

Electronic Supplementary Information for:

Statistical Analysis of C–H Activation by Oxo Complexes Supports Diverse Thermodynamic Control Over Reactivity

Joseph E. Schneider, McKenna K. Goetz, and John S. Anderson

Department of Chemistry, The University of Chicago, Chicago, IL 60637, United States

Correspondence to: jsanderson@uchicago.edu

Table of Contents

Summary of Experimental Data.....	5
Summary of csv File Contents.....	8
Detailed Statistics on DHA Regressions.....	16
Entropy Adjustment to Reaction Barriers.....	27
Effect of Solvent – Oxo Hydrogen Bonding on Regressions	29
Further Discussion of Steric Parameters.....	41
Attempts to Determine Reorganization Parameters.....	44
Robustness of Results to Computational Methodology.....	52
Analysis of Ru Oxo Kinetics with Several Substrates	64
Summary of Statistics on Regressions on the Co ^{III} Oxo Data.....	67
Regressions of Metal Oxo Complexes with Multiple Substrates.....	74
Availability of Data and Python Scripts	81
References.....	81

Figures, Tables, and Regressions

Figure S1. Metal oxo complexes in the training set.....	6
Figure S2. Metal oxo complexes in the test set.....	7
Figure S3. Correlation of main group oxides' hydrogen bond basicities and their calculated electronic energies of dimerization with water and the placement of relevant metal oxo complexes on the correlation line	30
Figure S4. Illustration of distance and angle steric metrics	41
Table S1. Metal oxo species analyzed with their experimental kinetics and barriers	5
Table S2. Description of what each column in the accompanying csv file contains.....	8
Table S3. Spin based parameters of each metal oxo complex	11
Table S4. Kinetics, barrier heights, and thermodynamic parameters of reactivity with 9,10-dihydroanthracene.....	12
Table S5. Kinetics, barrier heights, and thermodynamic parameters of reactivity with 1,4-cyclohexadiene.....	13
Table S6. Kinetics, barrier heights, and thermodynamic parameters of reactivity with xanthene	14
Table S7. Kinetics, barrier heights, and thermodynamic parameters of reactivity with fluorene	15
Table S8. Summary of statistics of regressions with DHA data	16
Table S9. Barrier heights predicted by the $\{\Delta G_{PCET}, \Delta G_{PT}, \Delta G_{ET}\}$ model and the contribution of each thermodynamic parameter.....	26
Table S10. Reference data used to construct the correlation between hydrogen bond basicity and electronic energy of dimerization and the resulting estimates of the hydrogen bond basicities of metal oxo complexes.....	30
Table S11. Summary of statistics of regressions with hydrogen bonding corrected DHA data.....	31
Table S12. Correlations between various steric metrics	41
Table S13. Steric parameters considered in this study	42
Table S14. Summary of statistics on regressions with measures of deformation energy.....	44
Table S15. Reorganization parameters considered in this study	45
Table S16. Summary of statistics on regressions with different computational methodology.....	52
Table S17. ΔE_{PCET} computed with different computational methodologies	53
Table S18. ΔE_{PT} computed with different computational methodologies.....	54
Table S19. ΔE_{ET} computed with different computational methodologies.....	55
Table S20. Summary of data for regressions with the Ru ^{IV} oxo data.....	64
Table S21. Summary of statistics on regressions with the Ru ^{IV} oxo data	64
Table S22. Summary of data for regressions with the Co ^{II} oxo data.....	67
Table S23. Summary of statistics on regressions with the Co ^{III} oxo data	67
Table S24. Summary of statistics on regressions with multiple substrates and multiple metal oxo complexes	74
Regression S1. DHA barriers against ΔG_{PCET} only.....	17
Regression S2. DHA barriers against ΔG_{PCET} and percent buried volume sterics	18
Regression S3. DHA barriers against ΔG_{PCET} and the IBO spin density on the oxo ligand.....	19
Regression S4. DHA barriers against ΔG_{PCET} and the Spin Excitation Energy	20
Regression S5. DHA barriers against ΔG_{PCET} and the magnitude of the asynchronicity.....	21
Regression S6. DHA barriers against $\Delta G_{PCET}, \Delta G_{PT}$, and ΔG_{ET}	22
Regression S7. DHA barriers against ΔG_{PCET} and ΔG_{PCET}^2	23
Regression S8. DHA barriers against ΔE_{PCET}	24
Regression S9. DHA barriers against $\Delta E_{PCET}, \Delta E_{PT}$, and ΔE_{ET}	25
Regression S10. DHA barriers against ΔG_{PCET} and RT	28
Regression S11. H-Bond corrected DHA barriers against ΔG_{PCET}	32
Regression S12. H-Bond adjusted DHA barriers against ΔG_{PCET} and percent buried volume sterics	33
Regression S13. H-Bond adjusted DHA barriers against ΔG_{PCET} and IBO spin density on the oxo ligand	34
Regression S14. H-Bond adjusted DHA barriers correction against ΔG_{PCET} and the spin excitation energy	35
Regression S15. H-Bond adjusted DHA barriers against ΔG_{PCET} and the magnitude of the asynchronicity	36
Regression S16. H-Bond adjusted DHA barriers against $\Delta G_{PCET}, \Delta G_{PT}$, and ΔG_{ET}	37
Regression S17. H-Bond adjusted DHA barriers against ΔG_{PCET} and ΔG_{PCET}^2	38
Regression S18. H-Bond adjusted DHA barriers against ΔE_{PCET}	39
Regression S19. H-Bond adjusted DHA barriers $\Delta E_{PCET}, \Delta E_{PT}$, and ΔE_{ET}	40

Regression S20. DHA barriers against ΔG_{PCET} and the height, max angle steric metrics.....	43
Regression S21. DHA barriers against ΔG_{PCET} and the oxo reorganization energy	46
Regression S22. DHA barriers against ΔG_{PCET} and stretching energies of M–O(H) bonds	47
Regression S23. DHA barriers against ΔG_{PCET} and change in metal–ligand bond lengths.....	48
Regression S24. DHA barriers against ΔG_{PCET} , reorganization, and the magnitude of the asynchronicity	49
Regression S25. DHA barriers against ΔG_{PCET} , stretching energies, and the magnitude of the asynchronicity	50
Regression S26. DHA barriers against ΔG_{PCET} , bond length changes, and the magnitude of the asynchronicity	51
Regression S27. DHA barriers against O3LYP's ΔE_{PCET}	56
Regression S28. DHA barriers against O3LYP's ΔE_{PCET} , ΔE_{PT} , and ΔE_{ET}	57
Regression S29. DHA barriers against B3LYP's ΔE_{PCET}	58
Regression S30. DHA barriers against B3LYP's ΔE_{PCET} , ΔE_{PT} , and ΔE_{ET}	59
Regression S31. DHA barriers against M06L's ΔE_{PCET}	60
Regression S32. DHA barriers against M06L's ΔE_{PCET} , ΔE_{PT} , and ΔE_{ET}	61
Regression S33. DHA barriers against O3LYP-ZORA's ΔE_{PCET}	62
Regression S34. DHA barriers against O3LYP-ZORA's ΔE_{PCET} , ΔE_{PT} , and ΔE_{ET}	63
Regression S35. Ru ^{IV} oxo barriers against ΔG_{PCET}	65
Regression S36. Ru ^{IV} oxo barriers against ΔG_{PCET} , ΔG_{PT} , and ΔG_{ET}	66
Regression S37. Co ^{III} oxo barriers against ΔG_{PT}	68
Regression S38. Co ^{III} oxo barriers against ΔG_{PCET}	69
Regression S39. Co ^{III} oxo barriers against ΔG_{PT} and ΔG_{PCET}	70
Regression S40. Co ^{III} oxo barriers against ΔG_{PT} , ΔG_{PCET} , and substrates' percent buried volume sterics	71
Regression S41. Co ^{III} oxo barriers against ΔG_{PT} and ΔG_{ET}	72
Regression S42. Co ^{III} oxo barriers against ΔG_{PT} , ΔG_{PCET} , and ΔG_{ET}	73
Regression S43. Multiple substrates' reaction barriers against ΔG_{PCET}	75
Regression S44. Multiple substrates' reaction barriers against ΔG_{PCET} and percent buried volume sterics	76
Regression S45. Multiple substrates' reaction barriers against ΔG_{PCET} and IBO spin density on the oxo ligand.....	77
Regression S46. Multiple substrates' reaction barriers against ΔG_{PCET} and the spin excitation energy	78
Regression S47. Multiple substrates' reaction barriers against ΔG_{PCET} and the magnitude of the asynchronicity	79
Regression S48. Multiple substrates' reaction barriers against ΔG_{PCET} , ΔG_{PT} , and ΔG_{ET}	80

Summary of Experimental Data

In Table S1 we list each metal oxo species considered, their references, their reported k_2 values for reactivity with 9,10-dihydroanthracene (DHA), any reported statistical or stoichiometric corrections to these k_2 values (the k_2 values were multiplied by these numbers prior to determining barrier heights), the temperature these k_2 values were collected at, and the resultant experimental reaction barriers (calculated as described in the main text methods). Where multiple temperatures or multiple experimental conditions are reported, only one set of those conditions was chosen to represent the metal oxo complex's reaction rate with DHA. We also list the experimental slope of $RT \log k_2$ vs. experimental substrate BDFE for cases with enough data to determine it (at least three different substrates with k_2 reported, counting DHA and xanthene as only one substrate due to their similar experimental BDFEs, and excepting the Co^{III} oxo complex whose kinetics trend not with BDFE but with pK_a). Chemdraws for each metal oxo complex are provided in Figure S1 (training set) and Figure S2 (test set).

Table S1. Metal oxo species analyzed with their experimental kinetics and barriers

Oxo	References	k_2^a (s^{-1})	Literature Correction	T (°C)	PCET Barrier ^a (kcal/mol)	BDFE Slope ^b
$[\text{Fe}^{\text{IV}}(\text{O})(\text{Me}_3\text{NTB})(\text{MeCN})]^{2+}$	1	780	4	-40	2.30	-0.18
$[\text{Fe}^{\text{IV}}(\text{O})(\text{TMG}_2\text{dien})(\text{MeCN})]^{2+}$	2	5		-30	4.38	
$[\text{Fe}^{\text{IV}}(\text{O})(\text{TMG}_3\text{tren})]^{2+}$	3	0.09		-30	7.46	
$[\text{Fe}^{\text{V}}(\text{O})(\text{TAML})]^-$	4,5	263	1	-37	3.54	-0.22
$[\text{Fe}^{\text{IV}}(\text{O})(\text{TMC})(\text{MeCN})]^{2+}$	6,7	0.2		0	7.99	
$[\text{Fe}^{\text{IV}}(\text{O})(\text{TMC})(\text{N}_3)]^+$	6	2.4		0	6.64	-0.28
$[\text{Fe}^{\text{IV}}(\text{O})(\text{TMC})(\text{OCOCF}_3)]^+$	6	1.3		0	6.93	-0.35
$[\text{Fe}^{\text{IV}}(\text{O})(\text{TMCS})]^+$	6,8	7.5		0	6.02	
$[\text{Mn}^{\text{IV}}(\text{O})(\text{H}_3\text{buea})]^-$	9,10	0.038	8	30	8.50	
$[\text{Fe}^{\text{IV}}(\text{O})(\text{TMP})]$	11	2.2		-15	6.18	
$[\text{Co}^{\text{III}}(\text{O})(\text{PhB}^{\text{tBu}}\text{Im}_3)]$	12,13	0.058	2	23	8.87	
$[\text{Ru}^{\text{IV}}(\text{O})(\text{H}^+\text{TPA})(\text{bpy})]^{3+}$	14	105		25	4.88	
$[\text{Fe}^{\text{IV}}(\text{O})(\text{tpfpp})]$	15	13	1	15	5.82	-0.15
$[\text{Mn}^{\text{VII}}(\text{O})_4]^-$	16,17	0.12	4	25	9.47	-0.67
$[\text{Mn}^{\text{V}}(\text{O})_2(\text{tf}_4\text{tmap})]^{3+}$	18	240	1	15	4.53	-0.25
$[\text{Mn}^{\text{IV}}(\text{O})(\text{OH})(\text{tf}_4\text{tmap})]^{3+}$	18	4.9	1	15	6.36	-0.35
$[\text{Cr}^{\text{IV}}(\text{O})(\text{TMC})(\text{Cl})]^+$	19,20	0.21	1	-10	7.69	
$[\text{Ru}^{\text{VI}}(\text{O})_2(\text{TMC})]^{2+}$	21,22	0.036	1	35	10.4	
$[\text{Fe}^{\text{IV}}(\text{O})(\text{N4Py})]^{2+}$	23,24	18		25	5.99	
$[\text{Fe}^{\text{IV}}(\text{O})(\text{BnTPEN})]^{2+}$	23	100		25	4.94	
$[\text{Fe}^{\text{IV}}(\text{O})(\text{Me}^2\text{TACN-Py}_2)]^{2+}$	23	7.4		25	6.54	
$[\text{Fe}^{\text{IV}}(\text{O})(\text{BP1})]^{2+}$	23	1.1		25	7.57	
$[\text{Fe}^{\text{IV}}(\text{O})(\text{BP2})]^{2+}$	23	40		25	5.44	
$[\text{Ru}^{\text{IV}}(\text{O})(\text{bpy})_2(\text{py})]^{2+}$	22,25	125	1	23	4.77	-0.54
$[\text{Mn}^{\text{IV}}(\text{O})_2(\text{Me}_2\text{EBC})]$	26	0.015		15	10.3	-0.09
$[\text{Mn}^{\text{IV}}(\text{O})(\text{N4Py})]^{2+}$	27	3.6	1	25	6.94	
$[\text{Co}^{\text{IV}}(\text{O})(\text{13-TMC})]^{2+}$	28	0.083	1	-40	7.30	-0.20
$[\text{Fe}^{\text{IV}}(\text{O})(\text{13-TMC})]^{2+}$	29	4.7	1	-40	5.44	-0.51
$[\text{Ru}^{\text{VI}}(\text{O})_2(\text{L})]^{2+}$	30,31	7.45	4	25	6.08	-0.60
$[\text{Ru}^{\text{VI}}(\text{O})_2(\text{F}_{28}\text{-tpp})]$	32	22.5	1	25	6.08	-0.43

^aFor reactivity with 9,10-dihydroanthracene. ^bExperimental slope of $RT \log k_2$ vs. substrate BDFE.

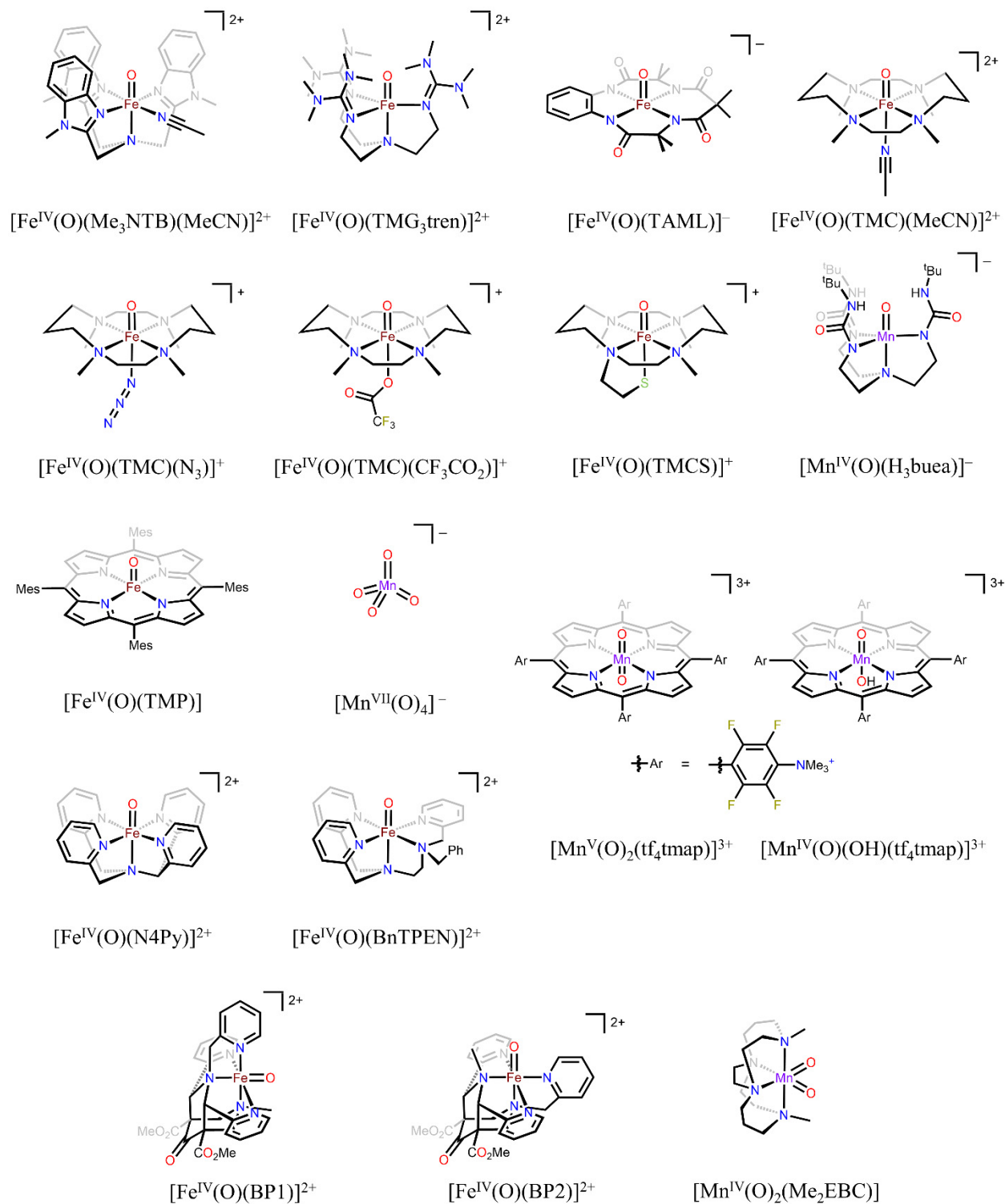


Figure S1. Metal oxo complexes in the training set. See Table S1 for references.

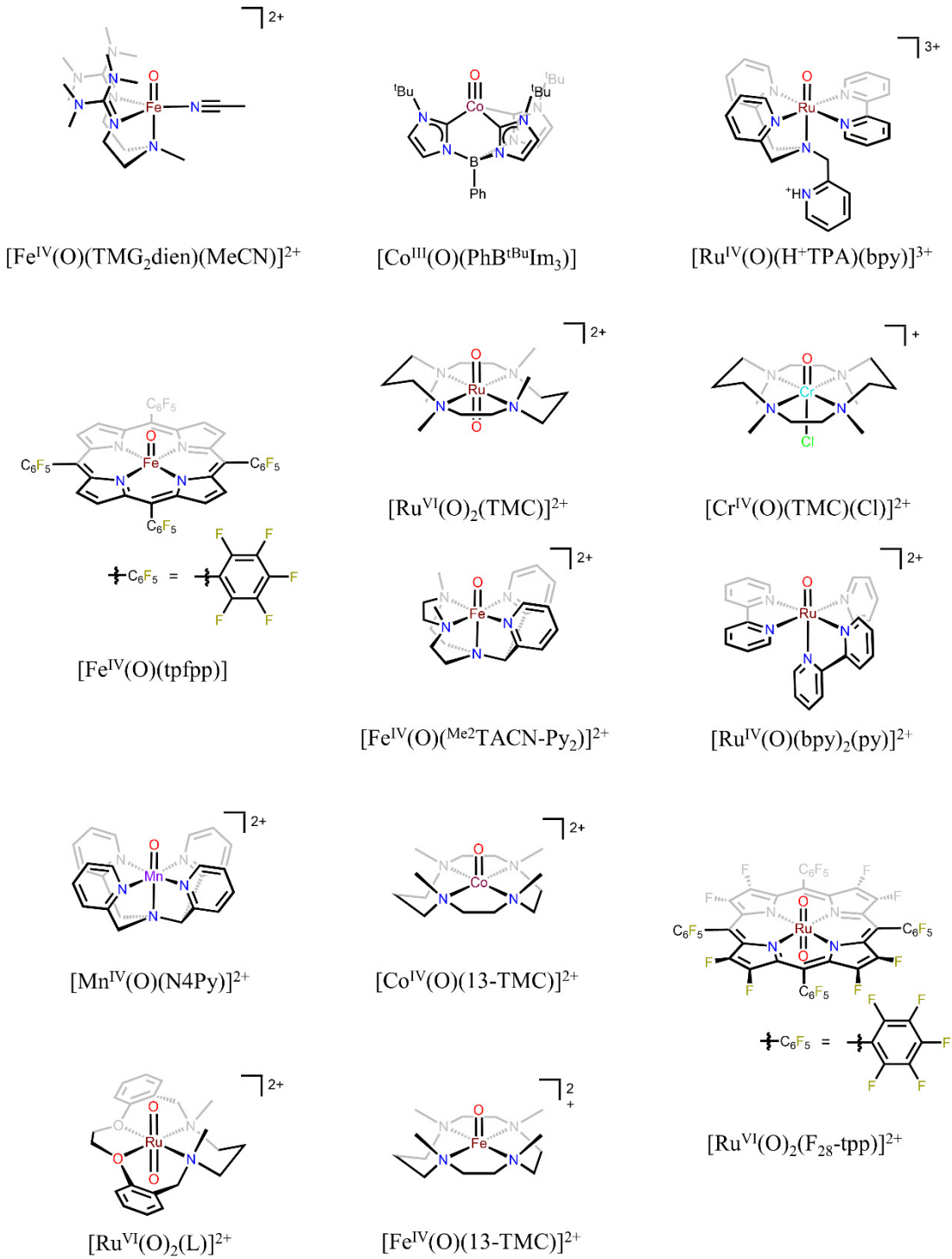


Figure S2. Metal oxo complexes in the test set. See Table S1 for references.

Summary of csv File Contents

In the accompanying data folder we include csv files containing all the data used in our regressions. For the data for various metal oxo complexes, each row corresponds to kinetic data of a particular metal oxo complex under a particular set of conditions; if a given metal oxo complex has k_2 values reported under different conditions (solvent, temperature, etc.) then multiple rows correspond to the same metal oxo complex. For the data on the kinetics of the Co^{III} oxo¹² each row pertains to a single substrate. In both spreadsheets each column has a short title for the data that is contained in that column. In Table S2, we give a longer description of what each column in the data files contains. The data directly used in our regressions are given in Table S3 (data relating to spin), Table S4 (data relating to reactivity with DHA), Table S6 (data related to reactivity with 1,4-cyclohexadiene (CHD)), Table S7 (data related to reactivity with fluorene), (data related to reactivity with xanthene), and Table S13 (steric parameters).

Table S2. Description of what each column in the accompanying csv file contains

Column Title	Description of Contents
Data Contained in “Oxos Data.csv”	
Name	The chemical formula of the oxo that the k_2 value(s) are reported for
Index	The numerical index assigned to the oxo that the k_2 value(s) are reported for
Training	1 if the row’s DHA k_2 value is included in the training set, 0 if not
Main Rate	1 if the row’s set of conditions is chosen to represent the metal oxo, 0 if not
Citation	The report the k_2 values are taken from
Note	Additional information relevant to the k_2 value
Metal	The metal of the metal oxo complex
Valency	The valency of the metal oxo complex
d count	The d-electron count of the metal oxo complex
Coordination	The coordination number (including the oxo) of the metal oxo complex
Axial Symmetry	The idealized axial symmetry about the M–O axis (C3 or C4); if the symmetry related ligands are not all equivalent then the symmetry is preceded by a “p”
N Oxos	The number of oxo ligands in the metal oxo complex
B(M,O)	The experimental M–O bond length, if reported (in Å)
v(M,O)	The experimental M–O stretching frequency, if reported (in cm ⁻¹)
BDE	The experimental bond dissociation (free) energy of MO–H, if reported (in kcal/mol)
pKa	The experimental pK _a of the protonated oxo, if reported
E0	The experimental reduction potential of the oxo, if reported (in V)
Charge	The charge of the metal oxo complex (in atomic charges)
Mass	The mass of the metal oxo complex (in AMU)
T	The temperature the k_2 value(s) are measured at (in °C)
kT	The thermal energy at temperature T (in kcal/mol), equivalently referred to as RT
Solvent	The solvent the k_2 value(s) are measured in
Abraham Alpha	Abraham’s hydrogen bond acidity of any protic component of the solvent; ^a 0 if the solvent is entirely aprotic.
Abraham Beta	The estimated hydrogen bond basicity of the metal oxo complex on Abraham’s scale
Abraham Alpha*Beta	The product of the hydrogen bond acidity and hydrogen bond basicity
Sub k2 ^b	The k_2 value for the reaction between the indicated substrate reacting with the indicated metal oxo complex in the given conditions (in M ⁻¹ s ⁻¹)
Sub Corr ^b	Any statistical and/or stoichiometric correction applied to the substrate’s k_2 value, if reported

Sub H_Act ^b	The experimental activation enthalpy of the reaction, if reported (in kcal/mol)
Sub S_Act ^b	The experimental activation entropy of the reaction, if reported (in cal/(mol K))
Sub KIE ^b	The experimental KIE on the substrate's k_2 value, if reported
Exp_BDFE_Slope	The experimental slope of the reaction between the metal oxo complex and various substrates at the given conditions, if there are enough k_2 values to determine it.
Mult_O	The ground state spin multiplicity of the metal oxo complex
Mult_OH	The ground state spin multiplicity of the corresponding metal hydroxide complex of the same overall charge
ΔMult	The change in spin multiplicity between the metal oxo complex and the corresponding metal hydroxide complex
Mult_O-	The spin multiplicity of the reduced metal oxo complex
Mult_OH+	The spin multiplicity of the protonated metal oxo complex
%BV_Tot	The total percent buried volume around the oxo ligand
%BV_Dir ^c	The percent buried volume for the quadrant in the given direction from the oxo ligand
%BV_Dev	The standard deviation of the percent buried volume of the four quadrants
Min_Angle	The minimum cone angle on top of the M–O bond
Max_Angle	The maximum cone angle on top of the M–O bond
Height	The height of the steric cavity the metal oxo resides in
Depth	The depth of the steric cavity the metal oxo resides in
Oxo_Reorganization	The calculated electronic energy needed to distort the metal oxo to the metal hydroxide geometry
Hydroxide_Reorganization	The calculated electronic energy needed to distort the metal hydroxide to the metal oxo geometry
Oxo_Frequency	The calculated dominant stretching frequency of the M–O bond
Hydroxide_Frequency	The calculated dominant stretching frequency of the M–OH bond
Length_M-O	The calculated length of the M–O bond
Length_M-OH	The calculated length of the M–OH bond
ΔLength_M-O	The calculated change in length between the M–O and M–OH bond
Oxo_Stretch	The energy needed to stretch the M–O bond to the length of the M–OH bond
Hydroxide_Stretch	The energy needed to compress the M–OH bond to the length of the M–O bond
Total_ΔLength_M-L	The calculated total change of metal–ligand bond lengths upon reduction from the oxo to the hydroxide complex, excluding the reduced oxo ligand
IBO_Spin_O	The IBO spin density on the oxo ligand in the metal oxo complex
IBO_Spin_M	The IBO spin density on the metal in the metal oxo complex
ΔIBO_Spin_O	The change in IBO spin density on the oxo ligand oxygen upon PCET reduction
ΔIBO_Spin_M	The change in IBO spin density on the metal upon PCET reduction
Spin_Excitation	The calculated energy needed for the metal oxo complex to access a spin surface within one spin multiplicity of the corresponding metal hydroxide complex
IBO_Charge_M_Oxo	The IBO charge density on the metal in the metal oxo complex
IBO_Charge_O_Oxo	The IBO charge density on the oxo ligand in the metal oxo complex
IBO_Charge_M_Hydroxide	The IBO charge density on the metal in the metal hydroxide complex
IBO_Charge_O_Hydroxide	The IBO charge on the hydroxide oxygen of the metal hydroxide complex
IBO_Charge_H_Hydroxide	The IBO charge on the hydroxide hydrogen of the metal hydroxide complex
ΔIBO_Charge_O(H)	The net amount of charge gained by the oxo ligand upon PCET as measured by IBO charges, including the proton and any IBO charge on the hydroxide hydrogen
Sub_ΔE_PCET ^b	The calculated change in the electronic energy upon PCET to the metal oxo complex from the indicated substrate
Sub_ΔE_PT ^b	The calculated change in the electronic energy upon PT to the metal oxo complex from the indicated substrate

Sub ΔE_ET ^b	The calculated change in the electronic energy upon ET to the metal oxo complex from the indicated substrate
Sub η (E) ^b	The calculated asynchronicity of PCET to the metal oxo complex from the indicated substrate calculated with electronic energies
Sub η (E) ^b	The calculated absolute value of the asynchronicity of PCET to the metal oxo complex from the indicated substrate calculated with electronic energies
Sub ΔE_CT Average ^b	The calculated average of Sub ΔE_PCET and Sub ΔE_PT
Sub ΔG_PCET ^b	The calculated change in the free energy upon PCET to the metal oxo complex from the indicated substrate
Sub ΔG_PT ^b	The calculated change in the free energy upon PT to the metal oxo complex from the indicated substrate
Sub ΔG_ET ^b	The calculated change in the free energy upon ET to the metal oxo complex from the indicated substrate
Sub η (G) ^b	The calculated asynchronicity of PCET to the metal oxo complex from the indicated substrate calculated with free energies
Sub η (G) ^b	The calculated absolute value of the asynchronicity of PCET to the metal oxo complex from the indicated substrate calculated with free energies
Sub ΔG_CT Average ^b	The calculated average of Sub ΔG_PCET and Sub ΔG_PT
Sub PCET Barrier ^b	The calculated experimental reaction barrier of PCET to the metal oxo complex from the indicated substrate with an adjustment for the entropy of association

Data Contained in “CoIII Oxo Data.csv”

Substrate	The substrate whose data is contained in the given row
k2	The k_2 value measured for reactivity between the Co ^{III} oxo and this substrate, or the reported k_{obs} value divided by the relevant substrate concentration (in M ⁻¹ s ⁻¹)
Mass	The mass of the substrate (in AMU)
BDE(kcal)	The experimental BDE of the substrate C–H bond (in kcal/mol), if reported ^d
pKa,exp (DMSO)	The experimental p K_a of the substrate C–H bond, if reported ^e
ΔG_PCET	The calculated change in free energy upon PCET from the substrate to the Co ^{III} oxo
ΔG_PT	The calculated change in free energy upon PT from the substrate to the Co ^{III} oxo
ΔG_ET	The calculated change in free energy upon ET from the substrate to the Co ^{III} oxo
%BV	The sterics surrounding the substrate’s reactive hydrogen

^aRef. ³³. ^bSub can be: DHA (9,10-dihydroanthracene), EtPh (ethylbenzene), CHD (1,4-cyclohexadiene), TPM (triphenylmethane), iPrPh (cumene), Tol (toluene), CyclOct (cyclooctane), DMB (2,3-dimethylbutane), CyclHex (cyclohexane), Xth (xanthene), F1 (fluorene), DPM (diphenylmethane), cCHD (1,3-cyclohexane), AcrH2 (10-methyl-9,10-dihydroacridine), BNAH (1-benzyl-1,4-dihydronicotinamide), Ind (indene), or CHxene (cyclohexene). Calculations were only performed with DHA, CHD, Xth, and F1. ^cDir can be: SW, NW, NE, SE. ^dRef. 34. ^eRef. 35–37.

Table S3. Spin based parameters of each metal oxo complex

Oxo	Mult. ^a Oxo	Mult. ^a Hydroxide	Mult. ^a Protonated Oxo	Mult. ^a Reduced Oxo	Spin Excitation ^b (kcal/mol)	IBO Spin Density
[Fe ^{IV} (O)(Me ₃ NTB)(MeCN)] ²⁺	3	6	3	6	16.0	0.852
[Fe ^{IV} (O)(TMG ₂ dien)(MeCN)] ²⁺	5	6	5	6	0	0.697
[Fe ^{IV} (O)(TMG ₃ tren)] ²⁺	5	6	5	6	0	0.662
[Fe ^V (O)(TAML)] ⁻	2	3	2	3	0	0.261
[Fe ^{IV} (O)(TMC)(MeCN)] ²⁺	3	6	3	6	10.6	0.760
[Fe ^{IV} (O)(TMC)(N ₃)] ⁺	3	6	3	6	7.2	0.691
[Fe ^{IV} (O)(TMC)(OCOCF ₃)] ⁺	3	6	3	6	8.3	0.699
[Fe ^{IV} (O)(TMCS)] ⁺	3	6	3	6	4.7	0.708
[Mn ^{IV} (O)(H ₃ buea)] ⁻	4	5	4	5	0	0.229
[Fe ^{IV} (O)(TMP)]	3	6	3	4	43.7	0.673
[Co ^{III} (O)(PhB ^t BuIm ₃)]	1	4	1	4	11.9	0.000
[Ru ^{IV} (O)(H ⁺ TPA)(bpy)] ³⁺	3	2	3	2	0	0.929
[Fe ^{IV} (O)(tpfpp)]	3	4	3	4	0	0.695
[Mn ^{VII} (O) ₄] ⁻	1	2	1	2	0	0.000
[Mn ^V (O) ₂ (tf ₄ tmap)] ³⁺	1	4	1	2	24.5	0.000
[Mn ^{IV} (O)(OH)(tf ₄ tmap)] ³⁺	4	5	4	5	0	0.546
[Cr ^{IV} (O)(TMC)(Cl)] ⁺	3	4	3	4	0	-0.133
[Ru ^{VI} (O) ₂ (TMC)] ²⁺	1	2	1	2	0	0.000
[Fe ^{IV} (O)(N4Py)] ²⁺	3	6	3	6	75.5	0.814
[Fe ^{IV} (O)(BnTPEN)] ²⁺	3	6	3	6	18.0	0.813
[Fe ^{IV} (O)(^{Me} ₂ TACN-Py ₂)] ²⁺	3	6	3	6	73.6	0.795
[Fe ^{IV} (O)(BP1)] ²⁺	3	6	3	6	19.6	0.821
[Fe ^{IV} (O)(BP2)] ²⁺	3	6	3	6	19.8	0.830
[Ru ^{IV} (O)(bpy) ₂ (py)] ²⁺	3	2	3	2	0	0.924
[Mn ^{IV} (O) ₂ (Me ₂ EBC)]	4	5	4	5	0	0.162
[Mn ^{IV} (O)(N4Py)] ²⁺	4	5	4	5	0	0.589
[Co ^{IV} (O)(13-TMC)] ²⁺	4	5	4	5	0	1.238
[Fe ^{IV} (O)(13-TMC)] ²⁺	3	6	3	6	17.7	0.691
[Ru ^{VI} (O) ₂ (L)] ²⁺	1	2	1	2	0	0.000
[Ru ^{VI} (O) ₂ (F ₂₈ -tpp)]	1	2	1	2	0	0.000

^aMultiplicity. ^bEnergy needed to access the lowest spin state of the oxo complex that is one multiplicity away from the multiplicity of the hydroxide; calculated at the ground spin state's optimized geometry.

Table S4. Kinetics, barrier heights, and thermodynamic parameters of reactivity with 9,10-dihydroanthracene

Oxo	k_2 (s ⁻¹) ^a	PCET Barrier (kcal/mol)	ΔG_{PCET} (kcal/mol)	ΔG_{PT} (kcal/mol)	ΔG_{ET} (kcal/mol)	$ \eta $ (kcal/mol)	ΔE_{PCET} (kcal/mol)	ΔE_{PT} (kcal/mol)	ΔE_{ET} (kcal/mol)
[Fe ^{IV} (O)(Me ₃ NTB)(MeCN)] ²⁺	780	2.3	-15.9	57.7	29.3	20.0	-8.9	61.4	37.8
[Fe ^{IV} (O)(TMG ₂ dien)(MeCN)] ²⁺	57	4.4	-9.3	57.5	39.2	12.9	-5	61.5	46
[Fe ^{IV} (O)(TMG ₃ tren)] ²⁺	0.09	7.5	-7.2	54.5	47.5	4.9	-3.1	57.6	54.4
[Fe ^V (O)(TAML)] ⁻	263	3.5	-10.1	39.2	40.2	0.72	-6.9	43.2	44.8
[Fe ^{IV} (O)(TMC)(MeCN)] ²⁺	0.2	8.0	-6.5	68.2	36.8	22.2	1.5	71.9	46.8
[Fe ^{IV} (O)(TMC)(N ₃)] ⁺	2.4	6.6	-9.4	47.1	46.6	0.4	-2.1	50.5	56.0
[Fe ^{IV} (O)(TMC)(OCOCF ₃)] ⁺	1.3	6.9	-8.7	56.7	42.7	9.9	-1.3	60.1	52.7
[Fe ^{IV} (O)(TMCS)] ⁺	7.5	6.0	-8.5	40.1	50.1	7.0	-2.1	42.7	59.3
[Mn ^{IV} (O)(H ₃ buea)] ⁻	0.038	8.5	0.71	27.6	62.3	24.6	5.3	29.5	69.3
[Fe ^{IV} (O)(TMP)]	2.2	6.2	-10.9	39.3	67.7	20.1	-6.2	44.3	73.5
[Co ^{III} (O)(PhB(tBu)Im ₃)]	0.0584	8.9	-8.8	15.9	74.3	41.3	-3.2	19.6	82.7
[Ru ^{IV} (O)(H ⁺ TPA)(bpy)] ³⁺	105	4.9	-4.5	75.9	41.9	24.1	-2.6	78.8	45.7
[Fe ^{IV} (O)(tpfpp)]	13	5.8	-8.0	50.1	57.3	5.1	-3.8	53.5	63.6
[Mn ^{VII} (O) ₄] ⁻	0.12	9.5	-0.4	55.5	49.6	4.1	3.5	58.7	54.4
[Mn ^V (O) ₂ (tf ₄ tmap)] ³⁺	240	4.5	-13.7	34.5	59.5	17.7	-9.0	36.7	66.2
[Mn ^{IV} (O)(OH)(tf ₄ tmap)] ³⁺	4.9	6.4	-9.2	20.0	60.8	28.9	-4.6	21.3	65.7
[Cr ^{IV} (O)(TMC)(Cl)] ⁺	0.21	7.7	-10.0	53.6	55.7	1.5	-7.5	56.9	61.5
[Ru ^{VI} (O) ₂ (TMC)] ²⁺	0.036	10.4	3.9	82.8	34.1	34.4	7.2	86.8	38.4
[Fe ^{IV} (O)(N4Py)] ²⁺	18	6.0	-5.8	65.0	38.0	19.1	1.5	69.0	46.4
[Fe ^{IV} (O)(BnTPEN)] ²⁺	100	4.9	-7.4	64.1	35.0	20.6	-1.2	66.7	43.0
[Fe ^{IV} (O)(^{Mc} ₂ TACN-Py ₂)] ²⁺	7.4	6.5	-6.3	63.7	37.3	18.7	1.4	67.5	46.6
[Fe ^{IV} (O)(BP1)] ²⁺	1.1	7.6	-6.2	69.9	35.6	24.3	0.4	74.0	43.5
[Fe ^{IV} (O)(BP2)] ²⁺	40	5.4	-9.6	68.1	31.7	25.7	-3.2	71.5	40.0
[Ru ^{IV} (O)(bpy) ₂ (py)] ²⁺	125	4.8	-5.5	68.5	43.4	17.7	-3.8	71.8	47.5
[Mn ^{IV} (O) ₂ (Me ₂ EBC)]	0.01496	10.3	-3.3	7.6	85.8	55.3	0.8	7.2	93.7
[Mn ^{IV} (O)(N4Py)] ²⁺	3.6	6.9	-8.1	51.5	36.6	10.6	-3.0	55.1	43.7
[Co ^{IV} (O)(13-TMC)] ²⁺	0.083	7.3	-15.0	69.0	11.5	40.6	-11.0	74.1	16.7
[Fe ^{IV} (O)(13-TMC)] ²⁺	4.7	5.4	-19.0	78.3	17.6	42.9	-13.8	83.4	24.1
[Ru ^{VI} (O) ₂ (L)] ²⁺	7.45	6.1	0.11	85.5	22.1	44.9	2.8	89.4	26.5
[Ru ^{VI} (O) ₂ (F ₂₈ -tpp)]	22.5	6.1	-4.6	64.9	37.2	19.6	-1.0	66.2	42.7

^aSee Table S1 for references and experimental conditions.

Table S5. Kinetics, barrier heights, and thermodynamic parameters of reactivity with 1,4-cyclohexadiene

Oxo	k_2 (s ⁻¹) ^a	PCET Barrier (kcal/mol)	ΔG_{PCET} (kcal/mol)	ΔG_{PT} (kcal/mol)	ΔG_{ET} (kcal/mol)	$ \eta $ (kcal/mol)	ΔE_{PCET} (kcal/mol)	ΔE_{PT} (kcal/mol)	ΔE_{ET} (kcal/mol)
[Fe ^{IV} (O)(Me ₃ NTB)(MeCN)] ²⁺	240	3.6	-19.2	64.8	26.5	27.1	-12.4	68.5	34.8
[Fe ^{IV} (O)(TMG ₂ dien)(MeCN)] ²⁺	18	5.4	-12.6	64.6	36.4	19.9	-8.5	68.5	42.9
[Fe ^{IV} (O)(TMG ₃ tren)] ²⁺	1.2	6.7	-10.6	61.6	44.7	12.0	-6.6	64.7	51.4
[Fe ^V (O)(TAML)] ⁻			-13.4	46.3	37.4	6.3	-10.4	50.3	41.8
[Fe ^{IV} (O)(TMC)(MeCN)] ²⁺			-9.8	75.3	34.0	29.2	-2.0	79.0	43.8
[Fe ^{IV} (O)(TMC)(N ₃)] ⁺	1.4	7.4	-12.8	54.2	43.8	7.4	-5.6	57.5	53.0
[Fe ^{IV} (O)(TMC)(OCOCF ₃)] ⁺	1.2	7.5	-12.0	63.8	39.9	16.9	-4.8	67.2	49.7
[Fe ^{IV} (O)(TMCS)] ⁺			-11.8	47.3	47.3	0.038	-5.6	49.8	56.2
[Mn ^{IV} (O)(H ₃ buea)] ⁻			-2.6	34.7	59.6	17.6	1.8	36.6	66.3
[Fe ^{IV} (O)(TMP)]			-14.2	46.4	64.9	13.1	-9.7	51.3	70.5
[Co ^{III} (O)(PhB ^{tBu} Im ₃)]			-12.1	23.0	71.5	34.3	-6.7	26.7	79.7
[Ru ^{IV} (O)(H ⁺ TPA)(bpy)] ³⁺			-7.8	83.0	39.1	31.0	-6.1	85.9	42.7
[Fe ^{IV} (O)(tpfpp)]	9	6.7	-11.3	57.2	54.5	1.9	-7.3	60.6	60.6
[Mn ^{VII} (O) ₄] ⁻			-3.7	62.6	46.9	11.1	0.029	65.8	51.3
[Mn ^V (O) ₂ (tf ₄ tmap)] ³⁺			-17	41.6	56.7	10.7	-12.5	43.8	63.2
[Mn ^{IV} (O)(OH)(tf ₄ tmap)] ³⁺	1.3	7.8	-12.5	27.1	58.1	21.9	-8.1	28.4	62.6
[Cr ^{IV} (O)(TMC)(Cl)] ⁺	0.096	8.6	-13.3	60.7	52.9	5.5	-11	64.0	58.5
[Ru ^{VI} (O) ₂ (TMC)] ²⁺	0.015	11.5	0.63	89.9	31.4	41.4	3.7	93.9	35.4
[Fe ^{IV} (O)(N4Py)] ²⁺			-9.1	72.1	35.3	26.0	-2.0	76.0	43.4
[Fe ^{IV} (O)(BnTPEN)] ²⁺			-10.7	71.2	32.2	27.6	-4.7	73.8	40.0
[Fe ^{IV} (O)(^{Mc2} TACN-Py ₂)] ²⁺			-9.7	70.8	34.6	25.6	-2.1	74.6	43.6
[Fe ^{IV} (O)(BP1)] ²⁺			-9.5	77.0	32.9	31.2	-3.1	81.1	40.5
[Fe ^{IV} (O)(BP2)] ²⁺			-12.9	75.2	29.0	32.7	-6.7	78.5	37.0
[Ru ^{IV} (O)(bpy) ₂ (py)] ²⁺			-8.8	75.6	40.7	24.7	-7.3	78.9	44.5
[Mn ^{IV} (O) ₂ (Me ₂ EBC)]	0.0159	10.8	-6.7	14.7	83.0	48.3	-2.7	14.3	90.7
[Mn ^{IV} (O)(N4Py)] ²⁺			-11.4	58.6	33.8	17.5	-6.5	62.2	40.7
[Co ^{IV} (O)(13-TMC)] ²⁺	0.037	8.1	-18.4	76.1	8.7	47.6	-14.5	81.1	13.7
[Fe ^{IV} (O)(13-TMC)] ²⁺	5.4	5.8	-22.3	85.4	14.8	50.0	-17.3	90.5	21.1
[Ru ^{VI} (O) ₂ (L)] ²⁺			-3.2	92.7	19.3	51.8	-0.72	96.5	23.5
[Ru ^{VI} (O) ₂ (F ₂₈ -tpp)]	240		-7.9	72.0	34.5	26.5	-4.5	73.3	39.7

^aSee Table S1 for references and experimental conditions.

Table S6. Kinetics, barrier heights, and thermodynamic parameters of reactivity with xanthene

Oxo	k_2 (s ⁻¹) ^a	PCET Barrier (kcal/mol)	ΔG_{PCET} (kcal/mol)	ΔG_{PT} (kcal/mol)	ΔG_{ET} (kcal/mol)	$ \eta $ (kcal/mol)	ΔE_{PCET} (kcal/mol)	ΔE_{PT} (kcal/mol)	ΔE_{ET} (kcal/mol)
[Fe ^{IV} (O)(Me ₃ NTB)(MeCN)] ²⁺			-18.7	57.0	21.0	25.4	-12.3	61.3	27.1
[Fe ^{IV} (O)(TMG ₂ dien)(MeCN)] ²⁺			-12.1	56.8	31.0	18.3	-8.4	61.3	35.3
[Fe ^{IV} (O)(TMG ₃ tren)] ²⁺			-10.1	53.8	39.2	10.3	-6.5	57.5	43.8
[Fe ^V (O)(TAML)] ⁻			-12.9	38.5	32.0	4.6	-10.3	43.1	34.2
[Fe ^{IV} (O)(TMC)(MeCN)] ²⁺			-9.3	67.4	28.6	27.5	-1.9	71.8	36.1
[Fe ^{IV} (O)(TMC)(N ₃)] ⁺	9.6	5.5	-12.2	46.4	38.4	5.7	-5.5	50.3	45.4
[Fe ^{IV} (O)(TMC)(OCOCF ₃)] ⁺	7.6	5.6	-11.5	55.9	34.4	15.2	-4.7	60.0	42.1
[Fe ^{IV} (O)(TMCS)] ⁺			-11.3	39.4	41.9	1.7	-5.5	42.5	48.6
[Mn ^{IV} (O)(H ₃ buea)] ⁻			-2	26.8	54.2	19.3	1.8	29.3	58.6
[Fe ^{IV} (O)(TMP)]	4.3	5.5	-13.7	38.6	59.4	14.7	-9.6	44.1	62.8
[Co ^{III} (O)(PhB ^t BuIm ₃)]			-11.5	15.1	66.1	36	-6.6	19.4	72.1
[Ru ^{IV} (O)(H ⁺ TPA)(bpy)] ³⁺			-7.2	75.2	33.7	29.3	-6.0	78.6	35.1
[Fe ^{IV} (O)(tpfpp)]	14	5.4	-10.8	49.4	49.1	0.17	-7.3	53.3	53.0
[Mn ^{VII} (O) ₄] ⁻	0.56	8.6	-3.2	54.7	41.5	9.4	0.092	58.6	43.7
[Mn ^V (O) ₂ (tf ₄ tmap)] ³⁺	570	3.6	-16.5	33.7	51.3	12.4	-12.5	36.5	55.5
[Mn ^{IV} (O)(OH)(tf ₄ tmap)] ³⁺	3.8	6.1	-12	19.2	52.6	23.6	-8.0	21.1	55.0
[Cr ^{IV} (O)(TMC)(Cl)] ⁺	0.86	6.6	-12.8	52.8	47.4	3.8	-10.9	56.7	50.9
[Ru ^{VI} (O) ₂ (TMC)] ²⁺	0.057	9.7	1.2	82.0	26.0	39.6	3.8	86.7	27.8
[Fe ^{IV} (O)(N4Py)] ²⁺			-8.5	64.3	29.9	24.3	-1.9	68.8	35.8
[Fe ^{IV} (O)(BnTPEN)] ²⁺			-10.2	63.4	26.8	25.8	-4.6	66.6	32.4
[Fe ^{IV} (O)(^{Mc2} TACN-Py ₂)] ²⁺			-9.1	63.0	29.2	23.9	-2.0	67.4	35.9
[Fe ^{IV} (O)(BP1)] ²⁺			-9	69.2	27.5	29.5	-3.0	73.8	32.8
[Fe ^{IV} (O)(BP2)] ²⁺			-12.4	67.4	23.6	31.0	-6.7	71.3	29.3
[Ru ^{IV} (O)(bpy) ₂ (py)] ²⁺	577	3.5	-8.2	67.7	35.3	22.9	-7.2	71.6	36.9
[Mn ^{IV} (O) ₂ (Me ₂ EBC)]	0.048	9.3	-6.1	6.9	77.6	50.0	-2.6	7.0	83.1
[Mn ^{IV} (O)(N4Py)] ²⁺			-10.9	50.7	28.4	15.8	-6.4	54.9	33.1
[Co ^{IV} (O)(13-TMC)] ²⁺	0.15	6.7	-17.9	68.3	3.2.0	46.0	-14.4	73.9	6.1
[Fe ^{IV} (O)(13-TMC)] ²⁺		4.5	-21.8	77.6	9.3.0	48.3	-17.3	83.3	13.5
[Ru ^{VI} (O) ₂ (L)] ²⁺	49.7	4.9	-2.6	84.8	13.9	50.1	-0.65	89.2	15.9
[Ru ^{VI} (O) ₂ (F ₂₈ -tpp)]	59	5.1	-7.4	64.2	29.1	24.8	-4.5	66.1	32.1

^aSee Table S1 for references and experimental conditions.

Table S7. Kinetics, barrier heights, and thermodynamic parameters of reactivity with fluorene

Oxo	k_2 (s ⁻¹) ^a	PCET Barrier (kcal/mol)	ΔG_{PCET} (kcal/mol)	ΔG_{PT} (kcal/mol)	ΔG_{ET} (kcal/mol)	$ \eta $ (kcal/mol)	ΔE_{PCET} (kcal/mol)	ΔE_{PT} (kcal/mol)	ΔE_{ET} (kcal/mol)
[Fe ^{IV} (O)(Me ₃ NTB)(MeCN)] ²⁺			-11.6	47.8	25.9	15.5	-5.1	51.1	32.0
[Fe ^{IV} (O)(TMG ₂ dien)(MeCN)] ²⁺			-5.0	47.7	35.8	8.4	-1.2	51.1	40.2
[Fe ^{IV} (O)(TMG ₃ tren)] ²⁺			-3.0	44.6	44.1	0.41	0.74	47.3	48.6
[Fe ^V (O)(TAML)] ⁻			-5.8	29.4	36.8	5.3	-3.1	32.9	39.0
[Fe ^{IV} (O)(TMC)(MeCN)] ²⁺			-2.2	58.3	33.4	17.6	5.3	61.6	41.0
[Fe ^{IV} (O)(TMC)(N ₃)] ⁺	0.15	7.8	-5.2	37.2	43.2	4.2	1.7	40.1	50.2
[Fe ^{IV} (O)(TMC)(OCOCF ₃)] ⁺	0.051	8.4	-4.4	46.8	39.3	5.3	2.5	49.8	46.9
[Fe ^{IV} (O)(TMCS)] ⁺			-4.3	30.3	46.7	11.6	1.7	32.4	53.5
[Mn ^{IV} (O)(H ₃ buea)] ⁻			5.0	17.7	59.0	29.2	9.1	19.2	63.5
[Fe ^{IV} (O)(TMP)]	0.09	7.5	-6.6	29.5	64.3	24.6	-2.4	33.9	67.7
[Co ^{III} (O)(PhB ^{tBu} Im ₃)]	0.61	7.5	-4.5	6.1	70.9	45.9	0.64	9.3	76.9
[Ru ^{IV} (O)(H ⁺ TPA)(bpy)] ³⁺			-0.2	66.1	38.5	19.5	1.2	68.5	39.9
[Fe ^{IV} (O)(tpfpp)]	2.3	6.5	-3.8	40.3	53.9	9.7	-0.023	43.2	57.8
[Mn ^{VII} (O) ₄] ⁻			3.8	45.7	46.3	0.45	7.3	48.4	48.6
[Mn ^V (O) ₂ (tf ₄ tmap)] ³⁺	28	5.4	-9.5	24.6	56.1	22.2	-5.2	26.4	60.4
[Mn ^{IV} (O)(OH)(tf ₄ tmap)] ³⁺			-4.9	10.1	57.5	33.5	-0.8	11.0	59.9
[Cr ^{IV} (O)(TMC)(Cl)] ⁺			-5.7	43.7	52.3	6.0	-3.7	46.6	55.7
[Ru ^{VI} (O) ₂ (TMC)] ²⁺			8.2	72.9	30.8	29.8	11.0	76.5	32.6
[Fe ^{IV} (O)(N4Py)] ²⁺			-1.5	55.2	34.7	14.5	5.3	58.6	40.6
[Fe ^{IV} (O)(BnTPEN)] ²⁺			-3.1	54.3	31.6	16.0	2.6	56.4	37.2
[Fe ^{IV} (O)(^{Mc2} TACN-Py ₂)] ²⁺			-2.1	53.9	34.0	14.1	5.2	57.2	40.8
[Fe ^{IV} (O)(BP1)] ²⁺			-1.9	60.1	32.3	19.7	4.2	63.7	37.7
[Fe ^{IV} (O)(BP2)] ²⁺			-5.4	58.3	28.4	21.2	0.57	61.1	34.2
[Ru ^{IV} (O)(bpy) ₂ (py)] ²⁺	21.9	5.4	-1.2	58.6	40.1	13.1	-0.0089	61.5	41.7
[Mn ^{IV} (O) ₂ (Me ₂ EBC)]	0.00912	10.3	0.93	-2.2	82.4	59.8	4.6	-3.1	87.9
[Mn ^{IV} (O)(N4Py)] ²⁺			-3.8	41.6	33.2	6.0	0.81	44.8	37.9
[Co ^{IV} (O)(13-TMC)] ²⁺	0.0064	8.2	-10.8	59.1	8.1	36.1	-7.2	63.7	10.9
[Fe ^{IV} (O)(13-TMC)] ²⁺			-14.7	68.5	14.2	38.4	-10.0	73.1	18.3
[Ru ^{VI} (O) ₂ (L)] ²⁺	1.58	7	4.4	75.7	18.7	40.3	6.6	79.1	20.7
[Ru ^{VI} (O) ₂ (F ₂₈ -tpp)]	1.32	7.4	-0.34	55.1	33.9	15.0	2.8	55.9	36.9

^aSee Table S1 for references and experimental conditions.

Detailed Statistics on DHA Regressions

In Table S8, we report statistics on the regressions with DHA reaction barriers from Table 1. We also give regressions with ΔG_{PCET}^2 and with electronic energies instead of free energies. While the regression against $\{\Delta E_{PCET}, \Delta E_{PT}, \Delta E_{ET}\}$ fits the data better than the regression against $\{\Delta G_{PCET}, \Delta G_{PT}, \Delta G_{ET}\}$, there are good theoretical reasons to use free energies rather than electronic energies for LFER analyses and we therefore limit our discussion to free energies.²² The table is followed by a detailed summary of each regression and a breakdown of the $\{\Delta G_{PCET}, \Delta G_{PT}, \Delta G_{ET}\}$ model for each data point.

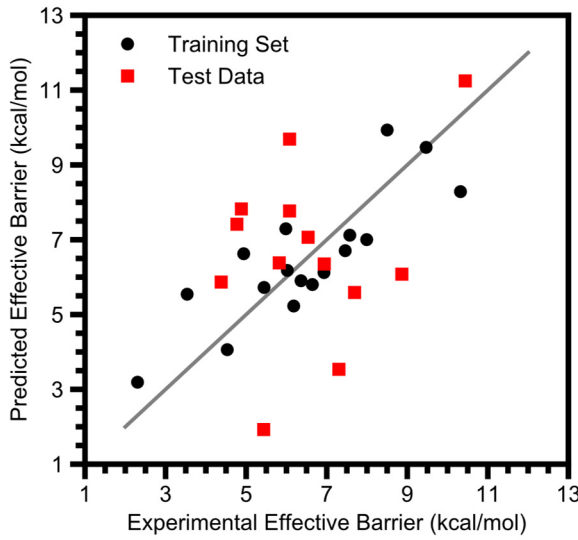
We report all the overall metrics as discussed in the methods section of the main text with more details specific to the parameters in each model and their corresponding coefficients. We report the correlation matrix of the parameters included in the model, their averages, and their standard deviations (all calculated with the training set). Within a linear regression, high correlation between two x-variables makes it difficult to untangle their effects on the y-variable, although the joint effect is unaffected.³⁸

For the coefficients, we report their values, their standard errors, 95% t-confidence intervals, and weighted coefficients. The coefficients' units are kcal/mol divided by the associated parameters' units. The standard errors do not directly inform on how reliable the coefficients are and are therefore scaled to give 95% t-confidence intervals. These rely on similar assumptions as the F-tests, and therefore have similar weaknesses.^{38,39} If the same analysis was performed on many different training sets – assuming the model is correctly formulated – one would expect to find the coefficients within the indicated interval 95% of the time (technically, this is the confidence in the method used to obtain the estimate of the coefficient, not in the estimate of the coefficient itself). If the interval contains zero, then there is no significant effect from the associated parameter and the coefficient and even its sign cannot be reliably interpreted. The weighted coefficients are the coefficients multiplied by the standard deviation of the associated parameter (within the training set). These can be used to compare the magnitude of disparate parameters' effects.⁴⁰

Table S8. Summary of statistics of regressions with DHA data

Parameter(s) Regressed with ΔG_{PCET}	R ²	MSE ^a	LOO ^b R ²	LOO ^b MSE ^a	5-Fold CV ^c MSE ^a	p-value ^d
ΔG_{PCET} only	0.70	1.18	0.60	1.57	1.49	< 0.001 ^f
%BV Steric Metrics	0.77	0.88	0.64	1.39	1.46	0.15
Oxo Spin Density	0.70	1.18	0.55	1.77	1.73	0.78
Spin Excitation	0.71	1.14	0.50	1.95	1.97	0.49
η	0.73	1.06	0.53	1.82	1.76	0.22
$\Delta G_{PT}, \Delta G_{ET}$	0.86	0.57	0.71	1.14	1.34	0.0082 0.023 ^g 0.0038 ^h
ΔG_{PCET}^2	0.71	1.11	0.59	1.59	1.51	0.36
ΔE_{PCET} only ^e	0.62	1.47	0.52	1.89	1.90	< 0.001 ⁱ
$\Delta E_{PCET}, \Delta E_{PT}, \Delta E_{ET}$ ^e	0.86	0.53	0.75	0.96	1.16	0.0013 ^j

^aMean Squared Error, kcal² mol⁻². ^bLeave-One-Out. ^cCross Validation. ^dFrom an F-test where the null hypothesis is that only ΔG_{PCET} has an effect. ^e ΔG_{PCET} not included in the regression. ^fFrom an F-test where the null hypothesis is that ΔG_{PCET} has no effect. ^gFrom an F-test where the null hypothesis is that ΔG_{PT} has no effect. ^hFrom an F-test where the null hypothesis is that ΔG_{ET} has no effect. ⁱFrom an F-test where the null hypothesis is that ΔE_{PCET} has no effect. ^jFrom an F-test where the null hypothesis is that only ΔE_{PCET} has an effect.



Regression S1. DHA barriers against ΔG_{PCET} only.

['DHA ΔG_{PCET} '] Metrics:

Score on Training Data:	0.6967248832007887
MSE of Training Data:	1.1837466708175275
Score of LOO Cross Validation:	0.5971855224924804
MSE of LOO Cross Validation:	1.5722697652848394
MSE of 5-Fold Cross Validation:	1.49405736960365 (0.04323619491372769)
F-Test p-value of final 1 variables:	3.078601862627206e-05

Correlation Matrix of x-values:

DHA ΔG_{PCET}	1.0
DHA ΔG_{PCET}	1.0

['DHA ΔG_{PCET} '] Training Average:
[-7.77619718]

['DHA ΔG_{PCET} '] Training Deviation:
[4.05326542]

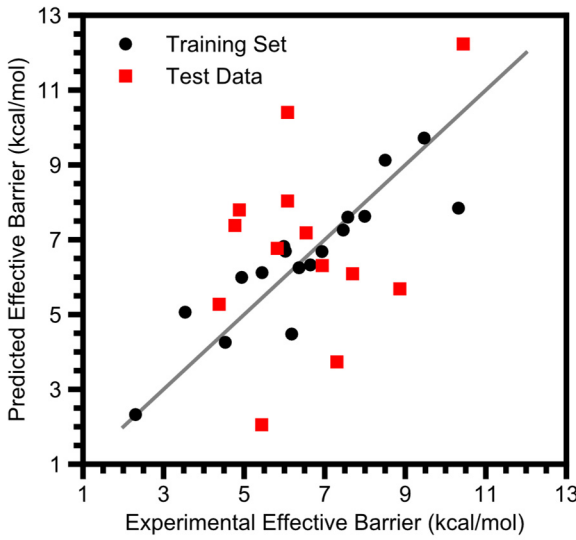
['DHA ΔG_{PCET} '] Coefficients:
[0.40685215]

['DHA ΔG_{PCET} '] Standard Error:
[0.06930726]

['DHA ΔG_{PCET} '] t-Test "Error":
[0.14772492]

['DHA ΔG_{PCET} '] Weighted Coefficients:
[1.64907974]

['DHA ΔG_{PCET} '] Intercept:
9.645819215174036



Regression S2. DHA barriers against ΔG_{PCET} and percent buried volume sterics.

`['DHA ΔG_PCET', '%BV Tot', '%BV Dev'] Metrics:`

Score on Training Data:	0.7746125436672053
MSE of Training Data:	0.8797347236852846
Score of LOO Cross Validation:	0.644354460933599
MSE of LOO Cross Validation:	1.3881594616273243
MSE of 5-Fold Cross Validation:	1.46372512865656 (0.059310929316259454)
F-Test p-value of final 2 variables:	0.14524602753892502

Correlation Matrix of x-values:

	DHA ΔG_PCET	%BV Tot	%BV Dev
DHA ΔG_PCET	1.000000	-0.107404	0.230500
%BV Tot	-0.107404	1.000000	0.134191
%BV Dev	0.230500	0.134191	1.000000

`['DHA ΔG_PCET', '%BV Tot', '%BV Dev'] Training Average:
[-7.77619718 64.39411765 5.35367331]`

`['DHA ΔG_PCET', '%BV Tot', '%BV Dev'] Training Deviation:
[4.05326542 10.53891783 4.76681449]`

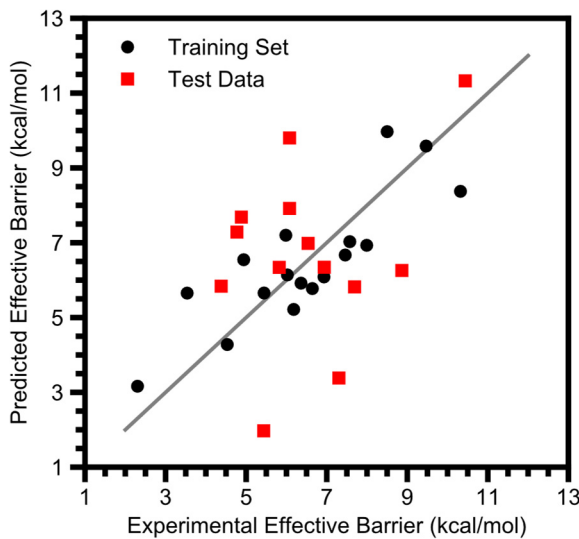
`['DHA ΔG_PCET', '%BV Tot', '%BV Dev'] Coefficients:
[0.44406794 0.01827786 -0.11845869]`

`['DHA ΔG_PCET', '%BV Tot', '%BV Dev'] Standard Error:
[0.06664533 0.02516922 0.05685555]`

`['DHA ΔG_PCET', '%BV Tot', '%BV Dev'] t-Test "Error":
[0.14397848 0.0543748 0.12282896]`

`['DHA ΔG_PCET', '%BV Tot', '%BV Dev'] Weighted Coefficients:
[1.79992522 0.19262889 -0.5646706]`

`['DHA ΔG_PCET', '%BV Tot', '%BV Dev'] Intercept:
9.392418865022623`



Regression S3. DHA barriers against ΔG_{PCET} and the IBO spin density on the oxo ligand.

`['DHA ΔG_PCET', 'IBO Spin O'] Metrics:`

Score on Training Data:	0.698551220951851
MSE of Training Data:	1.176618089826692
Score of LOO Cross Validation:	0.546795585374296
MSE of LOO Cross Validation:	1.7689523053359144
MSE of 5-Fold Cross Validation:	1.7301047476523321 (0.03545602037697516)
F-Test p-value of final 1 variables:	0.775139773791961

`Correlation Matrix of x-values:`

	DHA ΔG_PCET	IBO Spin O
DHA ΔG_PCET	1.000000	-0.346171
IBO Spin O	-0.346171	1.000000

`['DHA ΔG_PCET', 'IBO Spin O'] Training Average:`
`[-7.77619718 0.55994471]`

`['DHA ΔG_PCET', 'IBO Spin O'] Training Deviation:`
`[4.05326542 0.29315117]`

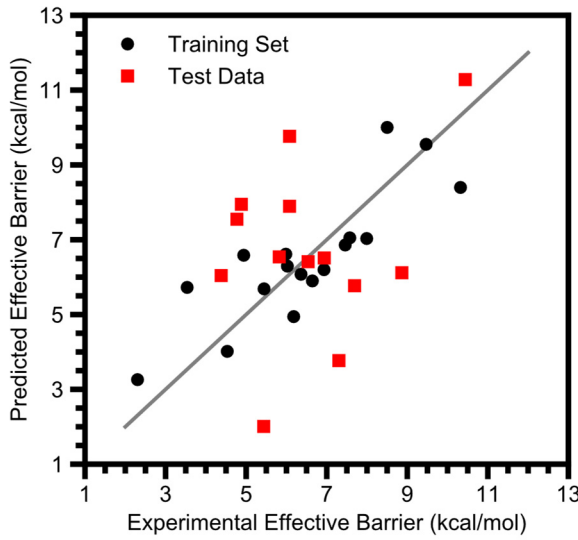
`['DHA ΔG_PCET', 'IBO Spin O'] Coefficients:`
`[0.39916608 -0.30699241]`

`['DHA ΔG_PCET', 'IBO Spin O'] Standard Error:`
`[0.07623711 1.05409519]`

`['DHA ΔG_PCET', 'IBO Spin O'] t-Test "Error":`
`[0.16351234 2.26080932]`

`['DHA ΔG_PCET', 'IBO Spin O'] Weighted Coefficients:`
`[1.61792606 -0.08999518]`

`['DHA ΔG_PCET', 'IBO Spin O'] Intercept:`
`9.757949587592675`



Regression S4. DHA barriers against ΔG_{PCET} and the Spin Excitation Energy.

`['DHA ΔG_PCET', 'Spin Excitation'] Metrics:`

Score on Training Data:	0.7072135314484478
MSE of Training Data:	1.1428072670986176
Score of LOO Cross Validation:	0.5009984749798582
MSE of LOO Cross Validation:	1.9477080751288274
MSE of 5-Fold Cross Validation:	1.970364948730487(0.0559990030724594)
F-Test p-value of final 1 variables:	0.49045257892652216

`Correlation Matrix of x-values:`

	DHA ΔG_PCET	Spin Excitation
DHA ΔG_PCET	1.00000	-0.20409
Spin Excitation	-0.20409	1.00000

`['DHA ΔG_PCET', 'Spin Excitation'] Training Average:
[-7.77619718 14.58587927]`

`['DHA ΔG_PCET', 'Spin Excitation'] Training Deviation:
[4.05326542 19.10348113]`

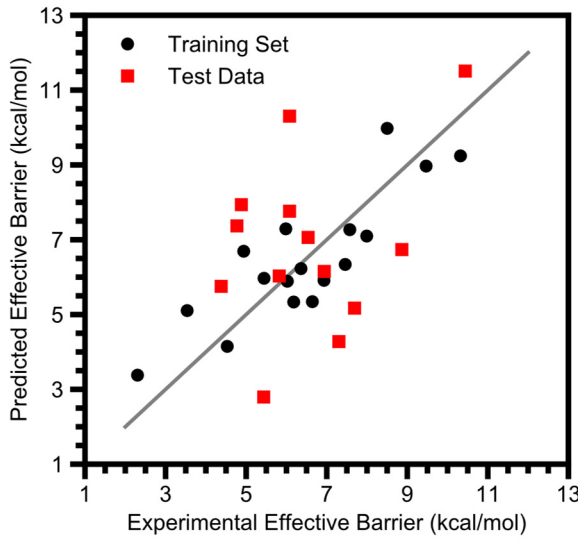
`['DHA ΔG_PCET', 'Spin Excitation'] Coefficients:
[0.39644513 -0.01081924]`

`['DHA ΔG_PCET', 'Spin Excitation'] Standard Error:
[0.0720039 0.01527737]`

`['DHA ΔG_PCET', 'Spin Excitation'] t-Test "Error":
[0.154433 0.03276669]`

`['DHA ΔG_PCET', 'Spin Excitation'] Weighted Coefficients:
[1.60689734 -0.20668517]`

`['DHA ΔG_PCET', 'Spin Excitation'] Intercept:
9.722700343793177`



Regression S5. DHA barriers against ΔG_{PCET} and the magnitude of the asynchronicity.

`['DHA ΔG_PCET', 'DHA |η| (G)'] Metrics:`

Score on Training Data:	0.7281325727412633
MSE of Training Data:	1.0611558419885931
Score of LOO Cross Validation:	0.5349640252644873
MSE of LOO Cross Validation:	1.815133376959526
MSE of 5-Fold Cross Validation:	1.7554887437479856 (0.08293293544608828)
F-Test p-value of final 1 variables:	0.2241810808486162

Correlation Matrix of x-values:

	DHA ΔG_PCET	DHA η (G)
DHA ΔG_PCET	1.000000	0.184231
DHA η (G)	0.184231	1.000000

`['DHA ΔG_PCET', 'DHA |η| (G)'] Training Average:`
`[-7.77619718 17.96727543]`

`['DHA ΔG_PCET', 'DHA |η| (G)'] Training Deviation:`
`[4.05326542 12.92730813]`

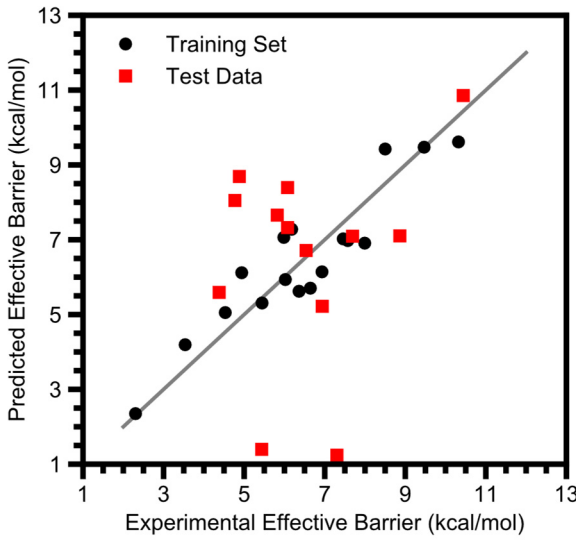
`['DHA ΔG_PCET', 'DHA |η| (G)'] Coefficients:`
`[0.39066077 0.02755618]`

`['DHA ΔG_PCET', 'DHA |η| (G)'] Standard Error:`
`[0.06910646 0.02166784]`

`['DHA ΔG_PCET', 'DHA |η| (G)'] t-Test "Error":`
`[0.14821863 0.04647289]`

`['DHA ΔG_PCET', 'DHA |η| (G)'] Weighted Coefficients:`
`[1.58345179 0.35622725]`

`['DHA ΔG_PCET', 'DHA |η| (G)'] Intercept:`
`9.024802368188036`



Regression S6. DHA barriers against ΔG_{PCET} , ΔG_{PT} , and ΔG_{ET} .

`['DHA ΔG_PCET', 'DHA ΔG_PT', 'DHA ΔG_ET'] Metrics:`

```

Score on Training Data:          0.8550607749306552
MSE of Training Data:          0.5657283293053714
Score of LOO Cross Validation: 0.708584021837019
MSE of LOO Cross Validation:   1.137457954395417
MSE of 5-Fold Cross Validation: 1.3430227389100244 (0.09649120302575805)
F-Test p-value of final 2 variables: 0.008237008538600432
F-Test p-value of 2nd to last variable (DHA ΔG_PT): 0.023223177281245677
F-Test p-value of final variable (DHA ΔG_ET): 0.00377509573731305

```

Correlation Matrix of x-values:

	DHA ΔG_PCET	DHA ΔG_PT	DHA ΔG_ET
DHA ΔG_PCET	1.000000	-0.116636	0.300610
DHA ΔG_PT	-0.116636	1.000000	-0.886456
DHA ΔG_ET	0.300610	-0.886456	1.000000

`['DHA ΔG_PCET', 'DHA ΔG_PT', 'DHA ΔG_ET'] Training Average:`
`[-7.77619718 47.94811989 48.18969167]`

`['DHA ΔG_PCET', 'DHA ΔG_PT', 'DHA ΔG_ET'] Training Deviation:`
`[4.05326542 17.72475347 14.50071323]`

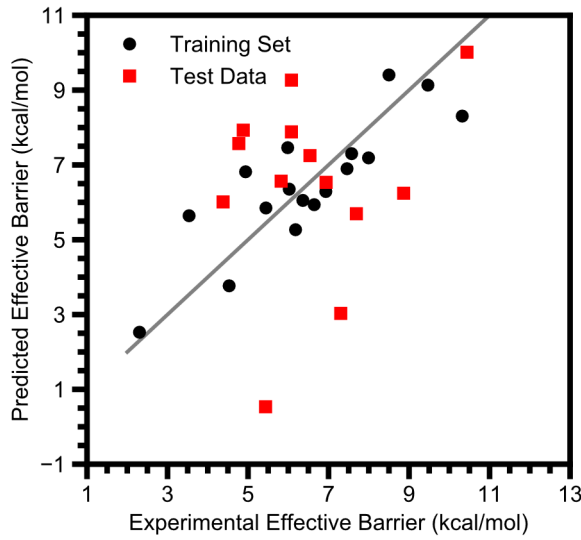
`['DHA ΔG_PCET', 'DHA ΔG_PT', 'DHA ΔG_ET'] Coefficients:`
`[0.3120842 0.06952437 0.12109262]`

`['DHA ΔG_PCET', 'DHA ΔG_PT', 'DHA ΔG_ET'] Standard Error:`
`[0.05736941 0.02703542 0.03441251]`

`['DHA ΔG_PCET', 'DHA ΔG_PT', 'DHA ΔG_ET'] t-Test "Error":`
`[0.12393907 0.05840647 0.07434371]`

`['DHA ΔG_PCET', 'DHA ΔG_PT', 'DHA ΔG_ET'] Weighted Coefficients:`
`[1.26496011 1.23230225 1.75592936]`

`['DHA ΔG_PCET', 'DHA ΔG_PT', 'DHA ΔG_ET'] Intercept:`
`-0.2600936876032849`



Regression S7. DHA barriers against ΔG_{PCET} and ΔG_{PCET}^2 .

```
[ 'DHA ΔG_PCET', 'DHA ΔG_PCET^2' ] Metrics:
```

Score on Training Data:	0.7149873903247832
MSE of Training Data:	1.112464258211542
Score of LOO Cross Validation:	0.5915803011130514
MSE of LOO Cross Validation:	1.5941481251619116
MSE of 5-Fold Cross Validation:	1.5101598742890083 (0.056935040823286265)
F-Test p-value of final 1 variables:	0.3596321487917926

```
Correlation Matrix of x-values:
```

	DHA ΔG_PCET	DHA ΔG_PCET^2
DHA ΔG_PCET	1.000000	-0.929028
DHA ΔG_PCET^2	-0.929028	1.000000

```
[ 'DHA ΔG_PCET', 'DHA ΔG_PCET^2' ] Training Average:  
[-7.77619718 76.89820308]
```

```
[ 'DHA ΔG_PCET', 'DHA ΔG_PCET^2' ] Training Deviation:  
[ 4.05326542 62.99805804]
```

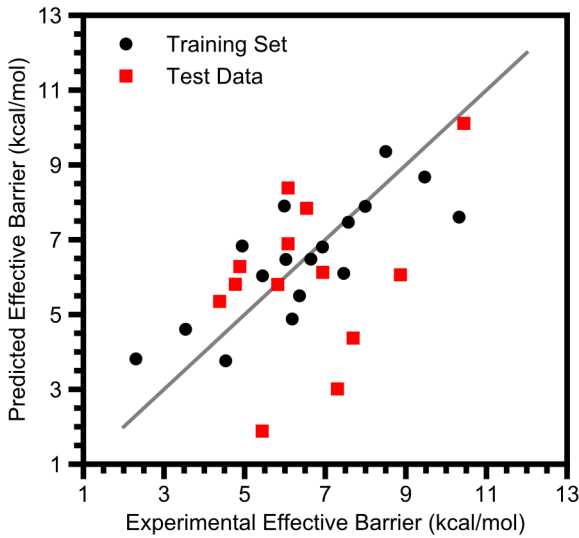
```
[ 'DHA ΔG_PCET', 'DHA ΔG_PCET^2' ] Coefficients:  
[ 0.24146465 -0.01145385]
```

```
[ 'DHA ΔG_PCET', 'DHA ΔG_PCET^2' ] Standard Error:  
[ 0.18795835 0.01209315]
```

```
[ 'DHA ΔG_PCET', 'DHA ΔG_PCET^2' ] t-Test "Error":  
[ 0.40313056 0.02593723]
```

```
[ 'DHA ΔG_PCET', 'DHA ΔG_PCET^2' ] Weighted Coefficients:  
[ 0.97872033 -0.72157062]
```

```
[ 'DHA ΔG_PCET', 'DHA ΔG_PCET^2' ] Intercept:  
9.240514307521131
```



Regression S8. DHA barriers against ΔE_{PCET} .

`['DHA ΔE _PCET'] Metrics:`

Score on Training Data:	0.6246046731001371
MSE of Training Data:	1.4652470441627932
Score of LOO Cross Validation:	0.5157469389983269
MSE of LOO Cross Validation:	1.8901417130553664
MSE of 5-Fold Cross Validation:	1.9017782503654304 (0.04647736834316938)
F-Test p-value of final 1 variables:	0.00015966818653256887

`Correlation Matrix of x-values:`

DHA ΔE _PCET	1.0
DHA ΔE _PCET	

`['DHA ΔE _PCET'] Training Average:`
`[-2.08594867]`

`['DHA ΔE _PCET'] Training Deviation:`
`[3.99325888]`

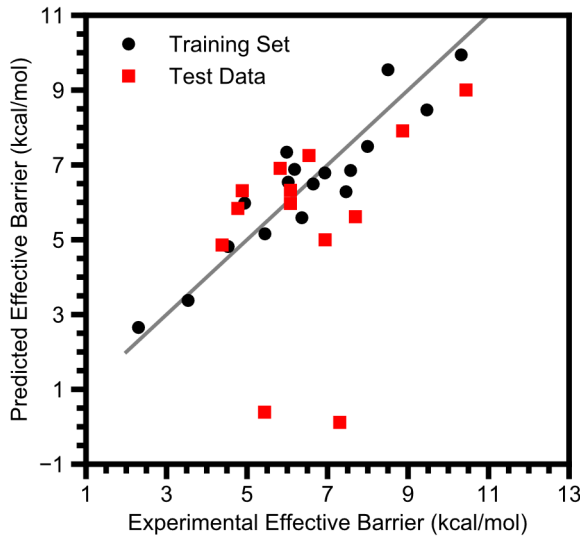
`['DHA ΔE _PCET'] Coefficients:`
`[0.39100845]`

`['DHA ΔE _PCET'] Standard Error:`
`[0.07826766]`

`['DHA ΔE _PCET'] t-Test "Error":`
`[0.16682356]`

`['DHA ΔE _PCET'] Weighted Coefficients:`
`[1.56139797]`

`['DHA ΔE _PCET'] Intercept:`
`7.297680247312937`



Regression S9. DHA barriers against ΔE_{PCET} , ΔE_{PT} , and ΔE_{ET} .

```
['DHA ΔE_PCET', 'DHA ΔE_PT', 'DHA ΔE_ET'] Metrics:
```

Score on Training Data:	0.8642292420790744
MSE of Training Data:	0.5299418705349127
Score of LOO Cross Validation:	0.7546196643252872
MSE of LOO Cross Validation:	0.9577711435895295
MSE of 5-Fold Cross Validation:	1.162034462523503(0.0776391752517394)
F-Test p-value of final 2 variables:	0.0013460555172805089

Correlation Matrix of x-values:

	DHA ΔE_PCET	DHA ΔE_PT	DHA ΔE_ET
DHA ΔE_PCET	1.000000	0.093539	0.119751
DHA ΔE_PT	0.093539	1.000000	-0.868929
DHA ΔE_ET	0.119751	-0.868929	1.000000

```
['DHA ΔE_PCET', 'DHA ΔE_PT', 'DHA ΔE_ET'] Training Average:  
[-2.08594867 50.96221826 55.73635424]
```

```
['DHA ΔE_PCET', 'DHA ΔE_PT', 'DHA ΔE_ET'] Training Deviation:  
[ 3.99325888 18.62129223 14.02559969]
```

```
['DHA ΔE_PCET', 'DHA ΔE_PT', 'DHA ΔE_ET'] Coefficients:  
[0.32595791 0.04033659 0.11282918]
```

```
['DHA ΔE_PCET', 'DHA ΔE_PT', 'DHA ΔE_ET'] Standard Error:  
[0.05562276 0.02392676 0.03185668]
```

```
['DHA ΔE_PCET', 'DHA ΔE_PT', 'DHA ΔE_ET'] t-Test "Error":  
[0.12016567 0.05169063 0.06882218]
```

```
['DHA ΔE_PCET', 'DHA ΔE_PT', 'DHA ΔE_ET'] Weighted Coefficients:  
[1.30163433 0.75111934 1.58249696]
```

```
['DHA ΔE_PCET', 'DHA ΔE_PT', 'DHA ΔE_ET'] Intercept:  
-1.1823410363409037
```

Table S9. Barrier heights predicted by the $\{\Delta G_{\text{PCET}}, \Delta G_{\text{PT}}, \Delta G_{\text{ET}}\}$ model and the contribution of each thermodynamic parameter

Oxo	Reference	0.31 × ΔG_{PCET} (kcal/mol)	0.070 × ΔG_{PT} (kcal/mol)	0.12 × ΔG_{ET} (kcal/mol)	Predicted Barrier ^a (kcal/mol)	Exp ^b Barrier (kcal/mol)
[Fe ^{IV} (O)(Me ₃ NTB)(MeCN)] ²⁺	1	-5.0	4.0	3.6	2.4	2.3
[Fe ^{IV} (O)(TMG ₂ dien)(MeCN)] ²⁺	2	-2.9	4.0	4.8	5.6	4.4
[Fe ^{IV} (O)(TMG ₃ tren)] ²⁺	3	-2.3	3.8	5.7	7.0	7.5
[Fe ^V (O)(TAML)] ⁻	4	-3.1	2.7	4.9	4.2	3.5
[Fe ^{IV} (O)(TMC)(MeCN)] ²⁺	6	-2.0	4.7	4.5	6.9	8.0
[Fe ^{IV} (O)(TMC)(N ₃)] ⁺	6	-2.9	3.3	5.6	5.7	6.6
[Fe ^{IV} (O)(TMC)(OCOCF ₃)] ⁺	6	-2.7	3.9	5.2	6.1	6.9
[Fe ^{IV} (O)(TMCS)] ⁺	6	-2.7	2.8	6.0	5.9	6.0
[Mn ^{IV} (O)(H ₃ buea)] ⁻	9	0.2	1.9	7.5	9.4	8.5
[Fe ^{IV} (O)(TMP)]	11	-3.4	2.7	8.2	7.3	6.2
[Co ^{III} (O)(PhB <i>t</i> BuIm ₃)]	12	-2.7	1.1	9.0	7.1	8.9
[Ru ^{IV} (O)(H ⁺ TPA)(bpy)] ³⁺	14	-1.4	5.3	5.0	8.7	4.9
[Fe ^{IV} (O)(tpfpp)]	15	-2.5	3.5	6.9	7.7	5.8
[Mn ^{VII} (O) ₄] ⁻	16	-0.14	3.9	6.0	9.5	9.5
[Mn ^V (O) ₂ (tf ₄ tmap)] ³⁺	18	-4.3	2.4	7.2	5.1	4.5
[Mn ^{IV} (O)(OH)(tf ₄ tmap)] ³⁺	18	-2.9	1.4	7.4	5.6	6.4
[Cr ^{IV} (O)(TMC)(Cl)] ⁺	19	-3.1	3.7	6.7	7.1	7.7
[Ru ^{VI} (O) ₂ (TMC)] ²⁺	21	1.2	5.8	4.1	10.9	10.4
[Fe ^{IV} (O)(N4Py)] ²⁺	23	-1.8	4.5	4.6	7.1	6.0
[Fe ^{IV} (O)(BnTPEN)] ²⁺	23	-2.3	4.5	4.2	6.1	4.9
[Fe ^{IV} (O)(^{Me2} TACN-Py ₂)] ²⁺	23	-2.0	4.4	4.5	6.7	6.5
[Fe ^{IV} (O)(BP1)] ²⁺	23	-1.9	4.9	4.3	7.0	7.6
[Fe ^{IV} (O)(BP2)] ²⁺	23	-3.0	4.7	3.8	5.3	5.4
[Ru ^{IV} (O)(bpy) ₂ (py)] ²⁺	25	-1.7	4.8	5.3	8.0	4.8
[Mn ^{IV} (O) ₂ (Me ₂ EBC)]	26	-1.0	0.5	10.4	9.6	10.3
[Mn ^{IV} (O)(N4Py)] ²⁺	27	-2.5	3.6	4.4	5.2	6.9
[Co ^{IV} (O)(13-TMC)] ²⁺	28	-4.7	4.8	1.4	1.2	7.3
[Fe ^{IV} (O)(13-TMC)] ²⁺	29	-5.9	5.4	2.1	1.4	5.4
[Ru ^{VI} (O) ₂ (L)] ²⁺	30	0.03	6.0	2.6	8.4	6.1
[Ru ^{VI} (O) ₂ (F ₂₈ tpp)]	32	-1.4	4.5	4.5	7.3	6.1

^a0.31ΔG_{PCET} + 0.070ΔG_{PT} + 0.12ΔG_{ET} - 0.26. ^bExperimental.

Entropy Adjustment to Reaction Barriers

As discussed in the main text, we subtracted from the experimental reaction barrier the loss of translational entropy upon metal oxo and substrate association. This correction is derived from the expression of the translational entropy of a chemical species of mass m and concentration C :⁴¹

$$TS_t = RT \ln \left(\left(\frac{2\pi m RT}{h^2} \right)^{\frac{3}{2}} C^{-1} \right) + \frac{5}{2} RT \quad (\text{S1})$$

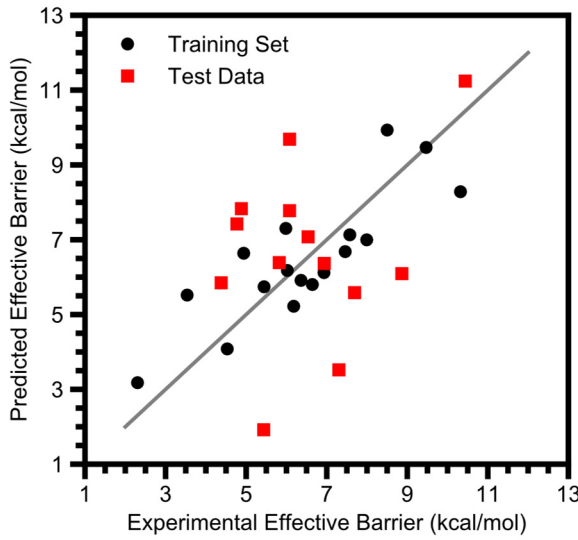
where RT is the thermal energy in kcal/mol and h is Plank's constant. With all species in the standard state of $C^\circ = 1 M$, the standard change in translational entropy upon association is:

$$(T\Delta S_t^\circ)_{assoc} = TS_{t, MO+CH} - (TS_{t, MO} - TS_{t, CH}) = RT \ln \left(\left(\frac{2\pi(m_{MO}+m_{CH})RT}{h^2} \right)^{\frac{3}{2}} C^\circ{}^{-1} \right) + \frac{5}{2} RT - \left(RT \ln \left(\left(\frac{2\pi m_{MO} RT}{h^2} \right)^{\frac{3}{2}} C^\circ{}^{-1} \right) + \frac{5}{2} RT + RT \ln \left(\left(\frac{2\pi m_{CH} RT}{h^2} \right)^{\frac{3}{2}} C^\circ{}^{-1} \right) + \frac{5}{2} RT \right) \quad (\text{S2})$$

in which the metal oxo is denoted as MO, the substrate as CH, and the associated complex as MO+CH. Simplifying this by combining the log terms via the identity $\ln a - \ln b - \ln c = -\ln \frac{bc}{a}$, canceling two of the $\frac{5}{2} RT$ terms, and factoring out RT gives:

$$(T\Delta S_t)_{assoc} = -RT \left[\ln \left(\left(\frac{2\pi(\frac{m_{Oxo}m_{Sub}}{m_{Oxo}+m_{Sub}})RT}{h^2} \right)^{\frac{3}{2}} C^\circ{}^{-1} \right) + \frac{5}{2} \right] \quad (\text{S3})$$

Combining the masses into $\mu = \frac{m_{Oxo}m_{Sub}}{m_{Oxo}+m_{Sub}}$ finishes the derivation of this expression as it appears in Equation 1 in the main text. We find this correction adequately accounts for the temperature dependence of the barriers; in Regression S10 we show that RT does not improve a fit to ΔG_{PCET} alone the fit. Inclusion of RT has a p -value of 0.97, barely affects the R^2 and MSE of the fit, and substantially worsens cross validation metrics.



Regression S10. DHA barriers against ΔG_{PCET} and kT .

```
['DHA ΔG_PCET', 'kT'] Metrics:
```

Score on Training Data:	0.6967643666901857
MSE of Training Data:	1.1835925584405569
Score of LOO Cross Validation:	0.5227899514128529
MSE of LOO Cross Validation:	1.8626513518737027
MSE of 5-Fold Cross Validation:	1.868642947451995 (0.09296746191926707)
F-Test p-value of final 1 variables:	0.9665472615379543

```
Correlation Matrix of x-values:
```

	DHA ΔG_PCET	kT
DHA ΔG_PCET	1.000000	0.575834
kT	0.575834	1.000000

```
['DHA ΔG_PCET', 'kT'] Training Average:  
[-7.77619718  0.55186587]
```

```
['DHA ΔG_PCET', 'kT'] Training Deviation:  
[4.05326542  0.04426339]
```

```
['DHA ΔG_PCET', 'kT'] Coefficients:  
[0.40469496  0.34304495]
```

```
['DHA ΔG_PCET', 'kT'] Standard Error:  
[0.08774231  8.03469455]
```

```
['DHA ΔG_PCET', 'kT'] t-Test "Error":  
[ 0.18818853 17.23270591]
```

```
['DHA ΔG_PCET', 'kT'] Weighted Coefficients:  
[1.64033608  0.01518433]
```

```
['DHA ΔG_PCET', 'kT'] Intercept:  
9.439729679880315
```

Effect of Solvent – Oxo Hydrogen Bonding on Regressions

Hydrogen bonding between protic solvents and the oxo ligand of metal oxo complexes likely results in raising the apparent barrier of PCET reactions,^{42,43} but we were unable to derive a reliable adjustment for this effect. Direct calculation of the equilibria between metal oxo complexes and solvent molecules was not feasible: DFT calculations of weak intermolecular interactions are unreliable,^{44–46} and even if largely electrostatic hydrogen bonds are an exception it would be difficult to determine the free energy of unbound solvent molecules in the variety of solvent mixtures which protic solvents appear in. We were, however, able to make a crude attempt at quantifying hydrogen bonding to demonstrate that our neglect of this effect does not affect our overall conclusions. Snelgrove et al.⁴² have shown that for hydrogen atom transfer reactions of O–H and N–H bonds the effect of hydrogen bonding to the solvent can be accounted for by means of Abraham’s hydrogen bonding parameters:^{33,47}

$$\log k^S = \log k^\circ + 8.3 \alpha \cdot \beta$$

where k^S is the rate in the presence of solvent hydrogen bonding, k° is the rate in the absence of solvent hydrogen bonding, α is Abraham’s hydrogen bond acidity of the substrate O–H or N–H bond, β is Abraham’s hydrogen bond basicity of the solvent, and all logarithms are base 10. This is very similar to a formula from Abraham for the equilibrium constant K of the formation of a hydrogen bond dimer between a donor with hydrogen bond acidity α and an acceptor with hydrogen bond basicity β (again with a common logarithm):⁴⁷

$$\log K = 7.354 \alpha \cdot \beta - 1.094$$

The similarity indicates that Snelgrove et al.’s expression is fundamentally related to the free energy of forming a hydrogen bonded dimer, and that it may be a good approximation for a more general situation than an O–H or N–H substrate donating a hydrogen bond to the solvent. However, the ability of protic solvents to form hydrogen bonds with each other renders it unclear if a simple application of the energy of dimer formation will apply as well to the case of hydrogen bonding to a protic solvent. It is further unclear how this formula’s applicability is affected by temperature changes, use of solvent mixtures, or the presence of electrolytes. The biggest hindrance to applying this formula, however, is that the Abraham hydrogen bond basicities of metal oxo complexes are not known. For all these reasons we are not confident that the use of this formula to adjust k_2 values for solvent hydrogen bonding will result in more accurate reaction barriers than neglect of this effect entirely. Nonetheless, we apply this formula as best we can to demonstrate that our results hold as well with or without and adjustment for hydrogen bonding.

We utilized the known β values of various carbon, nitrogen, phosphorus, and sulfur oxides to correlate the value of β with the DFT electronic energy of forming a dimer with water (calculated with the same level of theory as described in the main text, with the def2-TZVP basis on all atoms).^{47,48} The resulting correlation is shown in Figure S3 and the numerical data is given in Table S10. While the correlation is not spectacular ($r^2 = 0.61$), it allows us to come up with a reasonable estimate of β for each metal oxo complex with reported kinetics in a protic solvent via DFT calculations of the corresponding dimer between the metal oxo complex and water (calculated with the same level of theory as described in the main text, with the def2-TZVP basis on the water molecule).

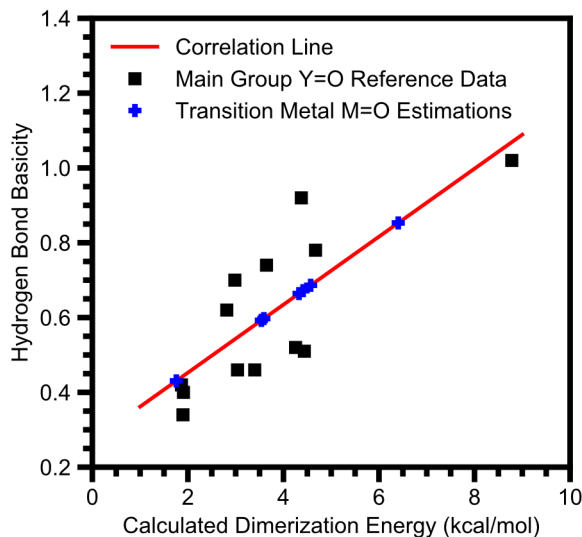


Figure S3. Correlation of main group oxides' hydrogen bond basicities and their calculated electronic energies of dimerization with water and the placement of relevant metal oxo complexes on the correlation line. The correlation coefficient r^2 is 0.61, and the regression equation is $y = 0.0909 x + 0.2709$.

Table S10. Reference data used to construct the correlation between hydrogen bond basicity and electronic energy of dimerization and the resulting estimates of the hydrogen bond basicities of metal oxo complexes

Main Group Y=O or Transition Metal M=O	Calculated Electronic Energy of Dimerization with Water (kcal/mol)	Hydrogen Bond Basicity (Abraham Scale)
Acetone	1.91	0.40 ^a
Methyl Isopropyl Ketone	3.40	0.46 ^a
Benzophenone	3.04	0.46 ^a
Benzaldehyde	1.86	0.42 ^a
Acetophenone	4.44	0.51 ^a
Nitrobenzene	1.90	0.34 ^a
N,N-Dimethyl- ^t Butylamide	2.98	0.70 ^a
Triethyl Phosphine	8.78	1.02 ^a
Dimethyl Sulfoxide	4.67	0.78 ^a
N,N-Dimethyl-Methanesulfinamide	4.25	0.52 ^a
N,N-Dimethyl-Methanesulfonamide	3.65	0.74 ^a
Triphenyl Phosphite	2.81	0.62 ^a
Triphenyl Phosphine	4.37	0.92 ^a
$[\text{Fe}^{\text{IV}}(\text{O})(\text{TMC}, \text{MeCN})]^{2+}$	1.76	0.43 ^d
$[\text{Fe}^{\text{IV}}(\text{O})(\text{TMC}, \text{N}_3)]^+$	3.54 ^b	0.59 ^d
$[\text{Fe}^{\text{IV}}(\text{O})(\text{TMCS})]^+$	4.33	0.66 ^d
$[\text{Mn}^{\text{V}}(\text{O})(\text{tf}_4\text{tmap}, \text{O})]^{3+}$	4.57	0.69 ^d
$[\text{Mn}^{\text{IV}}(\text{O})(\text{tf}_4\text{tmap}, \text{OH})]^{3+}$	6.40	0.85 ^d
$[\text{Mn}^{\text{IV}}(\text{O})(\text{Me}_2\text{EBC}, \text{O})]$	4.41 ^c	0.67 ^d
$[\text{Mn}^{\text{IV}}(\text{O})(\text{N}4\text{Py})]^{2+}$	3.59	0.60 ^d

^aReference 47. ^bThe conditions used in our analysis do not include a protic solvent, but an additional k_2 value is reported which was measured in a protic solvent mixture. ^cThis complex formed two hydrogen bonds upon dimerization, one for each of its oxo ligands and the water molecule's O–H bonds; the value given here is accordingly half the dimerization energy. ^dEstimated from the electronic dimerization energy.

With these estimates of hydrogen bond basicities in hand we were able to apply the formula of Snelgrove et al.⁴² to correct reaction barriers for solvent hydrogen bonding, giving as the overall formula for the reaction barrier:

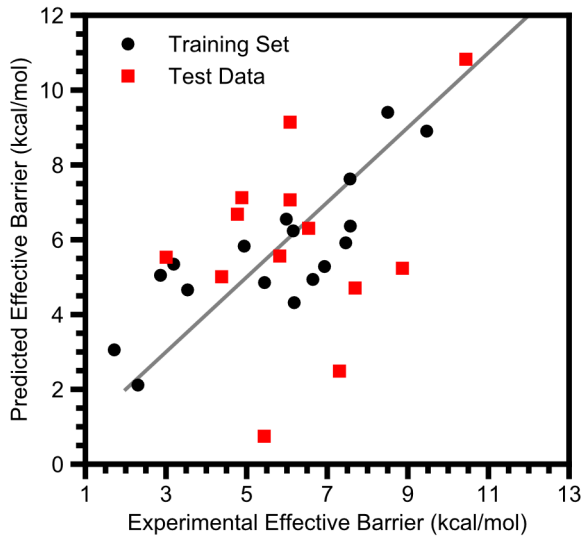
$$\Delta G_{PCET}^\ddagger = RT \ln \left(\frac{k_2 h}{n_{CH} n_O RT} \right) + (T\Delta S_t)_{assoc} - (1.4 \cdot 8.3) \alpha \cdot \beta \quad (\text{S4})$$

where α is the hydrogen bond acidity of the solvent (0 for aprotic solvents), β is this derived hydrogen bond basicity of the metal oxo complex, and 1.4 is the conversion from common logarithm units to kcal/mol at room temperature (we assume there is no temperature dependence of the hydrogen bonding correction). This amounts to a reduction of ~2–3 kcal/mol in the reaction barrier for metal oxo complexes with $\alpha \neq 0$. Using these barriers we repeated the regressions summarized in Table S8, summarizing the new results in Table S11 with a detailed summary of each regression following. These regressions should be viewed as examining how our results are affected by an adjustment for hydrogen bonding, not as tests of distinct hypotheses. While the overall fits are slightly worse, our main result – that only ΔG_{PT} and ΔG_{ET} offer a significant improvement to the ΔG_{PCET} only fit – is unchanged upon this hydrogen bonding adjustment of the reaction barriers. The only notable differences are: (a) cross validation no longer gives evidence for a small, statistically insignificant steric effect, (b) that the Ru^{VI} oxo is not predicted as accurately,²¹ although its prediction is still off by less than 2 kcal/mol, and (c) that the Co^{III} oxo is now an outlier,¹² but not grossly so. Our finding that the same free energies explain the kinetics of the broader set of metal oxo complexes and this Co^{III} oxo complex remains valid.

Table S11. Summary of statistics of regressions with hydrogen bonding corrected DHA data

Parameter(s) Regressed with ΔG_{PCET}	R ²	MSE ^a	LOO ^b R ²	LOO ^b MSE ^a	5-Fold CV ^c MSE ^a	p-value ^d
ΔG_{PCET} only	0.66	1.65	0.59	2.00	2.02	< 0.001 ^f
%BV Steric Metrics	0.68	1.56	0.36	3.11	3.10	0.68
Oxo Spin Density	0.69	1.51	0.59	1.96	1.98	0.27
Spin Excitation	0.66	1.63	0.39	2.93	3.00	0.70
η	0.67	1.60	0.55	2.18	2.15	0.53
ΔG_{PT} , ΔG_{ET}	0.80	0.94	0.71	1.40	1.54	0.027 0.0092 ^g 0.028 ^h
ΔG_{PCET}^2	0.66	1.63	0.53	2.25	2.23	0.69
ΔE_{PCET} only ^e	0.65	1.71	0.57	2.10	2.08	< 0.001 ⁱ
ΔE_{PCET} , ΔE_{PT} , ΔE_{ET} ^e	0.74	1.26	0.59	1.98	2.09	0.13 ^j

^aMean Squared Error, kcal² mol⁻². ^bLeave-One-Out. ^cCross Validation. ^dFrom an F-test where the null hypothesis is that only ΔG_{PCET} has an effect. ^e ΔG_{PCET} not included in the regression. ^fFrom an F-test where the null hypothesis is that ΔG_{PCET} has no effect. ^gFrom an F-test where the null hypothesis is that ΔG_{PT} has no effect. ^hFrom an F-test where the null hypothesis is that ΔG_{ET} has no effect. ⁱFrom an F-test where the null hypothesis is that ΔE_{PCET} has no effect. ^jFrom an F-test where the null hypothesis is that only ΔE_{PCET} has an effect.



Regression S11. H-Bond corrected DHA barriers against ΔG_{PCET} .

['DHA ΔG_{PCET} '] Metrics:

Score on Training Data:	0.6583716699943287
MSE of Training Data:	1.6502710857317893
Score of LOO Cross Validation:	0.5855573288938136
MSE of LOO Cross Validation:	2.0020083135629743
MSE of 5-Fold Cross Validation:	2.0163090946670144 (0.05795110828250081)
F-Test p-value of final 1 variables:	7.702231253337022e-05

Correlation Matrix of x-values:

DHA ΔG_{PCET}	1.0
DHA ΔG_{PCET}	

['DHA ΔG_{PCET} '] Training Average:
[-7.77619718]

['DHA ΔG_{PCET} '] Training Deviation:
[4.05326542]

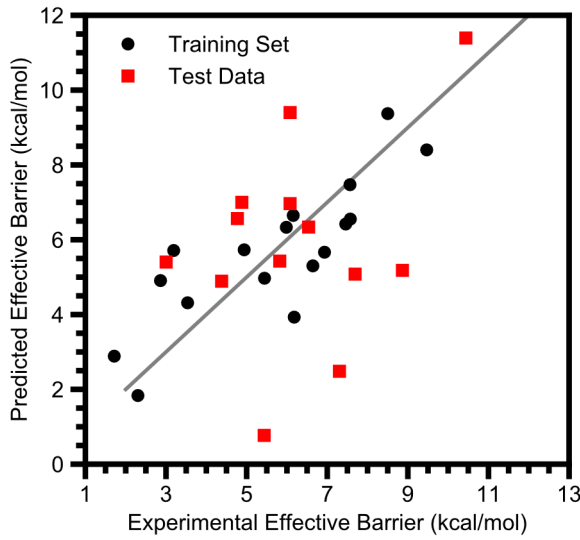
['DHA ΔG_{PCET} '] Coefficients:
[0.43997827]

['DHA ΔG_{PCET} '] Standard Error:
[0.08183272]

['DHA ΔG_{PCET} '] t-Test "Error":
[0.17442231]

['DHA ΔG_{PCET} '] Weighted Coefficients:
[1.78334872]

['DHA ΔG_{PCET} '] Intercept:
9.095284617394316



Regression S12. H-Bond adjusted DHA barriers against ΔG_{PCET} and percent buried volume sterics.

`['DHA ΔG_PCET', '%BV Tot', '%BV Dev'] Metrics:`

Score on Training Data:	0.6780065083153538
MSE of Training Data:	1.555422962469681
Score of LOO Cross Validation:	0.3568563395708818
MSE of LOO Cross Validation:	3.106772165997647
MSE of 5-Fold Cross Validation:	3.0971664143020705 (0.07200841580974428)
F-Test p-value of final 2 variables:	0.6806218722701031

Correlation Matrix of x-values:

	DHA ΔG_PCET	%BV Tot	%BV Dev
DHA ΔG_PCET	1.000000	-0.107404	0.230500
%BV Tot	-0.107404	1.000000	0.134191
%BV Dev	0.230500	0.134191	1.000000

`['DHA ΔG_PCET', '%BV Tot', '%BV Dev'] Training Average:`
`[-7.77619718 64.39411765 5.35367331]`

`['DHA ΔG_PCET', '%BV Tot', '%BV Dev'] Training Deviation:`
`[4.05326542 10.53891783 4.76681449]`

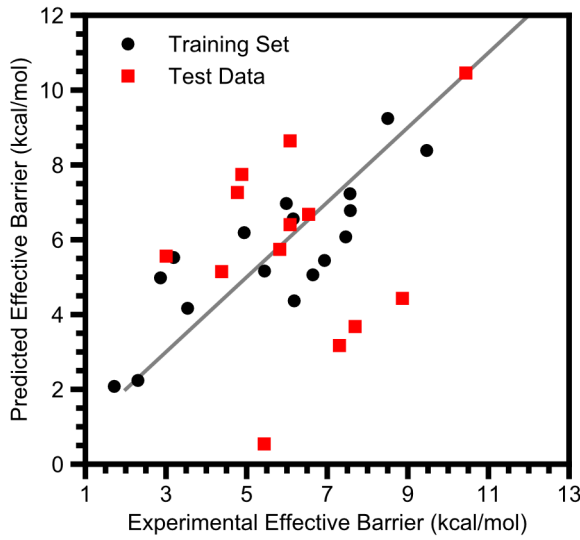
`['DHA ΔG_PCET', '%BV Tot', '%BV Dev'] Coefficients:`
`[0.45769236 0.02716673 -0.03736001]`

`['DHA ΔG_PCET', '%BV Tot', '%BV Dev'] Standard Error:`
`[0.08861722 0.03346711 0.07559991]`

`['DHA ΔG_PCET', '%BV Tot', '%BV Dev'] t-Test "Error":`
`[0.19144586 0.07230129 0.16332368]`

`['DHA ΔG_PCET', '%BV Tot', '%BV Dev'] Weighted Coefficients:`
`[1.85514862 0.28630793 -0.17808825]`

`['DHA ΔG_PCET', '%BV Tot', '%BV Dev'] Intercept:`
`7.683668572672475`



Regression S13. H-Bond adjusted DHA barriers against ΔG_{PCET} and IBO spin density on the oxo ligand.

```
['DHA ΔG_PCET', 'IBO Spin O'] Metrics:
```

Score on Training Data:	0.6880892431477332
MSE of Training Data:	1.5067172659640655
Score of LOO Cross Validation:	0.5948329610682959
MSE of LOO Cross Validation:	1.9572014101683484
MSE of 5-Fold Cross Validation:	1.9794617560199796 (0.05727008301927087)
F-Test p-value of final 1 variables:	0.26745197027806

Correlation Matrix of x-values:

	DHA ΔG_PCET	IBO Spin O
DHA ΔG_PCET	1.000000	-0.346171
IBO Spin O	-0.346171	1.000000

```
['DHA ΔG_PCET', 'IBO Spin O'] Training Average:  
[-7.77619718  0.55994471]
```

```
['DHA ΔG_PCET', 'IBO Spin O'] Training Deviation:  
[4.05326542  0.29315117]
```

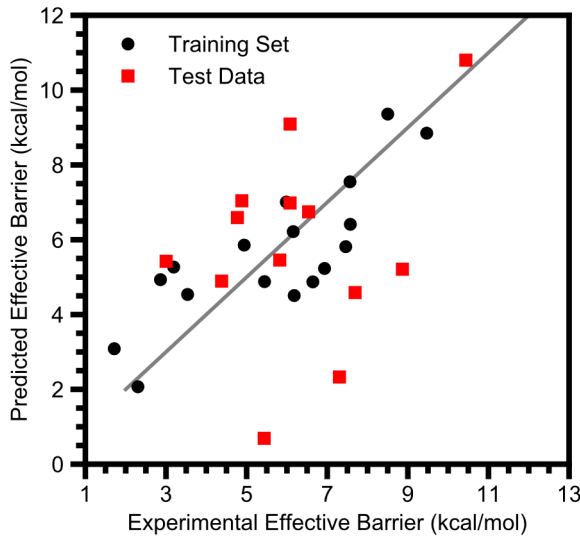
```
['DHA ΔG_PCET', 'IBO Spin O'] Coefficients:  
[0.47446962 1.37763277]
```

```
['DHA ΔG_PCET', 'IBO Spin O'] Standard Error:  
[0.08627094 1.19282835]
```

```
['DHA ΔG_PCET', 'IBO Spin O'] t-Test "Error":  
[0.18503277 2.55836236]
```

```
['DHA ΔG_PCET', 'IBO Spin O'] Weighted Coefficients:  
[1.92315131 0.40385466]
```

```
['DHA ΔG_PCET', 'IBO Spin O'] Intercept:  
8.592097982909333
```



Regression S14. H-Bond adjusted DHA barriers correction against ΔG_{PCET} and the spin excitation energy.

`['DHA ΔG _PCET', 'Spin Excitation'] Metrics:`

Score on Training Data:	0.6622103027351723
MSE of Training Data:	1.6317281720897845
Score of LOO Cross Validation:	0.3927294822859495
MSE of LOO Cross Validation:	2.9334832289354793
MSE of 5-Fold Cross Validation:	3.0032229238497066 (0.09884773576992516)
F-Test p-value of final 1 variables:	0.6960080190817327

`Correlation Matrix of x-values:`

	DHA ΔG _PCET	Spin Excitation
DHA ΔG _PCET	1.00000	-0.20409
Spin Excitation	-0.20409	1.00000

`['DHA ΔG _PCET', 'Spin Excitation'] Training Average:
[-7.77619718 14.58587927]`

`['DHA ΔG _PCET', 'Spin Excitation'] Training Deviation:
[4.05326542 19.10348113]`

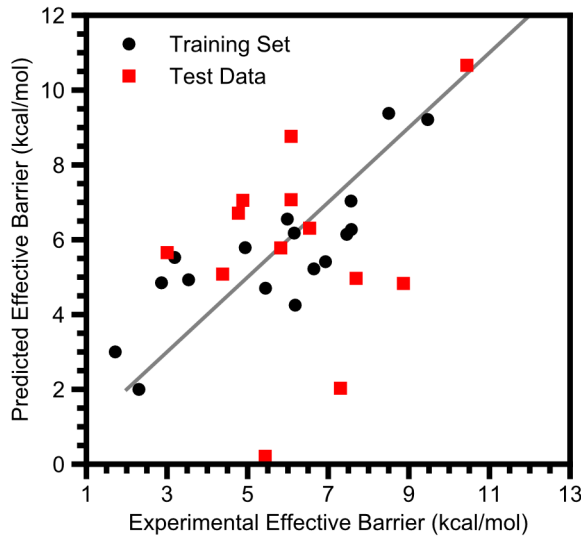
`['DHA ΔG _PCET', 'Spin Excitation'] Coefficients:
[0.44698225 0.0072814]`

`['DHA ΔG _PCET', 'Spin Excitation'] Standard Error:
[0.08603861 0.01825517]`

`['DHA ΔG _PCET', 'Spin Excitation'] t-Test "Error":
[0.18453447 0.03915345]`

`['DHA ΔG _PCET', 'Spin Excitation'] Weighted Coefficients:
[1.81173768 0.13910013]`

`['DHA ΔG _PCET', 'Spin Excitation'] Intercept:
9.043543240499048`



Regression S15. H-Bond adjusted DHA barriers against ΔG_{PCET} and the magnitude of the asynchronicity.

```
['DHA ΔG_PCET', 'DHA |η| (G)'] Metrics:
```

Score on Training Data:	0.6680402250602184
MSE of Training Data:	1.6035661275517157
Score of LOO Cross Validation:	0.5492930546538306
MSE of LOO Cross Validation:	2.1771866520289285
MSE of 5-Fold Cross Validation:	2.149580788555342(0.0830651883177897)
F-Test p-value of final 1 variables:	0.5334165382839267

Correlation Matrix of x-values:

	DHA ΔG_PCET	DHA η (G)
DHA ΔG_PCET	1.000000	0.184231
DHA η (G)	0.184231	1.000000

```
['DHA ΔG_PCET', 'DHA |η| (G)'] Training Average:  
[-7.77619718 17.96727543]
```

```
['DHA ΔG_PCET', 'DHA |η| (G)'] Training Deviation:  
[ 4.05326542 12.92730813]
```

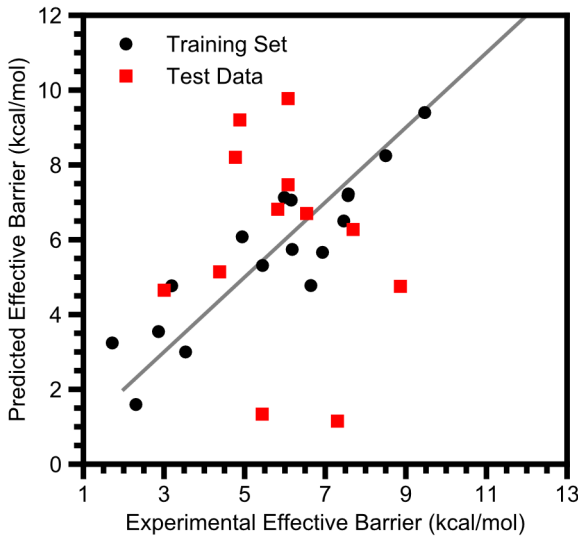
```
['DHA ΔG_PCET', 'DHA |η| (G)'] Coefficients:  
[ 0.4499722 -0.01700872]
```

```
['DHA ΔG_PCET', 'DHA |η| (G)'] Standard Error:  
[ 0.08495179 0.02663603]
```

```
['DHA ΔG_PCET', 'DHA |η| (G)'] t-Test "Error":  
[ 0.18220347 0.0571286 ]
```

```
['DHA ΔG_PCET', 'DHA |η| (G)'] Weighted Coefficients:  
[ 1.82385677 -0.21987692]
```

```
['DHA ΔG_PCET', 'DHA |η| (G)'] Intercept:  
9.478599679619604
```



Regression S16. H-Bond adjusted DHA barriers against ΔG_{PCET} , ΔG_{PT} , and ΔG_{ET} .

`['DHA ΔG_PCET', 'DHA ΔG_PT', 'DHA ΔG_ET'] Metrics:`

```

Score on Training Data:          0.8044848580527584
MSE of Training Data:          0.9444561742667039
Score of LOO Cross Validation: 0.7106357878785099
MSE of LOO Cross Validation:   1.397803842853806
MSE of 5-Fold Cross Validation: 1.5386337886747041 (0.08094085043482879)
F-Test p-value of final 2 variables: 0.026581064997124648
F-Test p-value of 2nd to last variable (DHA ΔG_PT): 0.009188466064706025
F-Test p-value of final variable (DHA ΔG_ET): 0.027671643184978723

```

Correlation Matrix of x-values:

	DHA ΔG_PCET	DHA ΔG_PT	DHA ΔG_ET
DHA ΔG_PCET	1.000000	-0.116636	0.300610
DHA ΔG_PT	-0.116636	1.000000	-0.886456
DHA ΔG_ET	0.300610	-0.886456	1.000000

`['DHA ΔG_PCET', 'DHA ΔG_PT', 'DHA ΔG_ET'] Training Average:`
`[-7.77619718 47.94811989 48.18969167]`

`['DHA ΔG_PCET', 'DHA ΔG_PT', 'DHA ΔG_ET'] Training Deviation:`
`[4.05326542 17.72475347 14.50071323]`

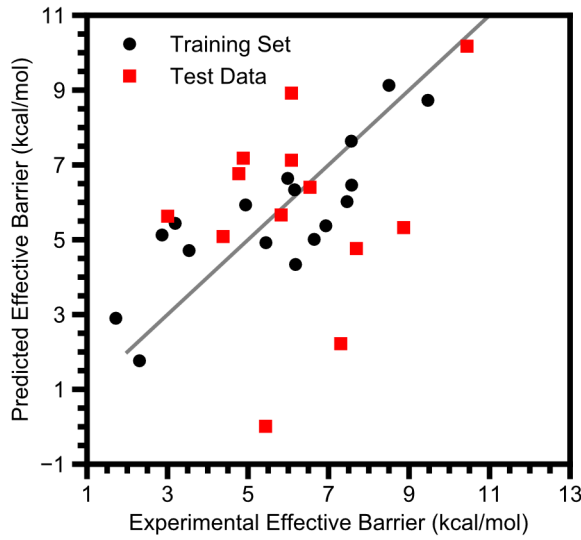
`['DHA ΔG_PCET', 'DHA ΔG_PT', 'DHA ΔG_ET'] Coefficients:`
`[0.37589886 0.10676076 0.11021676]`

`['DHA ΔG_PCET', 'DHA ΔG_PT', 'DHA ΔG_ET'] Standard Error:`
`[0.07412544 0.03493173 0.04446347]`

`['DHA ΔG_PCET', 'DHA ΔG_PT', 'DHA ΔG_ET'] t-Test "Error":`
`[0.16013829 0.07546541 0.09605748]`

`['DHA ΔG_PCET', 'DHA ΔG_PT', 'DHA ΔG_ET'] Weighted Coefficients:`
`[1.52361784 1.89230808 1.59822164]`

`['DHA ΔG_PCET', 'DHA ΔG_PT', 'DHA ΔG_ET'] Intercept:`
`-1.8332987921810613`



Regression S17. H-Bond adjusted DHA barriers against ΔG_{PCET} and ΔG_{PCET}^2 .

```
['DHA ΔG_PCET', 'DHA ΔG_PCET^2'] Metrics:
```

Score on Training Data:	0.6624878412462136
MSE of Training Data:	1.6303874935226972
Score of LOO Cross Validation:	0.5335369455694108
MSE of LOO Cross Validation:	2.2532981713669833
MSE of 5-Fold Cross Validation:	2.232966896805831 (0.07882751337208369)
F-Test p-value of final 1 variables:	0.685715324703223

Correlation Matrix of x-values:

	DHA ΔG_PCET	DHA ΔG_PCET^2
DHA ΔG_PCET	1.000000	-0.929028
DHA ΔG_PCET^2	-0.929028	1.000000

```
['DHA ΔG_PCET', 'DHA ΔG_PCET^2'] Training Average:  
[-7.77619718 76.89820308]
```

```
['DHA ΔG_PCET', 'DHA ΔG_PCET^2'] Training Deviation:  
[ 4.05326542 62.99805804]
```

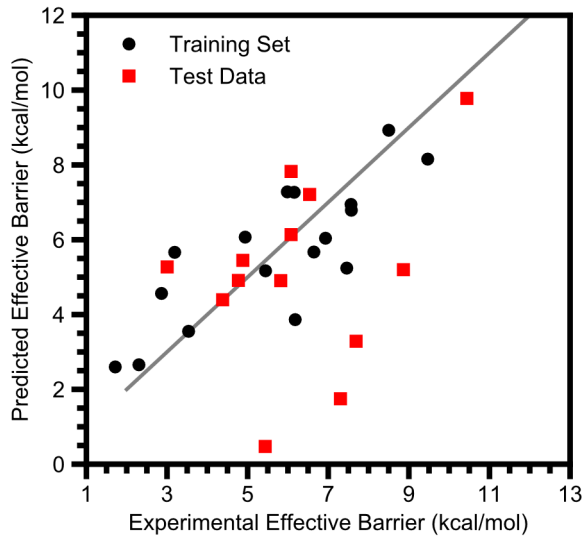
```
['DHA ΔG_PCET', 'DHA ΔG_PCET^2'] Coefficients:  
[ 0.35262908 -0.00604934]
```

```
['DHA ΔG_PCET', 'DHA ΔG_PCET^2'] Standard Error:  
[ 0.22754327 0.01464003]
```

```
['DHA ΔG_PCET', 'DHA ΔG_PCET^2'] t-Test "Error":  
[ 0.48803178 0.03139974]
```

```
['DHA ΔG_PCET', 'DHA ΔG_PCET^2'] Weighted Coefficients:  
[ 1.42929925 -0.38109659]
```

```
['DHA ΔG_PCET', 'DHA ΔG_PCET^2'] Intercept:  
8.881223350642781
```



Regression S18. H-Bond adjusted DHA barriers against ΔE_{PCET} .

['DHA ΔE _PCET'] Metrics:

Score on Training Data:	0.6454910010142754
MSE of Training Data:	1.7124924933718166
Score of LOO Cross Validation:	0.565956327438351
MSE of LOO Cross Validation:	2.0966929843360327
MSE of 5-Fold Cross Validation:	2.0816331006068287 (0.05733164762040685)
F-Test p-value of final 1 variables:	0.00010251166252062127

Correlation Matrix of x-values:

DHA ΔE _PCET	1.0
DHA ΔE _PCET	

['DHA ΔE _PCET'] Training Average:
[-2.08594867]

['DHA ΔE _PCET'] Training Deviation:
[3.99325888]

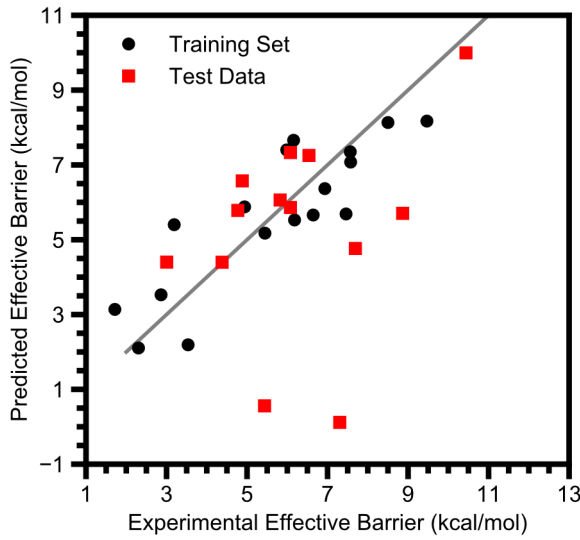
['DHA ΔE _PCET'] Coefficients:
[0.44219959]

['DHA ΔE _PCET'] Standard Error:
[0.08461381]

['DHA ΔE _PCET'] t-Test "Error":
[0.18035006]

['DHA ΔE _PCET'] Weighted Coefficients:
[1.76581744]

['DHA ΔE _PCET'] Intercept:
6.596332462651391



Regression S19. H-Bond adjusted DHA barriers ΔE_{PCET} , ΔE_{PT} , and ΔE_{ET} .

`['DHA ΔE_PCET', 'DHA ΔE_PT', 'DHA ΔE_ET'] Metrics:`

Score on Training Data:	0.7398301329358178
MSE of Training Data:	1.2567775306795423
Score of LOO Cross Validation:	0.5909484679893019
MSE of LOO Cross Validation:	1.975965856930953
MSE of 5-Fold Cross Validation:	2.089103798214306 (0.09558230895231092)
F-Test p-value of final 2 variables:	0.133842257174152

Correlation Matrix of x-values:

	DHA ΔE_PCET	DHA ΔE_PT	DHA ΔE_ET
DHA ΔE_PCET	1.000000	0.093539	0.119751
DHA ΔE_PT	0.093539	1.000000	-0.868929
DHA ΔE_ET	0.119751	-0.868929	1.000000

`['DHA ΔE_PCET', 'DHA ΔE_PT', 'DHA ΔE_ET'] Training Average:`
`[-2.08594867 50.96221826 55.73635424]`

`['DHA ΔE_PCET', 'DHA ΔE_PT', 'DHA ΔE_ET'] Training Deviation:`
`[3.99325888 18.62129223 14.02559969]`

`['DHA ΔE_PCET', 'DHA ΔE_PT', 'DHA ΔE_ET'] Coefficients:`
`[0.36471025 0.07661204 0.10478331]`

`['DHA ΔE_PCET', 'DHA ΔE_PT', 'DHA ΔE_ET'] Standard Error:`
`[0.08565794 0.03684674 0.04905865]`

`['DHA ΔE_PCET', 'DHA ΔE_PT', 'DHA ΔE_ET'] t-Test "Error":`
`[0.18505273 0.07960254 0.10598478]`

`['DHA ΔE_PCET', 'DHA ΔE_PT', 'DHA ΔE_ET'] Weighted Coefficients:`
`[1.45638243 1.42661521 1.46964876]`

`['DHA ΔE_PCET', 'DHA ΔE_PT', 'DHA ΔE_ET'] Intercept:`
`-3.309865589515569`

Further Discussion of Steric Parameters

There is little discussion in the literature about quantitative steric metrics for metal oxo mediated PCET, but in other systems such as asymmetric catalysis the nature of steric parameters is important.⁴⁹ Therefore, in addition to the percent buried volume (%BV) metric discussed in the main text we also determined distance and angle metrics (see Figure S4). These metrics ultimately do not fit the data any better than the %BV metrics.

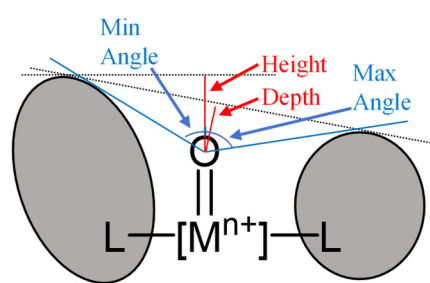


Figure S4. Illustration of distance and angle steric metrics.

Distance metrics were defined as how far from the oxo atom an infinitely wide flat substrate could approach without being encumbered by another atom in the complex. For this determination we used Bondi radii scaled by 1.17 with the Rowland-Taylor radii for hydrogen.^{50,51} The “height” as we defined it is the distance if the substrate is restricted to approaching along the metal-oxygen axis; that is, how much higher than the oxygen atom is there no steric bulk in any direction. The “depth” does not have this directionality restriction; it is the closest a substrate can approach along any direction with no steric encumbrance perpendicular to its approach.

Angle metrics were based on cones with a vertex on the oxo atom and an axis along the M–O bond. We recorded the minimum angle of a cone which touches at least one other atom in the complex (using the same radii as with distance metrics) as well as the maximum angle of a cone in which at least one segment of the surface does not go through another atom.

After collecting these parameters, we analyzed the correlations between them to determine which were statistically distinct (Table S12). There were high correlations among many of them, such that it only took two parameters to convey most of the statistical information contained within this set of parameters. We used %BV sterics as the pair within the main text, for which we observed a small, statistically insignificant improvement to the ΔG_{PCET} fit (which disappears in the H-bonding correction discussed above). In Regression S20 we demonstrate that height and max angle perform worse; unlike %BV sterics, these metrics even behave poorly under cross validation. Overall, while we cannot decisively rule out a small correlation with %BV sterics there is no clear and irrefutable evidence for the influence of sterics on the reaction rates. This is surprising and demonstrates that oxo ligands are in general very unencumbered. However, it is chemically unfathomable that sterics have absolutely no influence on the reaction barrier; thus, the question of whether we observe a small effect or no effect is immaterial. Regardless, within our data set sterics are not as important as free energies in explaining and predicting reaction barriers.

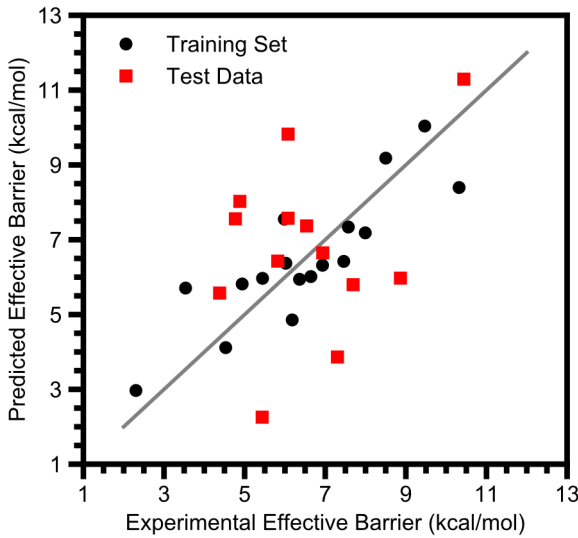
Table S12. Correlations between various steric metrics

	%BV Tot	%BV Dev	Height	Depth	Min Angle	Max Angle
%BV Tot	1	0.14236	0.33877	0.40745	-0.78889	-0.68510
%BV Dev	0.14236	1	0.64977	0.47271	-0.61376	0.01750
Height	0.33877	0.64977	1	0.90480	-0.75467	-0.09366
Depth	0.40745	0.47271	0.90480	1	-0.69931	-0.25180
Min Angle	-0.78889	-0.61376	-0.75467	-0.69931	1	0.41571
Max Angle	-0.68510	0.01750	-0.09366	-0.25180	0.41571	1

Table S13. Steric parameters considered in this study

Oxo	Total %BV	%BV Deviation	Height	Depth	Minimum Angle	Maximum Angle
[Fe ^{IV} (O)(Me ₃ NTB)(MeCN)] ²⁺	66.3	10.4	3.43	2.57	31.0	81.3
[Fe ^{IV} (O)(TMG ₂ dien)(MeCN)] ²⁺	68.0	10.5	3.42	2.84	31.1	86.3
[Fe ^{IV} (O)(TMG ₃ tren)] ²⁺	79.6	3.2	3.40	3.4	29.5	52.1
[Fe ^V (O)(TAML)] ⁻	56.0	7.4	1.80	1.17	49.2	98.7
[Fe ^{IV} (O)(TMC)(MeCN)] ²⁺	74.1	2.0	1.70	1.70	44.8	61.0
[Fe ^{IV} (O)(TMC)(N ₃)] ⁺	74.1	1.9	1.70	1.70	44.7	61.0
[Fe ^{IV} (O)(TMC)(OCOCF ₃)] ⁺	74.2	1.8	1.73	1.73	44.1	61.4
[Fe ^{IV} (O)(TMCS)] ⁺	74.1	2.3	1.75	1.74	42.5	59.2
[Mn ^{IV} (O)(H ₃ buea)] ⁻	72.3	16.0	4.75	3.99	14.7	50.2
[Fe ^{IV} (O)(TMP)]	58.2	9.8	3.74	3.62	42.3	92.9
[Co ^{III} (O)(PhB ^{tBu} Im ₃)]	67.8	8.9	2.75	1.99	40.6	83.1
[Ru ^{IV} (O)(H ⁺ TPA)(bpy)] ³⁺	58.1	5.6	1.49	1.15	52.2	88.5
[Fe ^{IV} (O)(tpfpp)]	52.4	0.15	2.16	2.14	65.3	91.6
[Mn ^{VII} (O) ₄] ⁻	35.2	1.1	0.00	0.00	101.3	101.3
[Mn ^V (O) ₂ (tf ₄ tmap)] ³⁺	55.3	0.43	2.36	2.36	63.3	84.8
[Mn ^{IV} (O)(OH)(tf ₄ tmap)] ³⁺	53.1	0.23	2.24	2.23	64.8	88.9
[Cr ^{IV} (O)(TMC)(Cl)] ⁺	75.0	2.1	1.74	1.74	44.3	59.9
[Ru ^{VI} (O) ₂ (TMC)] ²⁺	73.1	2.0	1.75	1.73	43.8	74.0
[Fe ^{IV} (O)(N4Py)] ²⁺	60.6	9.4	1.40	1.32	55.3	63.5
[Fe ^{IV} (O)(BnTPEN)] ²⁺	69.0	11.5	5.17	2.75	22.4	85.7
[Fe ^{IV} (O)(^{Mc2} TACN-Py ₂)] ²⁺	63.8	4.7	1.26	1.26	61.5	65.9
[Fe ^{IV} (O)(BP1)] ²⁺	65.6	2.0	1.57	1.57	48.5	57.5
[Fe ^{IV} (O)(BP2)] ²⁺	64.5	1.5	1.58	1.51	48.0	70.5
[Ru ^{IV} (O)(bpy) ₂ (py)] ²⁺	58.8	5.5	1.73	1.21	46.2	88.5
[Mn ^{IV} (O) ₂ (Me ₂ EBC)]	62.5	10.2	1.72	1.38	46.6	106.2
[Mn ^{IV} (O)(N4Py)] ²⁺	59.1	4.8	1.35	1.27	57.0	65.7
[Co ^{IV} (O)(13-TMC)] ²⁺	63.3	1.2	1.42	1.35	55.7	94.9
[Fe ^{IV} (O)(13-TMC)] ²⁺	66.7	1.1	1.57	1.49	52.4	92.2
[Ru ^{VI} (O) ₂ (L)] ²⁺	63.7	1.7	1.56	1.54	52.2	86.4
[Ru ^{VI} (O) ₂ (F ₂₈ -tpp)]	54.9	2.6	2.88	2.25	58.9	92.0

^aMultiplicity. ^bEnergy needed to access the lowest spin state of the oxo complex that is one multiplicity away from the multiplicity of the hydroxide; calculated at the ground spin state's optimized geometry.



Regression S20. DHA barriers against ΔG_{PCET} and the height, max angle steric metrics.

```
['DHA ΔG_PCET', 'Height', 'Max Angle'] Metrics:
```

Score on Training Data:	0.7296160767550646
MSE of Training Data:	1.0553654132979189
Score of LOO Cross Validation:	0.4869671105616551
MSE of LOO Cross Validation:	2.0024754463934866
MSE of 5-Fold Cross Validation:	2.343099781826322(0.09930972506610071)
F-Test p-value of final 2 variables:	0.47417271859314414

Correlation Matrix of x-values:

	DHA ΔG_PCET	Height	Max Angle
DHA ΔG_PCET	1.000000	-0.115239	-0.114024
Height	-0.115239	1.000000	-0.138121
Max Angle	-0.114024	-0.138121	1.000000

```
['DHA ΔG_PCET', 'Height', 'Max Angle'] Training Average:  
[-7.77619718 2.35675364 75.05752356]
```

```
['DHA ΔG_PCET', 'Height', 'Max Angle'] Training Deviation:  
[ 4.05326542 1.27930252 17.85106944]
```

```
['DHA ΔG_PCET', 'Height', 'Max Angle'] Coefficients:  
[ 0.39618155 -0.28333271 -0.00072724]
```

```
['DHA ΔG_PCET', 'Height', 'Max Angle'] Standard Error:  
[ 0.07139195 0.22689345 0.0162581 ]
```

```
['DHA ΔG_PCET', 'Height', 'Max Angle'] t-Test "Error":  
[ 0.15423294 0.4901735 0.03512348]
```

```
['DHA ΔG_PCET', 'Height', 'Max Angle'] Weighted Coefficients:  
[ 1.60582897 -0.36246825 -0.01298204]
```

```
['DHA ΔG_PCET', 'Height', 'Max Angle'] Intercept:  
10.28517288957433
```

Attempts to Determine Reorganization Parameters

A common theme in chemistry is that reaction barriers are in large part determined by the reorganization energy needed to deform to the transition state geometry without accounting for interaction between reactants; PCET chemistry is no exception to this. In one case, the deformation energy needed to reach a transition state geometry has been shown to correlate well with computed reaction barriers;⁵² in another case, the reorganization energy was the primary factor differentiating the reactivity between a Ru^{IV} oxo and a V^V oxo.⁵³ In light of both these studies and our hypothesis that anomalously low reorganization energies could contribute to the overestimation of Ru^{IV} oxo reaction barriers^{14,25} we have made several attempts to quantify reorganization and fit it to the data. Ultimately, no parameter examined demonstrated a significant effect.

The classical definition of reorganization energy is the energy needed to deform the products into the reactant geometry, or vice-versa, without the reaction actually occurring.^{54,55} We calculated a reorganization energy for the oxo complexes in just this manner, removing the hydroxide hydrogen from our optimized metal hydroxide structures and determining the energy of the metal oxo species at the resultant geometry (with the same level of theory as described in the main text). Wherever relevant, we checked multiple spin-states at this geometry and used the lowest energy obtained, regardless of the ground spin-state of the oxo. We performed a similar calculation for metal hydroxides by constraining the cartesian position of all oxo atoms and optimizing a hydrogen atom on top of this structure.

As alternative measurements of distortions, we used the predominant M–O stretching frequency in both the metal hydroxide and metal oxo complexes to determine the energies of stretching or compressing this specific bond into the other structure. The result heavily correlated with the change in the M–O bond distance, indicating similar information could be obtained without incorporating the vibrational frequency. Therefore, because mixing with other ligand vibrational modes made finding “stretching energies” for the non-oxo M–L bonds infeasible we instead tabulated the total change in M–L bond lengths.

The results of regressions with these parameters are given in Table S14. While the stretching energies and change in bond lengths offer some improvement to the fit, cross validation indicates this is mere overfitting and none of these regressions are statistically significant. Similarly, regressions along with the asynchronicity parameter (which is thought to work in concert with reorganization energy⁵⁶) do not provide a significant improvement.

Table S14. Summary of statistics on regressions with measures of deformation energy

Parameter(s) Regressed with ΔG_{PCET}	R ²	MSE ^a	LOO ^b R ²	LOO ^b MSE ^a	5-Fold CV ^c MSE ^a	p-value ^d
ΔG_{PCET} only	0.70	1.18	0.60	1.57	1.49	< 0.001 ^e
Reorganization Energies	0.70	1.18	0.44	2.18	2.20	0.96
Stretching Energies	0.74	1.00	0.46	2.09	2.27	0.34
Bond Length Changes	0.75	0.97	0.47	2.07	2.01	0.27
Reorganization Energies, $ \eta $	0.75	0.97	0.48	2.03	2.12	0.48
Stretching Energies, $ \eta $	0.78	0.87	0.43	2.21	2.50	0.27
Bond Length Changes, $ \eta $	0.78	0.88	0.47	2.08	2.36	0.29

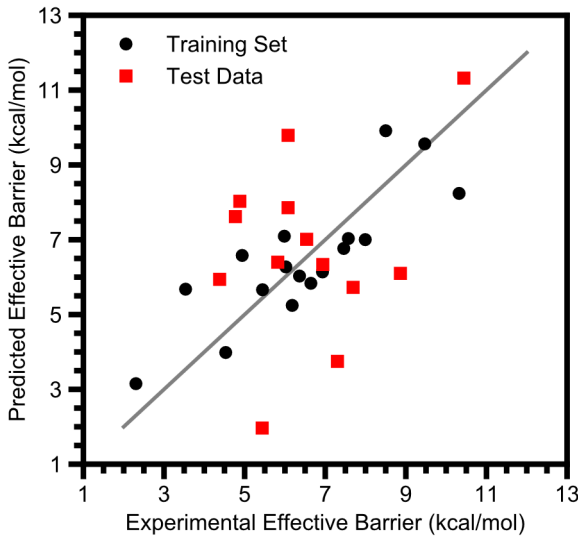
^aMean Squared Error, kcal² mol⁻². ^bLeave-One-Out. ^cCross Validation. ^dFrom an F-test where the null hypothesis is that only ΔG_{PCET} has an effect. ^eFrom an F-test where the null hypothesis is that ΔG_{PCET} has no effect.

Table S15. Reorganization parameters considered in this study

Oxo	Oxo Reorg ^a	Hydroxide Reorg ^a	Oxo Stretch ^b	Hydroxide Stretch ^b	M–O ΔLength ^c	ΣM–L ΔLength ^c
[Fe ^{IV} (O)(Me ₃ NTB)(MeCN)] ²⁺	23.1	35.5	42.5	21.4	0.19	0.92
[Fe ^{IV} (O)(TMG ₂ dien)(MeCN)] ²⁺	17.8	17.1	45.5	22.3	0.20	0.33
[Fe ^{IV} (O)(TMG ₃ tren)] ²⁺	18.5	16.1	50.8	23.3	0.21	0.33
[Fe ^V (O)(TAML)] ⁻	13.6	15.7	48.2	21.4	0.20	0.0092
[Fe ^{IV} (O)(TMC)(MeCN)] ²⁺	21.0	22.7	41.8	20.0	0.19	0.58
[Fe ^{IV} (O)(TMC)(N ₃)] ⁺	19.5	22.1	62.3	25.7	0.24	0.512
[Fe ^{IV} (O)(TMC)(OCOCF ₃)] ⁺	20.1	23.3	59.6	25.0	0.23	0.47
[Fe ^{IV} (O)(TMCS)] ⁺	15.1	19.8	57.3	17.7	0.24	0.56
[Mn ^{IV} (O)(H ₃ buea)] ⁻	20.8	21.2	37.1	16.0	0.21	0.20
[Fe ^{IV} (O)(TMP)]	20.7	23.8	64.2	24.0	0.23	0.44
[Co ^{III} (O)(PhB <i>t</i> BuIm ₃)]	20.9	19.6	43.1	17.7	0.22	0.38
[Ru ^{IV} (O)(H ⁺ TPA)(bpy)] ³⁺	8.5	8.6	24.5	13.7	0.16	-0.13
[Fe ^{IV} (O)(tpfpp)]	21.0	19.5	87.5	28.8	0.27	0.045
[Mn ^{VII} (O) ₄] ⁻	14.7	13.0	43.4	21.0	0.18	0.025
[Mn ^V (O) ₂ (tf ₄ tmap)] ³⁺	29.3	22.1	116.9	32.4	0.33	0.023
[Mn ^{IV} (O)(OH)(tf ₄ tmap)] ³⁺	14.7	13.4	30.4	14.8	0.18	0.19
[Cr ^{IV} (O)(TMC)(Cl)] ⁺	12.9	17.4	61.9	26.7	0.25	0.0060
[Ru ^{VI} (O) ₂ (TMC)] ²⁺	14.6	13.9	43.9	20.5	0.19	-0.032
[Fe ^{IV} (O)(N4Py)] ²⁺	34.7	28.4	37.0	20.0	0.18	0.93
[Fe ^{IV} (O)(BnTPEN)] ²⁺	24.4	24.6	39.9	20.5	0.19	0.89
[Fe ^{IV} (O)(^{Me2} TACN-Py ₂)] ²⁺	23.6	28.5	30.3	16.8	0.16	0.89
[Fe ^{IV} (O)(BP1)] ²⁺	26.2	28.7	33.8	18.6	0.17	0.89
[Fe ^{IV} (O)(BP2)] ²⁺	24.1	31.9	42.0	21.5	0.19	0.86
[Ru ^{IV} (O)(bpy) ₂ (py)] ²⁺	8.9	8.6	25.8	13.8	0.16	-0.13
[Mn ^{IV} (O) ₂ (Me ₂ EBC)]	22.8	26.2	62.6	21.2	0.25	0.20
[Mn ^{IV} (O)(N4Py)] ²⁺	22.9	21.5	22.6	11.9	0.14	0.63
[Co ^{IV} (O)(13-TMC)] ²⁺	10.1	11.6	5.7	4.8	0.084	0.41
[Fe ^{IV} (O)(13-TMC)] ²⁺	20.9	25.1	50.6	25.4	0.19	0.57
[Ru ^{VI} (O) ₂ (L)] ²⁺	13.9	13.3	44.1	21.3	0.19	-0.033
[Ru ^{VI} (O) ₂ (F ₂₈ -tpp)]	15.9	14.8	50.4	21.3	0.22	-0.032

^aReorganization; i.e. energy of the oxo at the hydroxide geometry or vice versa (kcal/mol). The position of the transferring H-atom was optimized for the hydroxide reorganization. ^bEnergy needed to distort the metal–oxygen bond of the oxo complex to its length in the hydroxide, or vice versa (kcal/mol); determined from frequency calculations.

^cThe change in the length of the metal–oxygen bond between the oxo complex and the hydroxide complex (Å). ^cThe sum of the change in the lengths of all metal–ligand bonds besides the metal–oxygen bond between the oxo complex and the hydroxide complex (Å).



Regression S21. DHA barriers against ΔG_{PCET} and the oxo reorganization energy.

`['DHA ΔG_PCET', 'Oxo λ', 'Hydroxide λ'] Metrics:`

Score on Training Data:	0.6985337405659753
MSE of Training Data:	1.1766863194552986
Score of LOO Cross Validation:	0.4413190508659992
MSE of LOO Cross Validation:	2.1806494399090437
MSE of 5-Fold Cross Validation:	2.1995049703717857 (0.06742190086236298)
F-Test p-value of final 2 variables:	0.9618615594550874

`Correlation Matrix of x-values:`

	DHA ΔG_PCET	Oxo λ	Hydroxide λ
DHA ΔG_PCET	1.000000	-0.113949	-0.336879
Oxo λ	-0.113949	1.000000	0.685471
Hydroxide λ	-0.336879	0.685471	1.000000

`['DHA ΔG_PCET', 'Oxo λ', 'Hydroxide λ'] Training Average:
[-7.77619718 21.37229441 22.86499201]`

`['DHA ΔG_PCET', 'Oxo λ', 'Hydroxide λ'] Training Deviation:
[4.05326542 5.37099513 6.03190216]`

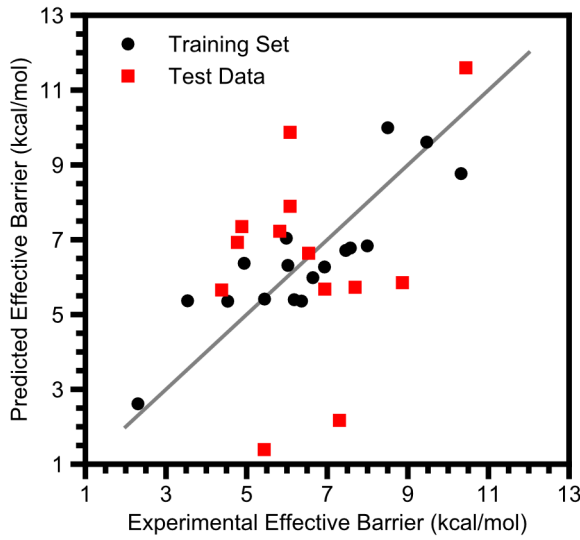
`['DHA ΔG_PCET', 'Oxo λ', 'Hydroxide λ'] Coefficients:
[0.40306166 -0.0127441 -0.00372249]`

`['DHA ΔG_PCET', 'Oxo λ', 'Hydroxide λ'] Standard Error:
[0.08000681 0.07807801 0.07335822]`

`['DHA ΔG_PCET', 'Oxo λ', 'Hydroxide λ'] t-Test "Error":
[0.17284421 0.16867729 0.1584808]`

`['DHA ΔG_PCET', 'Oxo λ', 'Hydroxide λ'] Weighted Coefficients:
[1.6337159 -0.06844851 -0.0224537]`

`['DHA ΔG_PCET', 'Oxo λ', 'Hydroxide λ'] Intercept:
9.973829077770457`



Regression S22. DHA barriers against ΔG_{PCET} and stretching energies of M–O(H) bonds.

`['DHA ΔG_PCET', 'Oxo Stretch', 'Hydroxide Stretch'] Metrics:`

Score on Training Data:	0.7429488443721649
MSE of Training Data:	1.0033248125190048
Score of LOO Cross Validation:	0.46372208300228446
MSE of LOO Cross Validation:	2.09320568590959
MSE of 5-Fold Cross Validation:	2.266485644527874(0.09874421962655447)
F-Test p-value of final 2 variables:	0.34134070652340187

`Correlation Matrix of x-values:`

	DHA ΔG_PCET	Oxo Stretch	Hydroxide Stretch
DHA ΔG_PCET	1.000000	-0.399234	-0.481905
Oxo Stretch	-0.399234	1.000000	0.865424
Hydroxide Stretch	-0.481905	0.865424	1.000000

`['DHA ΔG_PCET', 'Oxo Stretch', 'Hydroxide Stretch'] Training Average:
[-7.77619718 51.16490969 21.37839275]`

`['DHA ΔG_PCET', 'Oxo Stretch', 'Hydroxide Stretch'] Training Deviation:
[4.05326542 19.44134649 3.86935373]`

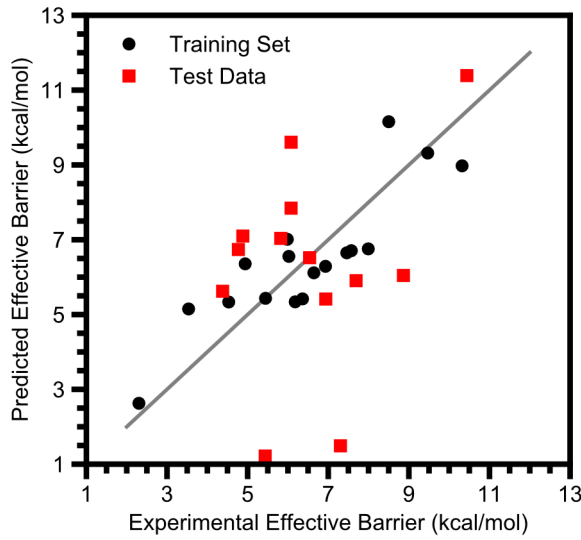
`['DHA ΔG_PCET', 'Oxo Stretch', 'Hydroxide Stretch'] Coefficients:
[0.45176185 0.02455864 -0.00460389]`

`['DHA ΔG_PCET', 'Oxo Stretch', 'Hydroxide Stretch'] Standard Error:
[0.07828656 0.02854359 0.15006501]`

`['DHA ΔG_PCET', 'Oxo Stretch', 'Hydroxide Stretch'] t-Test "Error":
[0.16912782 0.06166468 0.32419574]`

`['DHA ΔG_PCET', 'Oxo Stretch', 'Hydroxide Stretch'] Weighted Coefficients:
[1.83111067 0.47745294 -0.01781408]`

`['DHA ΔG_PCET', 'Oxo Stretch', 'Hydroxide Stretch'] Intercept:
8.836929319321026`



Regression S23. DHA barriers against ΔG_{PCET} and change in metal–ligand bond lengths.

```
['DHA ΔG_PCET', 'ΔLength M-O', 'Total ΔLength M-L'] Metrics:
```

Score on Training Data:	0.751448256020735
MSE of Training Data:	0.9701498183121323
Score of LOO Cross Validation:	0.46889535893792444
MSE of LOO Cross Validation:	2.073013300096122
MSE of 5-Fold Cross Validation:	2.0136398644927245 (0.07838159315728596)
F-Test p-value of final 2 variables:	0.27432806144440447

Correlation Matrix of x-values:

	DHA ΔG_PCET	ΔLength M-O	Total ΔLength M-L
DHA ΔG_PCET	1.000000	-0.308863	-0.233562
ΔLength M-O	-0.308863	1.000000	-0.440362
Total ΔLength M-L	-0.233562	-0.440362	1.000000

```
['DHA ΔG_PCET', 'ΔLength M-O', 'Total ΔLength M-L'] Training Average:  
[-7.77619718 0.2135339 0.47312783]
```

```
['DHA ΔG_PCET', 'ΔLength M-O', 'Total ΔLength M-L'] Training Deviation:  
[4.05326542 0.03836354 0.32487374]
```

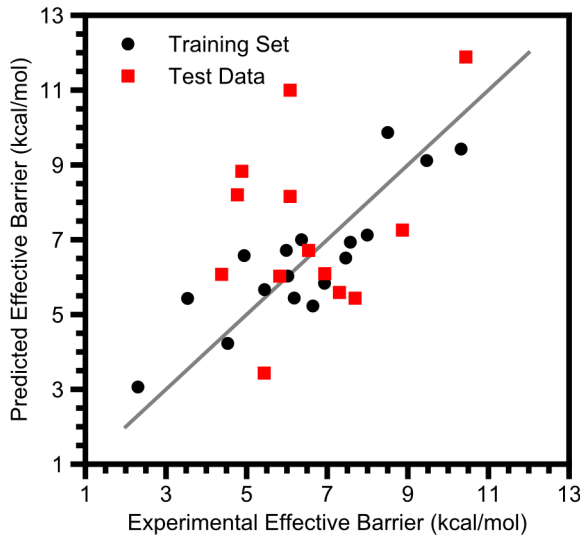
```
['DHA ΔG_PCET', 'ΔLength M-O', 'Total ΔLength M-L'] Coefficients:  
[ 0.44882346 13.36221923 0.15539224]
```

```
['DHA ΔG_PCET', 'ΔLength M-O', 'Total ΔLength M-L'] Standard Error:  
[0.07860524 8.99430283 1.03891916]
```

```
['DHA ΔG_PCET', 'ΔLength M-O', 'Total ΔLength M-L'] t-Test "Error":  
[ 0.1698163 19.43100991 2.24444839]
```

```
['DHA ΔG_PCET', 'ΔLength M-O', 'Total ΔLength M-L'] Weighted Coefficients:  
[1.8192006 0.51262207 0.05048286]
```

```
['DHA ΔG_PCET', 'ΔLength M-O', 'Total ΔLength M-L'] Intercept:  
7.045389227464227
```



Regression S24. DHA barriers against ΔG_{PCET} , reorganization, and the magnitude of the asynchronicity.

`['DHA ΔG_PCET', 'Oxo λ', 'Hydroxide λ', 'DHA |η| (G)'] Metrics:`

Score on Training Data:	0.7508389994578081
MSE of Training Data:	0.9725278750272693
Score of LOO Cross Validation:	0.47878455120218033
MSE of LOO Cross Validation:	2.034413699365813
MSE of 5-Fold Cross Validation:	2.1242747875853207 (0.07222199871900489)
F-Test p-value of final 3 variables:	0.48404896214361404

Correlation Matrix of x-values:

	DHA ΔG_PCET	Oxo λ	Hydroxide λ	DHA η (G)
DHA ΔG_PCET	1.000000	-0.113949	-0.336879	0.184231
Oxo λ	-0.113949	1.000000	0.685471	0.360767
Hydroxide λ	-0.336879	0.685471	1.000000	0.411410
DHA η (G)	0.184231	0.360767	0.411410	1.000000

`['DHA ΔG_PCET', 'Oxo λ', 'Hydroxide λ', 'DHA |η| (G)'] Training Average:`

`[-7.77619718 21.37229441 22.86499201 17.96727543]`

`['DHA ΔG_PCET', 'Oxo λ', 'Hydroxide λ', 'DHA |η| (G)'] Training Deviation:`

`[4.05326542 5.37099513 6.03190216 12.92730813]`

`['DHA ΔG_PCET', 'Oxo λ', 'Hydroxide λ', 'DHA |η| (G)'] Coefficients:`

`[0.35613308 -0.01975543 -0.04662405 0.04146195]`

`['DHA ΔG_PCET', 'Oxo λ', 'Hydroxide λ', 'DHA |η| (G)'] Standard Error:`

`[0.08127479 0.07401256 0.0744917 0.02612321]`

`['DHA ΔG_PCET', 'Oxo λ', 'Hydroxide λ', 'DHA |η| (G)'] t-Test "Error":`

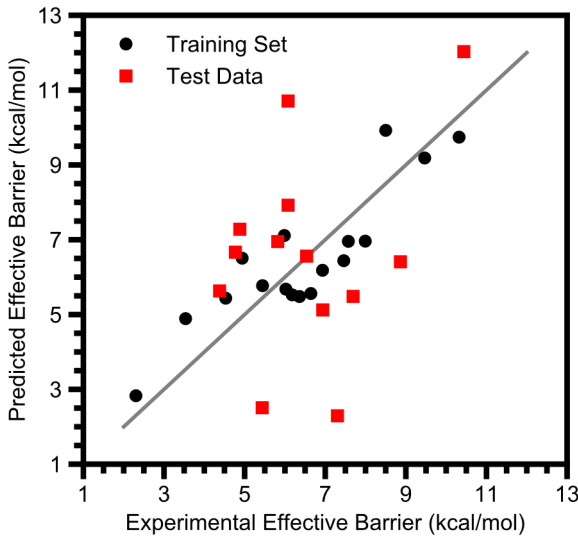
`[0.17708255 0.16125951 0.16230347 0.05691758]`

`['DHA ΔG_PCET', 'Oxo λ', 'Hydroxide λ', 'DHA |η| (G)'] Weighted Coefficients:`

`[1.44350191 -0.10610634 -0.28123169 0.53599146]`

`['DHA ΔG_PCET', 'Oxo λ', 'Hydroxide λ', 'DHA |η| (G)'] Intercept:`

`9.994736811747302`



Regression S25. DHA barriers against ΔG_{PCET} , stretching energies, and the magnitude of the asynchronicity.

```
['DHA ΔG_PCET', 'Oxo Stretch', 'Hydroxide Stretch', 'DHA |η| (G)'] Metrics:
```

Score on Training Data:	0.7778036840135025
MSE of Training Data:	0.8672790306468683
Score of LOO Cross Validation:	0.4336095053173339
MSE of LOO Cross Validation:	2.2107414203295503
MSE of 5-Fold Cross Validation:	2.4951787280872217 (0.09740659325306181)
F-Test p-value of final 3 variables:	0.27479651348982703

Correlation Matrix of x-values:

	DHA ΔG_PCET	Oxo Stretch	Hydroxide Stretch	DHA η (G)
DHA ΔG_PCET	1.000000	-0.399234	-0.481905	0.184231
Oxo Stretch	-0.399234	1.000000	0.865424	-0.078940
Hydroxide Stretch	-0.481905	0.865424	1.000000	-0.241536
DHA η (G)	0.184231	-0.078940	-0.241536	1.000000

```
['DHA ΔG_PCET', 'Oxo Stretch', 'Hydroxide Stretch', 'DHA |η| (G)'] Training Average:  
[-7.77619718 51.16490969 21.37839275 17.96727543]
```

```
['DHA ΔG_PCET', 'Oxo Stretch', 'Hydroxide Stretch', 'DHA |η| (G)'] Training Deviation:  
[ 4.05326542 19.44134649 3.86935373 12.92730813]
```

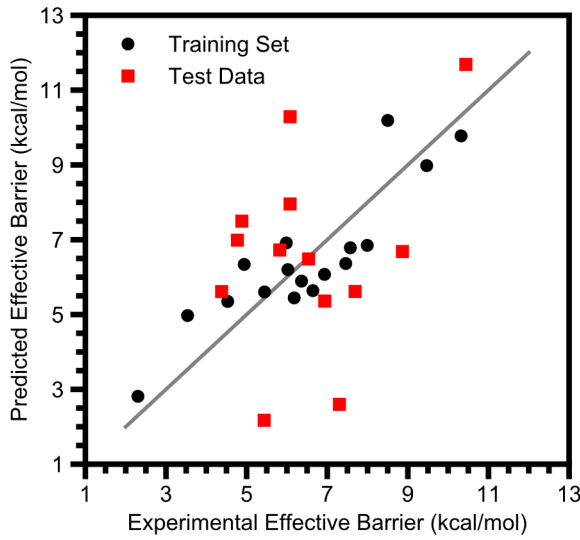
```
['DHA ΔG_PCET', 'Oxo Stretch', 'Hydroxide Stretch', 'DHA |η| (G)'] Coefficients:  
[0.44430222 0.01412713 0.0616774 0.03059378]
```

```
['DHA ΔG_PCET', 'Oxo Stretch', 'Hydroxide Stretch', 'DHA |η| (G)'] Standard Error:  
[0.07595257 0.02864889 0.15304247 0.02229869]
```

```
['DHA ΔG_PCET', 'Oxo Stretch', 'Hydroxide Stretch', 'DHA |η| (G)'] t-Test "Error":  
[0.16548644 0.06242056 0.3334509 0.04858468]
```

```
['DHA ΔG_PCET', 'Oxo Stretch', 'Hydroxide Stretch', 'DHA |η| (G)'] Weighted Coefficients:  
[1.80087482 0.27465053 0.23865166 0.39549526]
```

```
['DHA ΔG_PCET', 'Oxo Stretch', 'Hydroxide Stretch', 'DHA |η| (G)'] Intercept:  
7.3459742258465806
```



Regression S26. DHA barriers against ΔG_{PCET} , bond length changes, and the magnitude of the asynchronicity.

```
['DHA ΔG_PCET', 'ΔLength M-O', 'Total ΔLength M-L', 'DHA |η| (G)'] Metrics:
```

Score on Training Data:	0.7754144322642288
MSE of Training Data:	0.8766047835599248
Score of LOO Cross Validation:	0.4683307976976163
MSE of LOO Cross Validation:	2.075216901551265
MSE of 5-Fold Cross Validation:	2.361928941102483(0.0997562689075115)
F-Test p-value of final 3 variables:	0.29022403136241515

Correlation Matrix of x-values:

	DHA ΔG_PCET	ΔLength M-O	Total ΔLength M-L	DHA η (G)
DHA ΔG_PCET	1.000000	-0.308863	-0.233562	0.184231
ΔLength M-O	-0.308863	1.000000	-0.440362	0.036738
Total ΔLength M-L	-0.233562	-0.440362	1.000000	0.117113
DHA η (G)	0.184231	0.036738	0.117113	1.000000

```
['DHA ΔG_PCET', 'ΔLength M-O', 'Total ΔLength M-L', 'DHA |η| (G)'] Training Average:  
[-7.77619718 0.2135339 0.47312783 17.96727543]
```

```
['DHA ΔG_PCET', 'ΔLength M-O', 'Total ΔLength M-L', 'DHA |η| (G)'] Training Deviation:  
[ 4.05326542 0.03836354 0.32487374 12.92730813]
```

```
['DHA ΔG_PCET', 'ΔLength M-O', 'Total ΔLength M-L', 'DHA |η| (G)'] Coefficients:  
[ 0.42084833 10.92517568 -0.16992622 0.02512143]
```

```
['DHA ΔG_PCET', 'ΔLength M-O', 'Total ΔLength M-L', 'DHA |η| (G)'] Standard Error:  
[ 0.08160516 9.15568025 1.0673317 0.0221996 ]
```

```
['DHA ΔG_PCET', 'ΔLength M-O', 'Total ΔLength M-L', 'DHA |η| (G)'] t-Test "Error":  
[ 0.17780238 19.94851359 2.325516 0.04836878]
```

```
['DHA ΔG_PCET', 'ΔLength M-O', 'Total ΔLength M-L', 'DHA |η| (G)'] Weighted Coefficients:  
[ 1.70581 0.41912845 -0.05520457 0.32475242]
```

```
['DHA ΔG_PCET', 'ΔLength M-O', 'Total ΔLength M-L', 'DHA |η| (G)'] Intercept:  
7.050794199068996
```

Robustness of Results to Computational Methodology

Calculated free energies of reactions for transition metal complexes can depend greatly on the DFT functional used. This is particularly true for reactions which involve a transition from low-spin reactants to high-spin products, as is the case here.^{45,57} To confirm that our results are not an artifact of our computational methodology we recalculated the electronic energies with different computational methods at the O3LYP optimized geometries. These alternate methods were the B3LYP functional, the M06L functional, and O3LYP with the zeroth order regular approximation (ZORA) scalar relativistic correction. Importantly, the functionals tested incorporate varying amounts of Hartree Fock Exchange. Because M06L and ZORA are relatively sensitive to the integration grid used (per the ORCA manual),^{58,59} we used a finer integration grid than in our other calculations (Grid7/FinalGrid7, the finest grid setting available) and recalculated the O3LYP energies at this finer grid for comparison. As shown in Table S16 and the following regressions, we find ΔE_{PT} and ΔE_{ET} have significant contributions to reaction barriers regardless of the computational method used to calculate them.

Table S16. Summary of statistics on regressions with different computational methodology

Method	Parameter(s)	R ²	MSE ^a	LOO ^b R ²	LOO ^b MSE ^a	5-Fold CV ^c MSE ^a	p-value
O3LYP	ΔE_{PCET}	0.62	1.46	0.52	1.89	1.90	< 0.001 ^d
	$\Delta E_{\text{PCET}}, \Delta E_{\text{PT}}, \Delta E_{\text{ET}}$	0.87	0.52	0.76	0.95	1.15	0.001 ^e
B3LYP	ΔE_{PCET}	0.72	1.10	0.58	1.66	1.70	< 0.001 ^d
	$\Delta E_{\text{PCET}}, \Delta E_{\text{PT}}, \Delta E_{\text{ET}}$	0.88	0.47	0.76	0.95	1.24	0.004 ^e
M06L	ΔE_{PCET}	0.65	1.37	0.54	1.81	1.94	< 0.001 ^d
	$\Delta E_{\text{PCET}}, \Delta E_{\text{PT}}, \Delta E_{\text{ET}}$	0.85	0.58	0.71	1.14	1.46	0.004 ^e
O3LYP-	ΔE_{PCET}	0.58	1.62	0.46	2.10	2.10	< 0.001 ^d
ZORA	$\Delta E_{\text{PCET}}, \Delta E_{\text{PT}}, \Delta E_{\text{ET}}$	0.85	0.59	0.75	0.99	1.21	0.001 ^e

^aMean Squared Error, kcal² mol⁻². ^bLeave-One-Out. ^cCross Validation. ^dFrom an F-test where the null hypothesis is that ΔG_{PCET} has no effect. ^eFrom an F-test where the null hypothesis is that ΔG_{PT} and ΔG_{ET} have no effect.

Table S17. ΔE_{PCET} computed with different computational methodologies

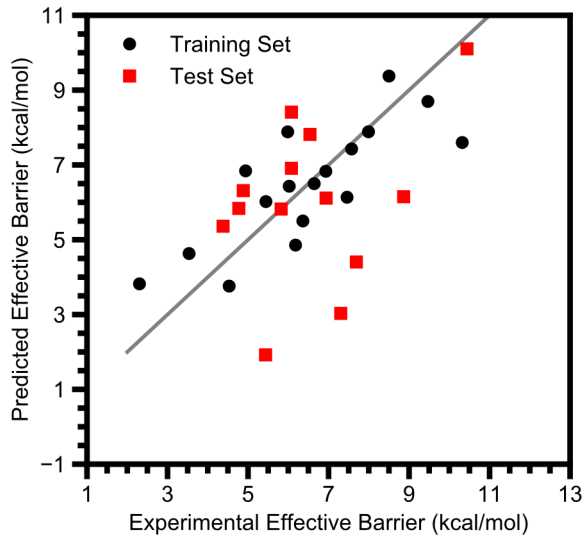
Oxo	O3LYP ΔE_{PCET}	B3LYP ΔE_{PCET}	M06L ΔE_{PCET}	O3LYP-ZORA ΔE_{PCET}
[Fe ^{IV} (O)(Me ₃ NTB)(MeCN)] ²⁺	-9.0	-17.9	-15.7	-6.3
[Fe ^{IV} (O)(TMG ₂ dien)(MeCN)] ²⁺	-5.0	-12.0	-7.9	-3.3
[Fe ^{IV} (O)(TMG ₃ tren)] ²⁺	-3.0	-10.0	-5.7	-1.4
[Fe ^V (O)(TAML)] ⁻	-6.9	-14.2	-6.6	-5.2
[Fe ^{IV} (O)(TMC)(MeCN)] ²⁺	1.4	-6.9	-2.2	3.3
[Fe ^{IV} (O)(TMC)(N ₃)] ⁺	-2.1	-9.9	-5.2	-0.24
[Fe ^{IV} (O)(TMC)(OCOCF ₃)] ⁺	-1.3	-9.0	-4.3	0.18
[Fe ^{IV} (O)(TMCS)] ⁺	-2.3	-10.2	-5.8	-0.67
[Mn ^{IV} (O)(H ₃ buea)] ⁻	5.2	-1.6	1.8	6.9
[Fe ^{IV} (O)(TMP)]	-6.3	-13.7	-14.1	-4.4
[Co ^{III} (O)(PhB ^{tBu} Im ₃)]	-3.0	-17.6	-6.0	0.41
[Ru ^{IV} (O)(H ⁺ TPA)(bpy)] ³⁺	-2.6	-4.1	-1.7	-3.3
[Fe ^{IV} (O)(tpfpp)]	-3.8	-10.6	-3.1	-2.3
[Mn ^{VII} (O) ₄] ⁻	3.5	-5.5	8.2	5.6
[Mn ^V (O) ₂ (tf ₄ tmap)] ³⁺	-9.1	-19.6	-14.6	-7.0
[Mn ^{IV} (O)(OH)(tf ₄ tmap)] ³⁺	-4.7	-9.6	-5.6	-1.8
[Cr ^{IV} (O)(TMC)(Cl)] ⁺	-7.5	-14.0	-10.2	-5.9
[Ru ^{VI} (O) ₂ (TMC)] ²⁺	7.1	0.88	7.4	5.6
[Fe ^{IV} (O)(N4Py)] ²⁺	1.4	-9.2	-6.4	4.3
[Fe ^{IV} (O)(BnTPEN)] ²⁺	-1.2	-10.9	-7.1	1.2
[Fe ^{IV} (O)(^{Me₂} TACN-Py ₂)] ²⁺	1.3	-8.0	-4.9	3.7
[Fe ^{IV} (O)(BP1)] ²⁺	0.26	-9.8	-7.2	2.9
[Fe ^{IV} (O)(BP2)] ²⁺	-3.3	-12.5	-10.9	-0.71
[Ru ^{IV} (O)(bpy) ₂ (py)] ²⁺	-3.8	-5.1	-2.7	-4.6
[Mn ^{IV} (O) ₂ (Me ₂ EBC)]	0.70	-5.3	1.2	2.7
[Mn ^{IV} (O)(N4Py)] ²⁺	-3.1	-10.1	-5.4	-0.84
[Co ^{IV} (O)(13-TMC)] ²⁺	-11.0	-18.7	-10.7	-9.6
[Fe ^{IV} (O)(13-TMC)] ²⁺	-13.8	-21.2	-19.5	-12.4
[Ru ^{VI} (O) ₂ (L)] ²⁺	2.8	-3.6	4.3	1.2
[Ru ^{VI} (O) ₂ (F ₂₈ -tpp)]	-1.1	-7.2	-0.20	-2.4

Table S18. ΔE_{PT} computed with different computational methodologies

Oxo	O3LYP ΔE_{PT}	B3LYP ΔE_{PT}	M06L ΔE_{PT}	O3LYP-ZORA ΔE_{PT}
[Fe ^{IV} (O)(Me ₃ NTB)(MeCN)] ²⁺	61.4	64.4	63.8	60.9
[Fe ^{IV} (O)(TMG ₂ dien)(MeCN)] ²⁺	61.4	64.2	62.4	61.0
[Fe ^{IV} (O)(TMG ₃ tren)] ²⁺	57.6	61.0	59.4	56.8
[Fe ^V (O)(TAML)] ⁻	43.2	38.3	45.0	44.7
[Fe ^{IV} (O)(TMC)(MeCN)] ²⁺	72.0	73.8	74.7	71.5
[Fe ^{IV} (O)(TMC)(N ₃)] ⁺	50.5	53.4	54.4	50.0
[Fe ^{IV} (O)(TMC)(OCOCF ₃)] ⁺	60.1	62.2	62.7	58.4
[Fe ^{IV} (O)(TMCS)] ⁺	42.7	45.7	46.1	42.3
[Mn ^{IV} (O)(H ₃ buea)] ⁻	29.5	31.4	27.9	28.8
[Fe ^{IV} (O)(TMP)]	44.2	41.9	45.5	44.7
[Co ^{III} (O)(PhB <i>i</i> BuIm ₃)]	19.5	21.2	22.1	21.7
[Ru ^{IV} (O)(H ⁺ TPA)(bpy)] ³⁺	78.8	79.4	80.3	78.8
[Fe ^{IV} (O)(tpfpp)]	53.6	52.1	54.2	51.9
[Mn ^{VII} (O) ₄] ⁻	58.7	62.1	60.5	59.0
[Mn ^V (O) ₂ (tf ₄ tmap)] ³⁺	36.6	38.6	40.1	35.8
[Mn ^{IV} (O)(OH)(tf ₄ tmap)] ³⁺	21.3	24.4	23.2	20.1
[Cr ^{IV} (O)(TMC)(Cl)] ⁺	56.9	60.4	59.4	56.2
[Ru ^{VI} (O) ₂ (TMC)] ²⁺	86.9	89.5	88.6	86.8
[Fe ^{IV} (O)(N4Py)] ²⁺	68.9	69.7	71.6	68.5
[Fe ^{IV} (O)(BnTPEN)] ²⁺	66.7	68.1	69.3	66.1
[Fe ^{IV} (O)(^{Me} ₂ TACN-Py ₂)] ²⁺	67.5	68.8	70.2	67.0
[Fe ^{IV} (O)(BP1)] ²⁺	74.0	75.1	76.8	73.6
[Fe ^{IV} (O)(BP2)] ²⁺	71.4	72.9	74.0	70.9
[Ru ^{IV} (O)(bpy) ₂ (py)] ²⁺	71.8	72.7	74.1	71.9
[Mn ^{IV} (O) ₂ (Me ₂ EBC)]	7.1	10.2	10.0	6.4.0
[Mn ^{IV} (O)(N4Py)] ²⁺	55.1	57.3	56.7	54.4
[Co ^{IV} (O)(13-TMC)] ²⁺	74.0	76.5	75.1	73.9
[Fe ^{IV} (O)(13-TMC)] ²⁺	83.4	86.2	84.5	83.1
[Ru ^{VI} (O) ₂ (L)] ²⁺	89.3	92.9	90.0	88.9
[Ru ^{VI} (O) ₂ (F ₂₈ -tpp)]	66.3	69.9	67.3	61.9

Table S19. ΔE_{ET} computed with different computational methodologies

Oxo	O3LYP ΔE_{ET}	B3LYP ΔE_{ET}	M06L ΔE_{ET}	O3LYP-ZORA ΔE_{ET}
[Fe ^{IV} (O)(Me ₃ NTB)(MeCN)] ²⁺	37.8	29.3	27.1	41.1
[Fe ^{IV} (O)(TMG ₂ dien)(MeCN)] ²⁺	45.9	39.4	39.7	48.4
[Fe ^{IV} (O)(TMG ₃ tren)] ²⁺	54.4	47.9	48.9	56.8
[Fe ^V (O)(TAML)] ⁻	44.8	37.4	42.2	46.6
[Fe ^{IV} (O)(TMC)(MeCN)] ²⁺	46.7	40.3	41.4	49.2
[Fe ^{IV} (O)(TMC)(N ₃)] ⁺	56.0	49.9	50.1	58.4
[Fe ^{IV} (O)(TMC)(OCOCF ₃)] ⁺	52.7	47.2	48.0	55.7
[Fe ^{IV} (O)(TMCS)] ⁺	59.2	52.5	52.9	61.3
[Mn ^{IV} (O)(H ₃ buea)] ⁻	69.2	64.5	66.0	72.2
[Fe ^{IV} (O)(TMP)]	73.5	75.1	69.7	73.6
[Co ^{III} (O)(PhB <i>t</i> BuIm ₃)]	82.8	74.8	74.6	85.6
[Ru ^{IV} (O)(H ⁺ TPA)(bpy)] ³⁺	45.8	48.8	41.5	45.9
[Fe ^{IV} (O)(tpfpp)]	63.6	65.2	59.6	66.0
[Mn ^{VII} (O) ₄] ⁻	54.4	44	55.4	56.3
[Mn ^V (O) ₂ (tf ₄ tmap)] ³⁺	66.2	87.1	61.7	67.9
[Mn ^{IV} (O)(OH)(tf ₄ tmap)] ³⁺	65.7	67.9	60.4	67.6
[Cr ^{IV} (O)(TMC)(Cl)] ⁺	61.5	56.4	56.7	63.8
[Ru ^{VI} (O) ₂ (TMC)] ²⁺	38.5	33.1	35.1	37.5
[Fe ^{IV} (O)(N4Py)] ²⁺	46.4	36.4	34.9	49.9
[Fe ^{IV} (O)(BnTPEN)] ²⁺	42.9	34.7	34.6	46.1
[Fe ^{IV} (O)(^{Me2} TACN-Py ₂)] ²⁺	46.5	37.9	36.7	49.4
[Fe ^{IV} (O)(BP1)] ²⁺	43.3	33.9	32.2	46.5
[Fe ^{IV} (O)(BP2)] ²⁺	40.0	31.6	28.9	43.3
[Ru ^{IV} (O)(bpy) ₂ (py)] ²⁺	47.6	51.1	43.7	47.7
[Mn ^{IV} (O) ₂ (Me ₂ EBC)]	93.7	87.4	89.3	95.6
[Mn ^{IV} (O)(N4Py)] ²⁺	43.7	37.2	37.0	47.1
[Co ^{IV} (O)(13-TMC)] ²⁺	16.8	9.3	13.9	18.8
[Fe ^{IV} (O)(13-TMC)] ²⁺	24.2	17.5	16.2	26.3
[Ru ^{VI} (O) ₂ (L)] ²⁺	26.5	20.8	24	25.4
[Ru ^{VI} (O) ₂ (F ₂₈ -tpp)]	42.7	38.1	39	45.6



Regression S27. DHA barriers against O3LYP's ΔE_{PCET} .

['O3LYP ΔE_{PCET} '] Metrics:

Score on Training Data:	0.6248135531191439
MSE of Training Data:	1.4644317414445578
Score of LOO Cross Validation:	0.5155711219123456
MSE of LOO Cross Validation:	1.8908279641807464
MSE of 5-Fold Cross Validation:	1.9028770862454243 (0.04693830813373367)
F-Test p-value of final 1 variables:	0.0001589808441718743

Correlation Matrix of x-values:
 O3LYP ΔE_{PCET}
 O3LYP ΔE_{PCET} 1.0

['O3LYP ΔE_{PCET} '] Training Average:
 [-2.1557534]

['O3LYP ΔE_{PCET} '] Training Deviation:
 [3.99653951]

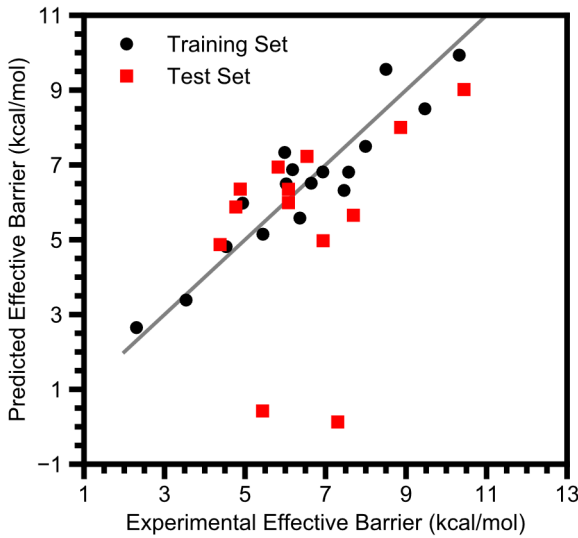
['O3LYP ΔE_{PCET} '] Coefficients:
 [0.39075281]

['O3LYP ΔE_{PCET} '] Standard Error:
 [0.07818165]

['O3LYP ΔE_{PCET} '] t-Test "Error":
 [0.16664024]

['O3LYP ΔE_{PCET} '] Weighted Coefficients:
 [1.56165903]

['O3LYP ΔE_{PCET} '] Intercept:
 7.3244233791333135



Regression S28. DHA barriers against O3LYP's ΔE_{PCET} , ΔE_{PT} , and ΔE_{ET} .

```
['O3LYP ΔE_PCET', 'O3LYP ΔE_PT', 'O3LYP ΔE_ET'] Metrics:
```

Score on Training Data:	0.8661041977336073
MSE of Training Data:	0.522623523624661
Score of LOO Cross Validation:	0.7561336561488596
MSE of LOO Cross Validation:	0.951861714554554
MSE of 5-Fold Cross Validation:	1.154890730587609(0.07663350650334944)
F-Test p-value of final 2 variables:	0.0012341809272257143

Correlation Matrix of x-values:

	O3LYP ΔE_PCET	O3LYP ΔE_PT	O3LYP ΔE_ET
O3LYP ΔE_PCET	1.000000	0.092458	0.118059
O3LYP ΔE_PT	0.092458	1.000000	-0.869440
O3LYP ΔE_ET	0.118059	-0.869440	1.000000

```
['O3LYP ΔE_PCET', 'O3LYP ΔE_PT', 'O3LYP ΔE_ET'] Training Average:  
[-2.1557534 50.94173114 55.69690677]
```

```
['O3LYP ΔE_PCET', 'O3LYP ΔE_PT', 'O3LYP ΔE_ET'] Training Deviation:  
[ 3.99653951 18.63116025 14.02743234]
```

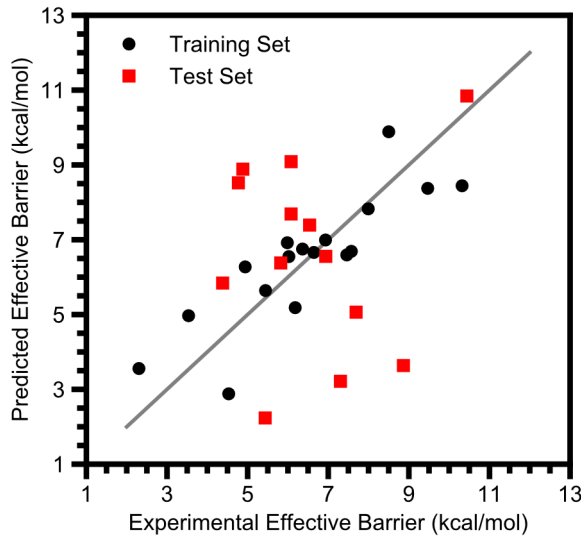
```
['O3LYP ΔE_PCET', 'O3LYP ΔE_PT', 'O3LYP ΔE_ET'] Coefficients:  
[0.32591958 0.04105499 0.11375599]
```

```
['O3LYP ΔE_PCET', 'O3LYP ΔE_PT', 'O3LYP ΔE_ET'] Standard Error:  
[0.05506456 0.02374144 0.03161931]
```

```
['O3LYP ΔE_PCET', 'O3LYP ΔE_PT', 'O3LYP ΔE_ET'] t-Test "Error":  
[0.11895975 0.05129026 0.06830937]
```

```
['O3LYP ΔE_PCET', 'O3LYP ΔE_PT', 'O3LYP ΔE_ET'] Weighted Coefficients:  
[1.30255047 0.76490212 1.59570441]
```

```
['O3LYP ΔE_PCET', 'O3LYP ΔE_PT', 'O3LYP ΔE_ET'] Intercept:  
-1.2426099746813781
```



Regression S29. DHA barriers against B3LYP's ΔE_{PCET} .

`['B3LYP ΔE_PCET'] Metrics:`

Score on Training Data:	0.7185873128148237
MSE of Training Data:	1.0984130023493341
Score of LOO Cross Validation:	0.5752474491511528
MSE of LOO Cross Validation:	1.6578986871562655
MSE of 5-Fold Cross Validation:	1.7027161796546295 (0.07407851365423393)
F-Test p-value of final 1 variables:	1.733634882372659e-05

`Correlation Matrix of x-values:`

B3LYP ΔE_PCET	
B3LYP ΔE_PCET	1.0

`['B3LYP ΔE_PCET'] Training Average:`
`[-10.33181066]`

`['B3LYP ΔE_PCET'] Training Deviation:`
`[4.30591229]`

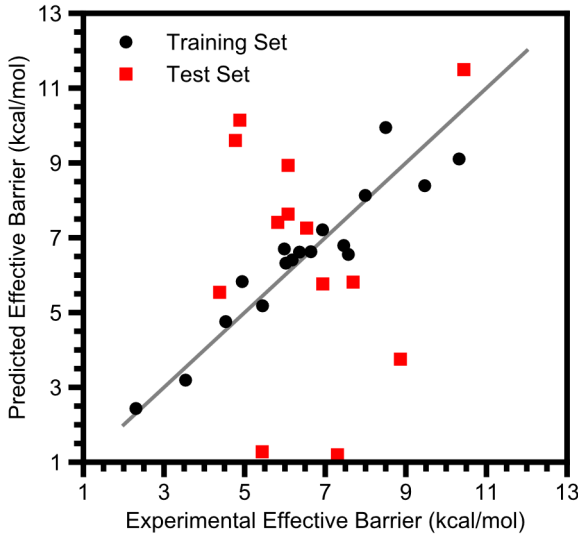
`['B3LYP ΔE_PCET'] Coefficients:`
`[0.38894267]`

`['B3LYP ΔE_PCET'] Standard Error:`
`[0.06284519]`

`['B3LYP ΔE_PCET'] t-Test "Error":`
`[0.13395135]`

`['B3LYP ΔE_PCET'] Weighted Coefficients:`
`[1.67475302]`

`['B3LYP ΔE_PCET'] Intercept:`
`10.500538700135094`



Regression S30. DHA barriers against B3LYP's ΔE_{PCET} , ΔE_{PT} , and ΔE_{ET} .

`['B3LYP ΔE_PCET', 'B3LYP ΔE_PT', 'B3LYP ΔE_ET'] Metrics:`

Score on Training Data:	0.8784702014938369
MSE of Training Data:	0.4743564058440075
Score of LOO Cross Validation:	0.7572853874456303
MSE of LOO Cross Validation:	0.947366264671894
MSE of 5-Fold Cross Validation:	1.2363937155719087 (0.09772669492501583)
F-Test p-value of final 2 variables:	0.004262890528072938

Correlation Matrix of x-values:

	B3LYP ΔE_PCET	B3LYP ΔE_PT	B3LYP ΔE_ET
B3LYP ΔE_PCET	1.000000	-0.127181	0.046790
B3LYP ΔE_PT	-0.127181	1.000000	-0.826294
B3LYP ΔE_ET	0.046790	-0.826294	1.000000

`['B3LYP ΔE_PCET', 'B3LYP ΔE_PT', 'B3LYP ΔE_ET'] Training Average:`
`[-10.33181066 52.5454078 50.98919915]`

`['B3LYP ΔE_PCET', 'B3LYP ΔE_PT', 'B3LYP ΔE_ET'] Training Deviation:`
`[4.30591229 18.62901372 18.26010309]`

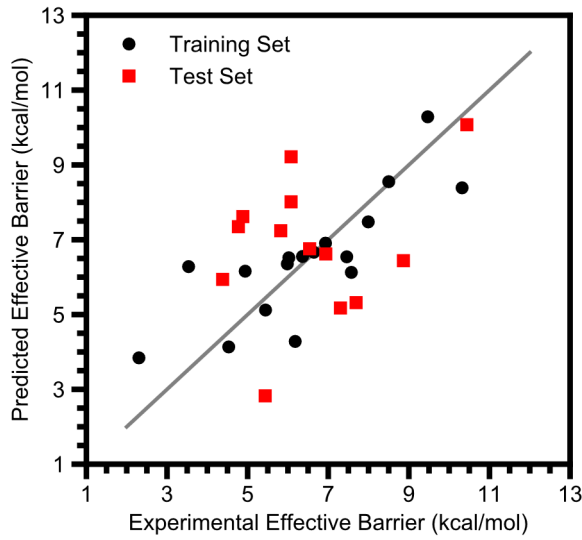
`['B3LYP ΔE_PCET', 'B3LYP ΔE_PT', 'B3LYP ΔE_ET'] Coefficients:`
`[0.40163668 0.04998103 0.07462551]`

`['B3LYP ΔE_PCET', 'B3LYP ΔE_PT', 'B3LYP ΔE_ET'] Standard Error:`
`[0.04497118 0.01843489 0.01867506]`

`['B3LYP ΔE_PCET', 'B3LYP ΔE_PT', 'B3LYP ΔE_ET'] t-Test "Error":`
`[0.09715433 0.03982616 0.04034501]`

`['B3LYP ΔE_PCET', 'B3LYP ΔE_PT', 'B3LYP ΔE_ET'] Weighted Coefficients:`
`[1.72941233 0.93109722 1.36266952]`

`['B3LYP ΔE_PCET', 'B3LYP ΔE_PT', 'B3LYP ΔE_ET'] Intercept:`
`4.200322441694215`



Regression S31. DHA barriers against M06L's ΔE_{PCET} .

`['M06L ΔE_PCET'] Metrics:`

Score on Training Data:	0.6489813916645575
MSE of Training Data:	1.3700995762444375
Score of LOO Cross Validation:	0.53623765519843
MSE of LOO Cross Validation:	1.810162131016007
MSE of 5-Fold Cross Validation:	1.943021323080626 (0.07769574536680626)
F-Test p-value of final 1 variables:	9.496453767954272e-05

`Correlation Matrix of x-values:`

	M06L ΔE_PCET
M06L ΔE_PCET	1.0

`['M06L ΔE_PCET'] Training Average:`
`[-5.8857926]`

`['M06L ΔE_PCET'] Training Deviation:`
`[5.90685145]`

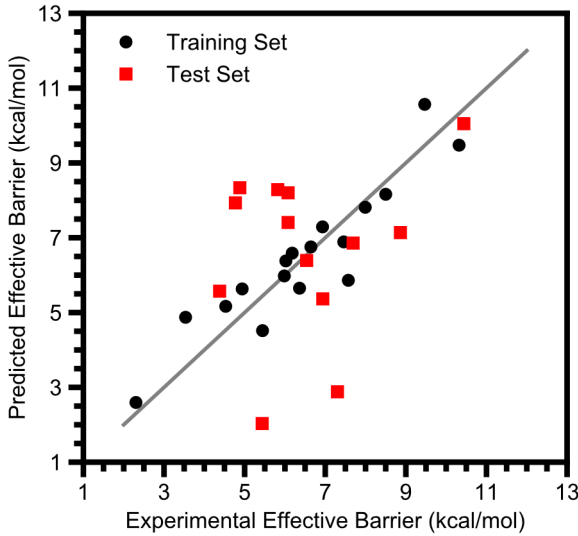
`['M06L ΔE_PCET'] Coefficients:`
`[0.26944558]`

`['M06L ΔE_PCET'] Standard Error:`
`[0.05116517]`

`['M06L ΔE_PCET'] t-Test "Error":`
`[0.10905597]`

`['M06L ΔE_PCET'] Weighted Coefficients:`
`[1.59157503]`

`['M06L ΔE_PCET'] Intercept:`
`8.067957508683563`



Regression S32. DHA barriers against M06L's ΔE_{PCET} , ΔE_{PT} , and ΔE_{ET} .

['M06L ΔE_{PCET} ', 'M06L ΔE_{PT} ', 'M06L ΔE_{ET} '] Metrics:

Score on Training Data:	0.8510495458264639
MSE of Training Data:	0.5813850015311927
Score of LOO Cross Validation:	0.7071919877823828
MSE of LOO Cross Validation:	1.1428913565658008
MSE of 5-Fold Cross Validation:	1.4555347084599448 (0.09713878607647679)
F-Test p-value of final 2 variables:	0.0038029971170726595

Correlation Matrix of x-values:

	M06L ΔE_{PCET}	M06L ΔE_{PT}	M06L ΔE_{ET}
M06L ΔE_{PCET}	1.000000	-0.207271	0.353413
M06L ΔE_{PT}	-0.207271	1.000000	-0.867418
M06L ΔE_{ET}	0.353413	-0.867418	1.000000

['M06L ΔE_{PCET} ', 'M06L ΔE_{PT} ', 'M06L ΔE_{ET} '] Training Average:
[-5.8857926 53.24122039 49.62308161]

['M06L ΔE_{PCET} ', 'M06L ΔE_{PT} ', 'M06L ΔE_{ET} '] Training Deviation:
[5.90685145 18.94195623 16.00741272]

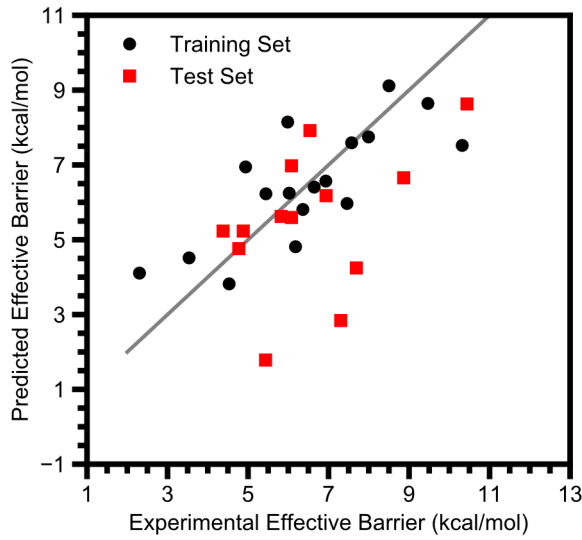
['M06L ΔE_{PCET} ', 'M06L ΔE_{PT} ', 'M06L ΔE_{ET} '] Coefficients:
[0.20521987 0.0711776 0.116457]

['M06L ΔE_{PCET} ', 'M06L ΔE_{PT} ', 'M06L ΔE_{ET} '] Standard Error:
[0.03917302 0.02296595 0.02842]

['M06L ΔE_{PCET} ', 'M06L ΔE_{PT} ', 'M06L ΔE_{ET} '] t-Test "Error":
[0.08462816 0.04961491 0.06139768]

['M06L ΔE_{PCET} ', 'M06L ΔE_{PT} ', 'M06L ΔE_{ET} '] Weighted Coefficients:
[1.21220329 1.34824305 1.86417519]

['M06L ΔE_{PCET} ', 'M06L ΔE_{PT} ', 'M06L ΔE_{ET} '] Intercept:
-1.8785991938222475



Regression S33. DHA barriers against O3LYP-ZORA's ΔE_{PCET} .

`['ZORA ΔE_PCET'] Metrics:`

Score on Training Data:	0.5837879956450376
MSE of Training Data:	1.6245631349823895
Score of LOO Cross Validation:	0.4632551558748629
MSE of LOO Cross Validation:	2.095028200853886
MSE of 5-Fold Cross Validation:	2.100418828317726(0.04913667840929494)
F-Test p-value of final 1 variables:	0.000356141781854169

`Correlation Matrix of x-values:`

ZORA ΔE_PCET	1.0
ZORA ΔE_PCET	

`['ZORA ΔE_PCET'] Training Average:`
`[-0.04816983]`

`['ZORA ΔE_PCET'] Training Deviation:`
`[3.95594462]`

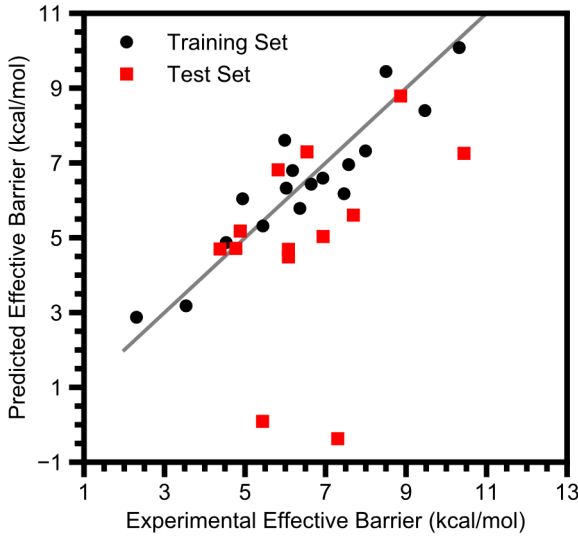
`['ZORA ΔE_PCET'] Coefficients:`
`[0.38158243]`

`['ZORA ΔE_PCET'] Standard Error:`
`[0.08319026]`

`['ZORA ΔE_PCET'] t-Test "Error":`
`[0.17731583]`

`['ZORA ΔE_PCET'] Weighted Coefficients:`
`[1.50951897]`

`['ZORA ΔE_PCET'] Intercept:`
`6.500437449829684`



Regression S34. DHA barriers against O3LYP-ZORA's ΔE_{PCET} , ΔE_{PT} , and ΔE_{ET} .

```
['ZORA ΔE_PCET', 'ZORA ΔE_PT', 'ZORA ΔE_ET'] Metrics:
```

Score on Training Data:	0.849900635628982
MSE of Training Data:	0.585869440069017
Score of LOO Cross Validation:	0.7468405586771689
MSE of LOO Cross Validation:	0.9881346317321933
MSE of 5-Fold Cross Validation:	1.20988798980493(0.07486597934720962)
F-Test p-value of final 2 variables:	0.0013210450640702698

Correlation Matrix of x-values:

	ZORA ΔE_PCET	ZORA ΔE_PT	ZORA ΔE_ET
ZORA ΔE_PCET	1.000000	0.115023	0.106737
ZORA ΔE_PT	0.115023	1.000000	-0.872438
ZORA ΔE_ET	0.106737	-0.872438	1.000000

```
['ZORA ΔE_PCET', 'ZORA ΔE_PT', 'ZORA ΔE_ET'] Training Average:  
[-4.81698302e-02 5.05000651e+01 5.81283061e+01]
```

```
['ZORA ΔE_PCET', 'ZORA ΔE_PT', 'ZORA ΔE_ET'] Training Deviation:  
[ 3.95594462 18.67471947 13.55389964]
```

```
['ZORA ΔE_PCET', 'ZORA ΔE_PT', 'ZORA ΔE_ET'] Coefficients:  
[0.31228114 0.04369815 0.12462006]
```

```
['ZORA ΔE_PCET', 'ZORA ΔE_PT', 'ZORA ΔE_ET'] Standard Error:  
[0.05972849 0.02574095 0.0354332 ]
```

```
['ZORA ΔE_PCET', 'ZORA ΔE_PT', 'ZORA ΔE_ET'] t-Test "Error":  
[0.12903556 0.05560993 0.07654877]
```

```
['ZORA ΔE_PCET', 'ZORA ΔE_PT', 'ZORA ΔE_ET'] Weighted Coefficients:  
[1.23536689 0.81605065 1.68908777]
```

```
['ZORA ΔE_PCET', 'ZORA ΔE_PT', 'ZORA ΔE_ET'] Intercept:  
-2.9536129994751716
```

Analysis of Ru Oxo Kinetics with Several Substrates

Due to the overestimation reaction barriers for Ru oxo complexes, we have investigated whether free energies other than ΔG_{PCET} have an effect on the kinetics of $[\text{Ru}^{\text{IV}}(\text{O})(\text{bpy})_2(\text{py})]^{2+}$ with several substrates. The experimental data is from two reports from Mayer and coworkers.^{25,60} The determination of barrier heights and computational methodology were the same as for the data on multiple oxo complexes.

Table S20. Summary of data for regressions with the Ru^{IV} oxo data

Substrate	Corr. ^a	k_2 (mol s ⁻¹)	PCET Barrier (kcal/mol)	ΔG_{PCET} (kcal/mol)	ΔG_{PCET} (kcal/mol)	ΔG_{PCET} (kcal/mol)
9,10-Dihydroanthracene	2	125 ^e	4.77	-5.48	68.5	43.4
Ethylbenzene	2	0.022 ^e	10.22	2.90	82.8	51.7
Isopropylbenzene	2	0.033 ^e	9.90	1.29	85.1	53.9
Toluene	1	0.0064 ^e	10.65	8.69	83.5	53.8
Xanthene	1	577 ^e	3.46	-8.24	67.7	35.3
Fluorene	1	21.9 ^e	5.44	-1.21	58.6	40.1
AcrH ₂ ^b	1	5,700 ^f	2.11	-11.4	70.5	19.5
BNAH ^c	1	70,000 ^f	0.457	-12.1	88.1	19.3
Indene	1	10.8 ^e	6.11	-2.61	54.5	40.0
Cyclohexene	1 ^c	0.92 ^e	7.81	-4.94	84.5	41.5

^aStoichiometric correction to the rate. ^b10-Methyl9,10-dihydroacridine. ^cN-Benzyl-1,4-dihydronicotinamide.

^cCyclohexenone is the only observed product, which we take to imply a 1:1 reaction stoichiometry. ^eReference 25.

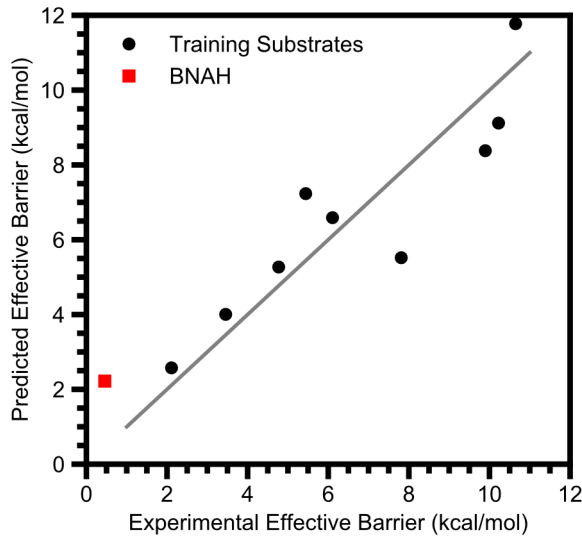
^fReference 60.

We find that ΔG_{PT} and ΔG_{ET} improve the fit to all substrates except *N*-benzyl-1,4-dihydronicotinamide (BNAH). It is unclear why BNAH does not fit the trend, as it is thought to react via the same PCET mechanism as the other substrates. Nonetheless there does not seem to be a broader issue with hydridic C–H bonds because 10-methyl-9,10-dihydroacridine (AcrH₂) fits well. The coefficients of the fits with ΔG_{PT} and ΔG_{ET} are similar to those seen in the fit with DHA (ΔG_{PCET} has a coefficient ~0.3; ΔG_{PT} and ΔG_{ET} have a coefficients ~0.1), which reinforces the conclusion that we are observing the same trends in both data sets.

Table S21. Summary of statistics on regressions with the Ru^{IV} oxo data

Parameter(s) Regressed with	R ²	MSE ^a	LOO ^b R ²	LOO ^b MSE ^a	5-Fold CV ^c MSE ^a	p-value
ΔG_{PCET} only	0.81	1.58	0.69	2.61	2.77	<0.001 ^d
ΔG_{PCET} , ΔG_{ET} , and ΔG_{ET}	0.94	0.48	0.79	1.79	2.18	0.051 ^e

^aMean Squared Error, kcal² mol⁻². ^bLeave-One-Out. ^cCross Validation. ^dFrom an F-test where the null hypothesis is that ΔG_{PCET} has no effect. ^eFrom an F-test where the null hypothesis is that ΔG_{PT} and ΔG_{ET} have no effect.



Regression S35. Ru^{IV} oxo barriers against ΔG_{PCET} .

`[' ΔG_{PCET} '] Metrics:`

```
Score on Training Data: 0.8141313040751759
MSE of Training Data: 1.5840108561567379
Score of LOO Cross Validation: 0.6935554692619883
MSE of LOO Cross Validation: 2.6115826609941655
MSE of 5-Fold Cross Validation: 2.769340429340532(0.09523255744448217)
F-Test p-value of final 1 variables: 0.0008715558586384065
```

`Correlation Matrix of x-values:`

```
 $\Delta G_{\text{PCET}}$ 
 $\Delta G_{\text{PCET}}$  1.0
```

`[' ΔG_{PCET} '] Training Average:`
`[-2.32885283]`

`[' ΔG_{PCET} '] Training Deviation:`
`[5.73889131]`

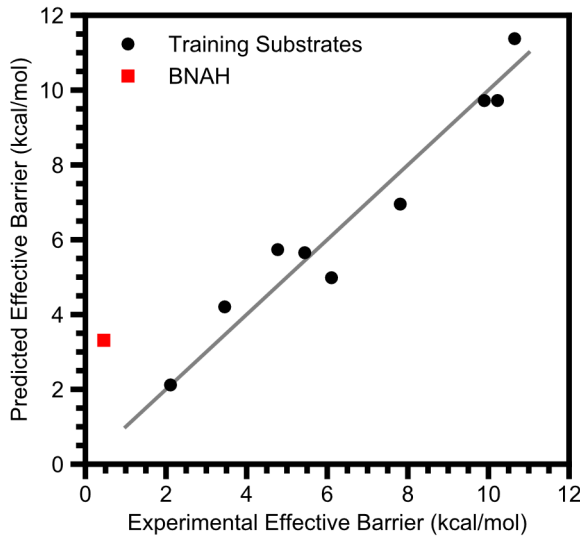
`[' ΔG_{PCET} '] Coefficients:`
`[0.4589815]`

`[' ΔG_{PCET} '] Standard Error:`
`[0.08288998]`

`[' ΔG_{PCET} '] t-Test "Error":`
`[0.19600367]`

`[' ΔG_{PCET} '] Weighted Coefficients:`
`[2.63404493]`

`[' ΔG_{PCET} '] Intercept:`
`7.787390135961275`



Regression S36. Ru^{IV} oxo barriers against ΔG_{PCET} , ΔG_{PT} , and ΔG_{ET} .

`[' ΔG_{PCET} ', ' ΔG_{PT} ', ' ΔG_{ET} '] Metrics:`

```
Score on Training Data: 0.9433272836504076
MSE of Training Data: 0.48297642321627954
Score of LOO Cross Validation: 0.789763533352954
MSE of LOO Cross Validation: 1.7916779577753412
MSE of 5-Fold Cross Validation: 2.1772658070507824(0.09820218535610042)
F-Test p-value of final 2 variables: 0.0513356946380471
```

Correlation Matrix of x-values:

	ΔG_{PCET}	ΔG_{PT}	ΔG_{ET}
ΔG_{PCET}	1.000000	0.418868	0.876863
ΔG_{PT}	0.418868	1.000000	0.501120
ΔG_{ET}	0.876863	0.501120	1.000000

`[' ΔG_{PCET} ', ' ΔG_{PT} ', ' ΔG_{ET} '] Training Average:`
`[-2.32885283 72.85902939 42.13973614]`

`[' ΔG_{PCET} ', ' ΔG_{PT} ', ' ΔG_{ET} '] Training Deviation:`
`[5.73889131 10.9865912 10.20429223]`

`[' ΔG_{PCET} ', ' ΔG_{PT} ', ' ΔG_{ET} '] Coefficients:`
`[0.24144858 0.07967059 0.09854522]`

`[' ΔG_{PCET} ', ' ΔG_{PT} ', ' ΔG_{ET} '] Standard Error:`
`[0.11278959 0.0327295 0.06656052]`

`[' ΔG_{PCET} ', ' ΔG_{PT} ', ' ΔG_{ET} '] t-Test "Error":`
`[0.28993488 0.08413386 0.17109926]`

`[' ΔG_{PCET} ', ' ΔG_{PT} ', ' ΔG_{ET} '] Weighted Coefficients:`
`[1.38564716 0.87530822 1.00558426]`

`[' ΔG_{PCET} ', ' ΔG_{PT} ', ' ΔG_{ET} '] Intercept:`
`-2.676603704473255`

Summary of Statistics on Regressions on the Co^{III} Oxo Data

Table S23 gives a summary of the regressions performed on the Co^{III} oxo complex. We reiterate the previously reported trend with ΔG_{PT} and lack of a trend with ΔG_{PCET}.¹² We also detail how the addition of ΔG_{PCET} to the regression with ΔG_{PT} is significant and demonstrate that addition of neither the substrates' %BV sterics nor ΔG_{ET} improve the fit further. The substrate 1,1,3,3-tetraphenylpropene was excluded from this analysis due to its relatively large steric hinderance.

Table S22. Summary of data for regressions with the Co^{II} oxo data

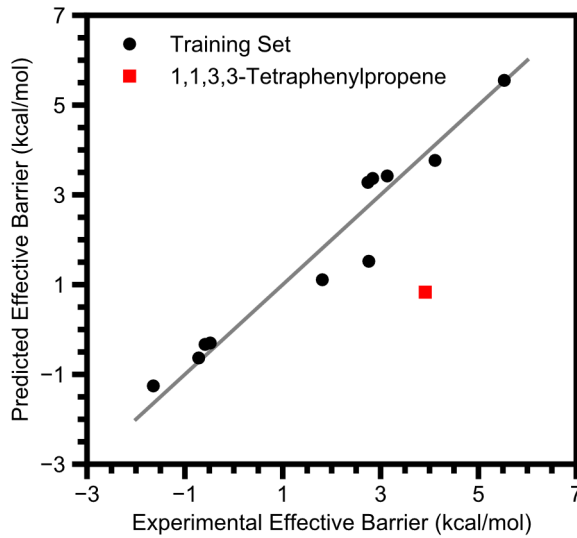
Substrate	k ₂ (mol/s) ^a	PCET Barrier (kcal/mol)	ΔG _{PCET} (kcal/mol)	ΔG _{PT} (kcal/mol)	ΔG _{ET} (kcal/mol)	%BV ^b
9,10-Dihydroanthracene	0.0584 ^c	3.1	-6.7	29.5	94.8	47.4
Fluorene	0.61	1.8	-3.3	19.3	90.5	43.2
1,3-Cyclohexadiene	0.0027 ^c	5.5	-11.8	38.9	82.8	41.9
9-(<i>p</i> -CF ₃ Ph)Fluorene	112	-1.6	-9.9	8.8	91.9	57.6
9-(<i>p</i> -MeOPh)Fluorene	17.6	-0.48	-11.1	13.0	84.6	57.8
9-(<i>p</i> -MePh)Fluorene	22.4	-0.59	-10.7	12.9	88.8	57.7
3-Methylxanthene	0.088	2.8	-11.2	29.2	82.3	46.0
Diphenylmethane	0.012	4.1	-2.4	31.0	99.4	48.2
9-Phenylfluorene	29.6	-0.72	-10.3	11.6	90.0	57.7
9- <i>tert</i> -Butylfluorene	0.088	2.8	-5.2	21.1	89.0	61.5
1,1,3,3-Tetraphenylpropene	0.008	2.7	-12.5	18.0	88.1	73.5
Xanthene	0.1128	3.1	-10.4	28.9	85.3	45.8

^aReference 12. ^bPercent buried volume of a sphere around the reactive hydrogen atom. ^cCorrected by a stoichiometric factor of 2.

Table S23. Summary of statistics on regressions with the Co^{III} oxo data

Parameter(s) Regressed with	R ²	MSE ^a	LOO ^b R ²	LOO ^b MSE ^a	5-Fold CV ^c MSE ^a	p-value
ΔG _{PT} only	0.94	0.28	0.93	0.36	0.39	< 0.001 ^d
ΔG _{PCET} only	0.09	4.39	-0.32	6.35	6.37	0.37 ^e
ΔG _{PT} and ΔG _{PCET}	0.97	0.13	0.94	0.27	0.29	0.017 ^e
ΔG _{PT} , ΔG _{PCET} , and %BV Sterics	0.98	0.10	0.83	0.80	0.80	0.21 ^f
ΔG _{PT} and ΔG _{ET}	0.95	0.25	0.93	0.36	0.52	0.41 ^g
ΔG _{PT} , ΔG _{PCET} , and ΔG _{ET}	0.98	0.08	0.95	0.23	0.29	0.072 ^g

^aMean Squared Error, kcal² mol⁻². ^bLeave-One-Out. ^cCross Validation. ^dFrom an F-test where the null hypothesis is that ΔG_{PT} has no effect. ^eFrom an F-test where the null hypothesis is that ΔG_{PCET} has no effect. ^fFrom an F-test where the null hypothesis is that %BV Sterics has no effect. ^gFrom an F-test where the null hypothesis is that ΔG_{ET} has no effect.



Regression S37. Co^{III} oxo barriers against ΔG_{PT}.

['ΔG_PT'] Metrics:

Score on Training Data:	0.9424632998739368
MSE of Training Data:	0.27729834873004827
Score of LOO Cross Validation:	0.9252474025325068
MSE of LOO Cross Validation:	0.36027043253438246
MSE of 5-Fold Cross Validation:	0.38974742022611514 (0.011222596536024027)
F-Test p-value of final 1 variables:	6.966522436702149e-07

Correlation Matrix of x-values:

ΔG_PT	1.0
ΔG_PT	

['ΔG_PT'] Training Average:

[22.19752727]

['ΔG_PT'] Training Deviation:

[9.42668502]

['ΔG_PT'] Coefficients:

[0.22608638]

['ΔG_PT'] Standard Error:

[0.01862059]

['ΔG_PT'] t-Test "Error":

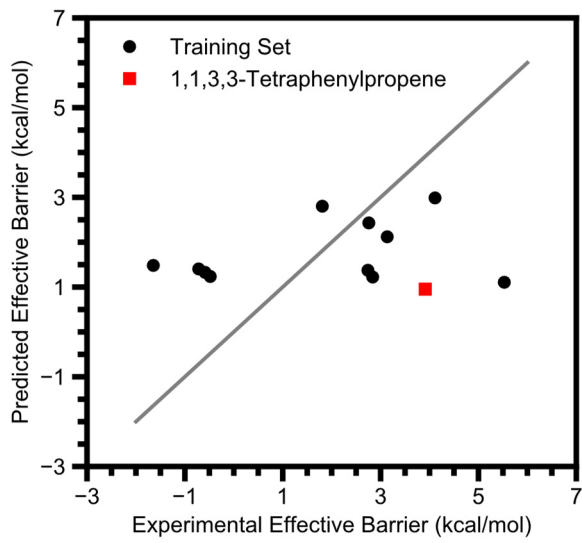
[0.0421227]

['ΔG_PT'] Weighted Coefficients:

[2.13124506]

['ΔG_PT'] Intercept:

-3.24666603888153



Regression S38. Co^{III} oxo barriers against ΔG_{PCET}.

['ΔG_PCET'] Metrics:

Score on Training Data:	0.08862503668507471
MSE of Training Data:	4.392375159635855
Score of LOO Cross Validation:	-0.31700265884710466
MSE of LOO Cross Validation:	6.34729940666087
MSE of 5-Fold Cross Validation:	6.37119453049353(0.09952217793998655)
F-Test p-value of final 1 variables:	0.3739434558155724

Correlation Matrix of x-values:

ΔG_PCET	1.0
ΔG_PCET	

['ΔG_PCET'] Training Average:
[-8.45470682]

['ΔG_PCET'] Training Deviation:
[3.26244406]

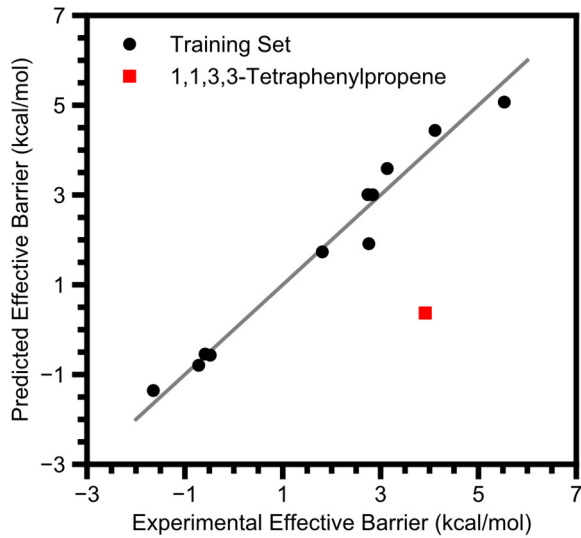
['ΔG_PCET'] Coefficients:
[0.20032553]

['ΔG_PCET'] Standard Error:
[0.21413388]

['ΔG_PCET'] t-Test "Error":
[0.48440449]

['ΔG_PCET'] Weighted Coefficients:
[0.65355084]

['ΔG_PCET'] Intercept:
3.465585563988545



Regression S39. Co^{III} oxo barriers against ΔG_{PT} and ΔG_{PCET} .

`[' ΔG_{PT} ', ' ΔG_{PCET} '] Metrics:`

```
Score on Training Data: 0.9728720534806891
MSE of Training Data: 0.13074324314324676
Score of LOO Cross Validation: 0.943560930601589
MSE of LOO Cross Validation: 0.2720083131940089
MSE of 5-Fold Cross Validation: 0.2929711051982866(0.01173660654476484)
F-Test p-value of final 1 variables: 0.01721332594582059
```

`Correlation Matrix of x-values:`

```
 $\Delta G_{PT}$   $\Delta G_{PCET}$ 
 $\Delta G_{PT}$  1.000000 0.128517
 $\Delta G_{PCET}$  0.128517 1.000000
```

`[' ΔG_{PT} ', ' ΔG_{PCET} '] Training Average:`
`[22.19752727 -8.45470682]`

`[' ΔG_{PT} ', ' ΔG_{PCET} '] Training Deviation:`
`[9.42668502 3.26244406]`

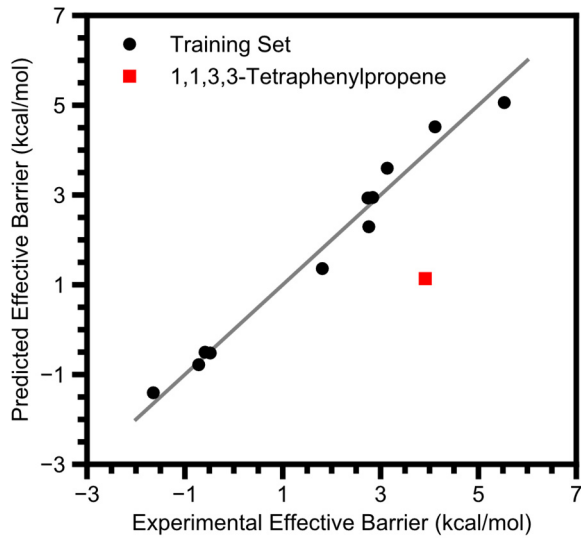
`[' ΔG_{PT} ', ' ΔG_{PCET} '] Coefficients:`
`[0.22082357 0.11832428]`

`[' ΔG_{PT} ', ' ΔG_{PCET} '] Standard Error:`
`[0.01367484 0.03951282]`

`[' ΔG_{PT} ', ' ΔG_{PCET} '] t-Test "Error":`
`[0.03153423 0.09111673]`

`[' ΔG_{PT} ', ' ΔG_{PCET} '] Weighted Coefficients:`
`[2.08163428 0.38602634]`

`[' ΔG_{PT} ', ' ΔG_{PCET} '] Intercept:`
`-2.129448313216325`



Regression S40. Co^{III} oxo barriers against ΔG_{PT}, ΔG_{PCET}, and substrates' percent buried volume sterics.

['ΔG_PT', 'ΔG_PCET', '%BV'] Metrics:

Score on Training Data:	0.9785995318612503
MSE of Training Data:	0.10313963894215689
Score of LOO Cross Validation:	0.8335055335504782
MSE of LOO Cross Validation:	0.8024207248241055
MSE of 5-Fold Cross Validation:	0.8002864721214152 (0.03212409826687691)
F-Test p-value of final 1 variables:	0.21338614672251444

Correlation Matrix of x-values:

	ΔG_PT	ΔG_PCET	%BV
ΔG_PT	1.000000	0.128517	-0.777256
ΔG_PCET	0.128517	1.000000	-0.121393
%BV	-0.777256	-0.121393	1.000000

['ΔG_PT', 'ΔG_PCET', '%BV'] Training Average:
 [22.19752727 -8.45470682 51.34545455]

['ΔG_PT', 'ΔG_PCET', '%BV'] Training Deviation:
 [9.42668502 3.26244406 6.77567355]

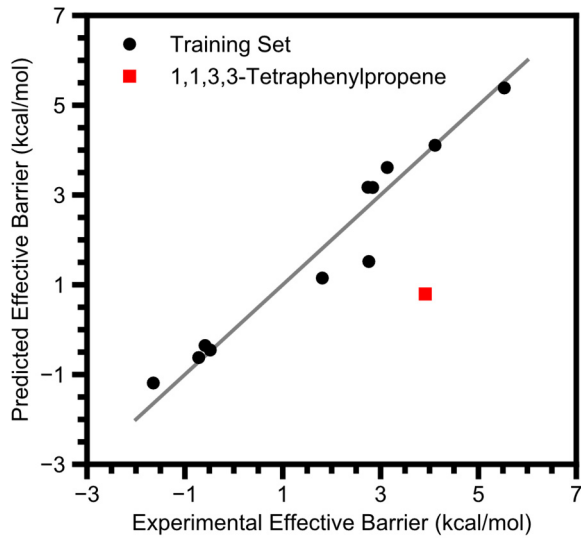
['ΔG_PT', 'ΔG_PCET', '%BV'] Coefficients:
 [0.24253036 0.120095 0.03899516]

['ΔG_PT', 'ΔG_PCET', '%BV'] Standard Error:
 [0.02049641 0.03754008 0.02848994]

['ΔG_PT', 'ΔG_PCET', '%BV'] t-Test "Error":
 [0.0484663 0.08876819 0.06736801]

['ΔG_PT', 'ΔG_PCET', '%BV'] Weighted Coefficients:
 [2.2862573 0.39180322 0.26421845]

['ΔG_PT', 'ΔG_PCET', '%BV'] Intercept:
 -4.598538368410885



Regression S41. Co^{III} oxo barriers against ΔG_{PT} and ΔG_{ET} .

`[' ΔG_{PT} ', ' ΔG_{ET} '] Metrics:`

Score on Training Data:	0.9473851700776209
MSE of Training Data:	0.2535773762523971
Score of LOO Cross Validation:	0.9257014183495356
MSE of LOO Cross Validation:	0.35808230154870657
MSE of 5-Fold Cross Validation:	0.5218007751115226 (0.09976949819374094)
F-Test p-value of final 1 variables:	0.4121834589527267

`Correlation Matrix of x-values:`

ΔG_{PT}	ΔG_{ET}
ΔG_{PT}	1.000000 -0.106709
ΔG_{ET}	-0.106709 1.000000

`[' ΔG_{PT} ', ' ΔG_{ET} '] Training Average:`
`[22.19752727 89.03654545]`

`[' ΔG_{PT} ', ' ΔG_{ET} '] Training Deviation:`
`[9.42668502 4.97130331]`

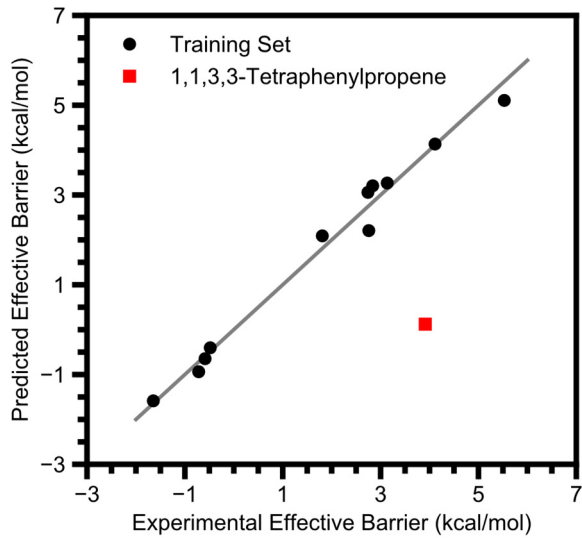
`[' ΔG_{PT} ', ' ΔG_{ET} '] Coefficients:`
`[0.22783984 0.03115895]`

`[' ΔG_{PT} ', ' ΔG_{ET} '] Standard Error:`
`[0.01899495 0.0360186]`

`[' ΔG_{PT} ', ' ΔG_{ET} '] t-Test "Error":`
`[0.04380243 0.08305904]`

`[' ΔG_{PT} ', ' ΔG_{ET} '] Weighted Coefficients:`
`[2.14777439 0.15490058]`

`[' ΔG_{PT} ', ' ΔG_{ET} '] Intercept:`
`-6.059874252255053`



Regression S42. Co^{III} oxo barriers against ΔG_{PT}, ΔG_{PCET}, and ΔG_{ET}.

['ΔG_PT', 'ΔG_PCET', 'ΔG_ET'] Metrics:

Score on Training Data:	0.9834815349371753
MSE of Training Data:	0.07961080624089117
Score of LOO Cross Validation:	0.9532389621068799
MSE of LOO Cross Validation:	0.2253650029330011
MSE of 5-Fold Cross Validation:	0.29298124182750607 (0.036112502254110106)
F-Test p-value of final 1 variables:	0.0716825286335695

Correlation Matrix of x-values:

	ΔG_PT	ΔG_PCET	ΔG_ET
ΔG_PT	1.000000	0.128517	-0.106709
ΔG_PCET	0.128517	1.000000	0.750813
ΔG_ET	-0.106709	0.750813	1.000000

['ΔG_PT', 'ΔG_PCET', 'ΔG_ET'] Training Average:
[22.19752727 -8.45470682 89.03654545]

['ΔG_PT', 'ΔG_PCET', 'ΔG_ET'] Training Deviation:
[9.42668502 3.26244406 4.97130331]

['ΔG_PT', 'ΔG_PCET', 'ΔG_ET'] Coefficients:
[0.21293067 0.20413059 -0.07243803]

['ΔG_PT', 'ΔG_PCET', 'ΔG_ET'] Standard Error:
[0.01199958 0.05219299 0.03416295]

['ΔG_PT', 'ΔG_PCET', 'ΔG_ET'] t-Test "Error":
[0.02837449 0.12341681 0.08078254]

['ΔG_PT', 'ΔG_PCET', 'ΔG_ET'] Weighted Coefficients:
[2.00723035 0.66596465 -0.3601114]

['ΔG_PT', 'ΔG_PCET', 'ΔG_ET'] Intercept:
5.2208535130795175

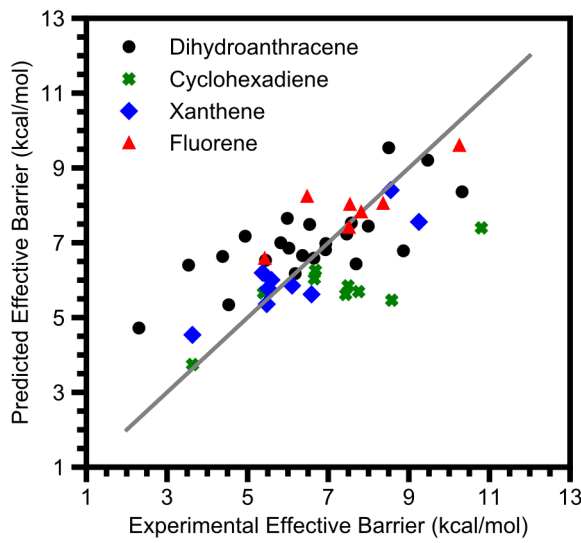
Regressions of Metal Oxo Complexes with Multiple Substrates

Table S24 gives details on the regressions between multiple substrates' barriers for reactivity with several metal oxo species. Most of the parameters we analyze do not change between substrate to substrate (the exceptions being the free energies), so we were wary of giving too much weight to metal oxo complexes which had k_2 values reported for an unusually large number of substrates. For that reason we limited our analysis to the substrates which have the largest number of k_2 values reported with metal oxo complexes in our data set: 9,10-dihydroanthracene (DHA), 1,4-cyclohexadiene (CHD), xanthene (Xth), and fluorene (Fl). Due to the same concern with extra weight being given to specific metal oxo complexes we only report the overall R^2 and MSE of the fit along with a modified LOO R^2 and MSE. This modification is that we did not leave out one individual data point at a time to predict with all other data points; instead we left out all data for a given metal oxo complex and predicted them with the rest of the metal oxo complexes' data. Ultimately, the results from this analysis cohere with what is seen for that regressions to only DHA data: when compared to the fit to only ΔG_{PCET} , only ΔG_{PT} and ΔG_{ET} show a convincing effect. The data used in these regressions is given in Table S3 (data relating to spin), Table S4 (data relating to reactivity with DHA), Table S6 (data related to reactivity with 1,4-cyclohexadiene (CHD)), Table S7 (data related to reactivity with fluorene), (data related to reactivity with xanthene), and Table S13 (steric parameters).

Table S24. Summary of statistics on regressions with multiple substrates and multiple metal oxo complexes

Parameter(s) Regressed with ΔG_{PCET}	R^2	MSE ^a	LOO ^b R^2	LOO ^b MSE ^a
ΔG_{PCET} only	0.45	1.79	0.36	2.10
%BV Sterics	0.48	1.71	0.28	2.37
Oxo Spin Density	0.53	1.55	0.37	2.08
Spin Excitation	0.50	1.66	0.39	2.01
$ \eta $	0.50	1.63	0.30	2.30
ΔG_{PT} , ΔG_{ET}	0.64	1.18	0.50	1.64

^aMean Squared Error, kcal² mol⁻². ^bLeave-One-Out.



Regression S43. Multiple substrates' reaction barriers against ΔG_{PCET} .

```
[ 'Sub ΔG_PCET' ] Metrics:
Score on Training Data: 0.45487429395449097
MSE of Training Data: 1.7936813739581947
Score of LOO Cross Validation: 0.3623252595400116
MSE of LOO Cross Validation: 2.0982046744851544

Correlation Matrix of x-values:
  Sub ΔG_PCET
Sub ΔG_PCET 1.0

[ 'Sub ΔG_PCET' ] Training Average:
[-8.86079851]

[ 'Sub ΔG_PCET' ] Training Deviation:
[4.20784163]

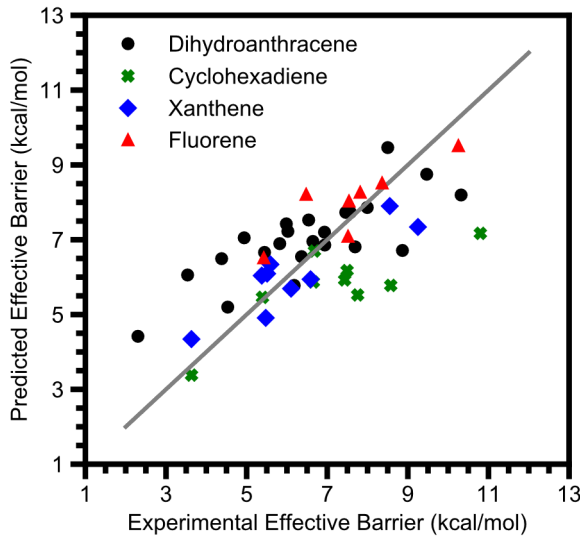
[ 'Sub ΔG_PCET' ] Coefficients:
[0.29074391]

[ 'Sub ΔG_PCET' ] Standard Error:
[0.04692825]

[ 'Sub ΔG_PCET' ] t-Test "Error":
[0.09446167]

[ 'Sub ΔG_PCET' ] Weighted Coefficients:
[1.22340434]

[ 'Sub ΔG_PCET' ] Intercept:
9.3326501024694
```



Regression S44. Multiple substrates' reaction barriers against ΔG_{PCET} and percent buried volume sterics.

```
['Sub ΔG_PCET', '%BV Tot', '%BV Dev'] Metrics:
```

Score on Training Data:	0.48027058057784117
MSE of Training Data:	1.710117444063089
Score of LOO Cross Validation:	0.2785190099479361
MSE of LOO Cross Validation:	2.373960719829397

Correlation Matrix of x-values:

	Sub ΔG_PCET	%BV Tot	%BV Dev
Sub ΔG_PCET	1.000000	-0.155632	0.192876
%BV Tot	-0.155632	1.000000	0.155131
%BV Dev	0.192876	0.155131	1.000000

```
['Sub ΔG_PCET', '%BV Tot', '%BV Dev'] Training Average:  
[-8.86079851 63.96875 4.65175846]
```

```
['Sub ΔG_PCET', '%BV Tot', '%BV Dev'] Training Deviation:  
[ 4.20784163 10.24309028 4.35809801]
```

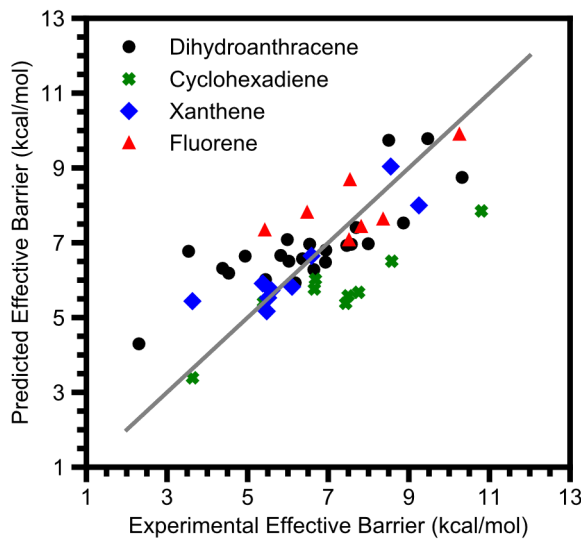
```
['Sub ΔG_PCET', '%BV Tot', '%BV Dev'] Coefficients:  
[ 0.30887955 0.02627491 -0.04095496]
```

```
['Sub ΔG_PCET', '%BV Tot', '%BV Dev'] Standard Error:  
[0.04864807 0.01984959 0.04696706]
```

```
['Sub ΔG_PCET', '%BV Tot', '%BV Dev'] t-Test "Error":  
[0.09804374 0.04000422 0.09465589]
```

```
['Sub ΔG_PCET', '%BV Tot', '%BV Dev'] Weighted Coefficients:  
[ 1.29971621 0.26913631 -0.17848572]
```

```
['Sub ΔG_PCET', '%BV Tot', '%BV Dev'] Intercept:  
8.003085518073675
```



Regression S45. Multiple substrates' reaction barriers against ΔG_{PCET} and IBO spin density on the oxo ligand.

```
['Sub ΔG_PCET', 'IBO Spin O'] Metrics:
```

Score on Training Data:	0.5287385429894587
MSE of Training Data:	1.5506384827018973
Score of LOO Cross Validation:	0.36879954216229527
MSE of LOO Cross Validation:	2.076901697904626

```
Correlation Matrix of x-values:
```

	Sub ΔG_PCET	IBO Spin O
Sub ΔG_PCET	1.000000	-0.170138
IBO Spin O	-0.170138	1.000000

```
['Sub ΔG_PCET', 'IBO Spin O'] Training Average:  
[-8.86079851  0.48515917]
```

```
['Sub ΔG_PCET', 'IBO Spin O'] Training Deviation:  
[4.20784163  0.32509068]
```

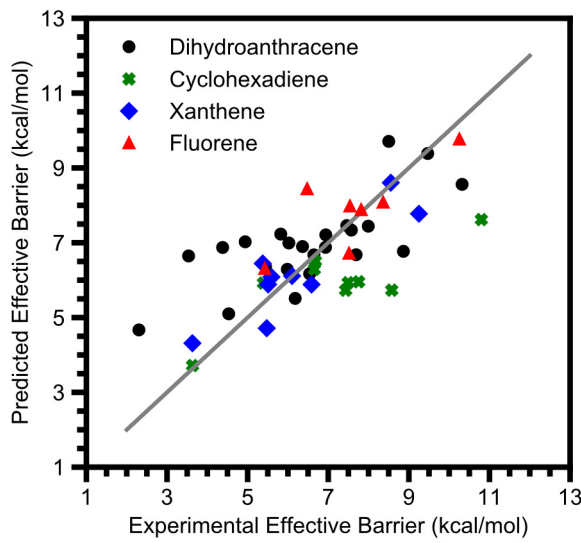
```
['Sub ΔG_PCET', 'IBO Spin O'] Coefficients:  
[ 0.27051544 -1.53891806]
```

```
['Sub ΔG_PCET', 'IBO Spin O'] Standard Error:  
[0.04476805  0.57945946]
```

```
['Sub ΔG_PCET', 'IBO Spin O'] t-Test "Error":  
[0.09016748  1.16709126]
```

```
['Sub ΔG_PCET', 'IBO Spin O'] Weighted Coefficients:  
[ 1.13828612 -0.50028792]
```

```
['Sub ΔG_PCET', 'IBO Spin O'] Intercept:  
9.900029869312357
```



Regression S46. Multiple substrates' reaction barriers against ΔG_{PCET} and the spin excitation energy.

```

['Sub ΔG_PCET', 'Spin Excitation'] Metrics:
Score on Training Data: 0.49613389580124573
MSE of Training Data: 1.6579207989041966
Score of LOO Cross Validation: 0.39044592960659175
MSE of LOO Cross Validation: 2.0056764345539455

Correlation Matrix of x-values:
      Sub ΔG_PCET  Spin Excitation
Sub ΔG_PCET       1.000000     -0.077451
Spin Excitation    -0.077451      1.000000

['Sub ΔG_PCET', 'Spin Excitation'] Training Average:
[-8.86079851 11.34056619]

['Sub ΔG_PCET', 'Spin Excitation'] Training Deviation:
[ 4.20784163 17.66873331]

['Sub ΔG_PCET', 'Spin Excitation'] Coefficients:
[ 0.28394156 -0.02091645]

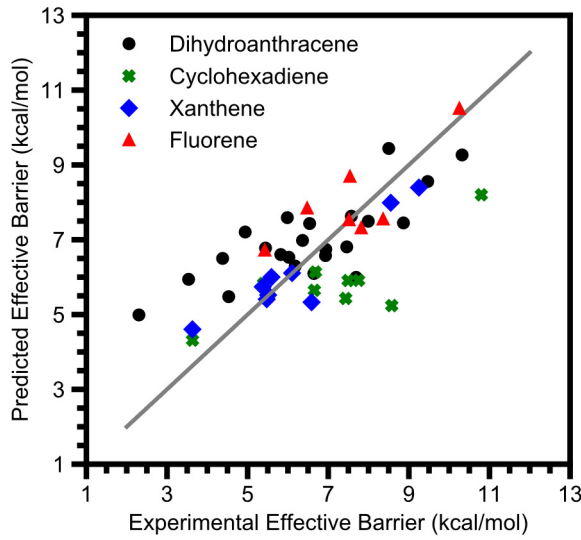
['Sub ΔG_PCET', 'Spin Excitation'] Standard Error:
[0.04575333 0.01089624]

['Sub ΔG_PCET', 'Spin Excitation'] t-Test "Error":
[0.09215195 0.02194616]

['Sub ΔG_PCET', 'Spin Excitation'] Weighted Coefficients:
[ 1.1947811 -0.36956713]

['Sub ΔG_PCET', 'Spin Excitation'] Intercept:
9.509580161062551

```



Regression S47. Multiple substrates' reaction barriers against ΔG_{PCET} and the magnitude of the asynchronicity.

['Sub ΔG_{PCET} ', 'Sub $|\eta| (G)$ '] Metrics:

Score on Training Data:	0.5041455584938033
MSE of Training Data:	1.6315592276432798
Score of LOO Cross Validation:	0.2998360096801256
MSE of LOO Cross Validation:	2.3038192736560474

Correlation Matrix of x-values:

	Sub ΔG_{PCET}	Sub $ \eta (G)$
Sub ΔG_{PCET}	1.000000	0.298842
Sub $ \eta (G)$	0.298842	1.000000

['Sub ΔG_{PCET} ', 'Sub $|\eta| (G)$ '] Training Average:
[-8.86079851 17.97838265]

['Sub ΔG_{PCET} ', 'Sub $|\eta| (G)$ '] Training Deviation:
[4.20784163 14.68415922]

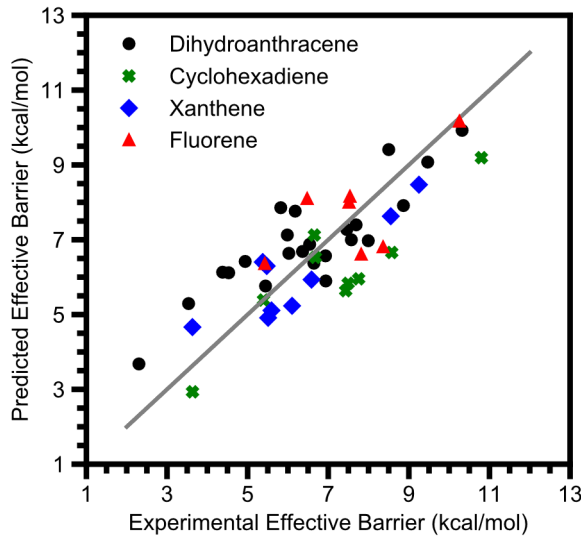
['Sub ΔG_{PCET} ', 'Sub $|\eta| (G)$ '] Coefficients:
[0.26077867 0.02873333]

['Sub ΔG_{PCET} ', 'Sub $|\eta| (G)$ '] Standard Error:
[0.04741871 0.01358814]

['Sub ΔG_{PCET} ', 'Sub $|\eta| (G)$ '] t-Test "Error":
[0.09550618 0.02736792]

['Sub ΔG_{PCET} ', 'Sub $|\eta| (G)$ '] Weighted Coefficients:
[1.09731536 0.42192485]

['Sub ΔG_{PCET} ', 'Sub $|\eta| (G)$ '] Intercept:
8.550555292333174



Regression S48. Multiple substrates' reaction barriers against ΔG_{PCET} , ΔG_{PT} , and ΔG_{ET} .

`['Sub ΔG_{PCET} ', 'Sub ΔG_{PT} ', 'Sub ΔG_{ET} '] Metrics:`

Score on Training Data:	0.6424983850662855
MSE of Training Data:	1.1763231503396485
Score of LOO Cross Validation:	0.5010163972835706
MSE of LOO Cross Validation:	1.6418554182588772

`Correlation Matrix of x-values:`

	Sub ΔG_{PCET}	Sub ΔG_{PT}	Sub ΔG_{ET}
Sub ΔG_{PCET}	1.000000	-0.308508	0.359117
Sub ΔG_{PT}	-0.308508	1.000000	-0.860287
Sub ΔG_{ET}	0.359117	-0.860287	1.000000

`['Sub ΔG_{PCET} ', 'Sub ΔG_{PT} ', 'Sub ΔG_{ET} '] Training Average:`
`[-8.86079851 44.08376701 50.44489208]`

`['Sub ΔG_{PCET} ', 'Sub ΔG_{PT} ', 'Sub ΔG_{ET} '] Training Deviation:`
`[4.20784163 18.89575872 14.48110578]`

`['Sub ΔG_{PCET} ', 'Sub ΔG_{PT} ', 'Sub ΔG_{ET} '] Coefficients:`
`[0.2286421 0.04120077 0.09643366]`

`['Sub ΔG_{PCET} ', 'Sub ΔG_{PT} ', 'Sub ΔG_{ET} '] Standard Error:`
`[0.04163513 0.01697321 0.02257307]`

`['Sub ΔG_{PCET} ', 'Sub ΔG_{PT} ', 'Sub ΔG_{ET} '] t-Test "Error":`
`[0.08391008 0.03420727 0.04549303]`

`['Sub ΔG_{PCET} ', 'Sub ΔG_{PT} ', 'Sub ΔG_{ET} '] Weighted Coefficients:`
`[0.96208973 0.77851978 1.39646609]`

`['Sub ΔG_{PCET} ', 'Sub ΔG_{PT} ', 'Sub ΔG_{ET} '] Intercept:`
`2.1015075758414623`

Availability of Data and Python Scripts

The data folder accompanying this supplementary information contains csv files with all the analyzed parameters and python scripts for running the regression output. It also contains the optimized geometries and ORCA output files of the relevant frequency calculations. Instructions for downloading the software needed to run the python script can be found at <https://www.scipy.org/install.html> and <https://www.python.org/downloads/>.

References

- (1) Sook Seo, M.; Hee Kim, N.; Cho, K.-B.; Eun So, J.; Kyung Park, S.; Clémancey, M.; Garcia-Serres, R.; Latour, J.-M.; Shaik, S.; Nam, W. A Mononuclear Nonheme Iron(IV)-Oxo Complex Which Is More Reactive than Cytochrome P450 Model Compound I. *Chem. Sci.* **2011**, *2* (6), 1039–1045. <https://doi.org/10.1039/C1SC00062D>.
- (2) England, J.; Guo, Y.; Van Heuvelen, K. M.; Cranswick, M. A.; Rohde, G. T.; Bominaar, E. L.; Münck, E.; Que, L. A More Reactive Trigonal-Bipyramidal High-Spin Oxoiron(IV) Complex with a Cis-Labile Site. *J. Am. Chem. Soc.* **2011**, *133* (31), 11880–11883. <https://doi.org/10.1021/ja2040909>.
- (3) England, J.; Martinho, M.; Farquhar, E. R.; Frisch, J. R.; Bominaar, E. L.; Münck, E.; Que, L. A Synthetic High-Spin Oxoiron(IV) Complex: Generation, Spectroscopic Characterization, and Reactivity. *Angew. Chem. Int. Ed.* **2009**, *48* (20), 3622–3626. <https://doi.org/10.1002/anie.200900863>.
- (4) Kundu, S.; Thompson, J. V. K.; Shen, L. Q.; Mills, M. R.; Bominaar, E. L.; Ryabov, A. D.; Collins, T. J. Activation Parameters as Mechanistic Probes in the TAML Iron(V)-Oxo Oxidations of Hydrocarbons. *Chem. Eur. J.* **2015**, *21* (4), 1803–1810. <https://doi.org/10.1002/chem.201405024>.
- (5) Oliveira, F. T. de; Chanda, A.; Banerjee, D.; Shan, X.; Mondal, S.; Que, L.; Bominaar, E. L.; Münck, E.; Collins, T. J. Chemical and Spectroscopic Evidence for an FeV-Oxo Complex. *Science* **2007**, *315* (5813), 835–838. <https://doi.org/10.1126/science.1133417>.
- (6) Sastri, C. V.; Lee, J.; Oh, K.; Lee, Y. J.; Lee, J.; Jackson, T. A.; Ray, K.; Hirao, H.; Shin, W.; Halfen, J. A.; Kim, J.; Que, L.; Shaik, S.; Nam, W. Axial Ligand Tuning of a Nonheme Iron(IV)-Oxo Unit for Hydrogen Atom Abstraction. *Proc. Natl. Acad. Sci. U.S.A.* **2007**, *104* (49), 19181–19186. <https://doi.org/10.1073/pnas.0709471104>.
- (7) Rohde, J.-U.; In, J.-H.; Lim, M. H.; Brennessel, W. W.; Bukowski, M. R.; Stubna, A.; Münck, E.; Nam, W.; Que, L. Crystallographic and Spectroscopic Characterization of a Nonheme Fe(IV)=O Complex. *Science* **2003**, *299* (5609), 1037–1039. <https://doi.org/10.1126/science.299.5609.1037>.
- (8) Bukowski, M. R.; Koehntop, K. D.; Stubna, A.; Bominaar, E. L.; Halfen, J. A.; Münck, E.; Nam, W.; Que, L. A Thiolate-Ligated Nonheme Oxoiron(IV) Complex Relevant to Cytochrome P450. *Science* **2005**, *310* (5750), 1000–1002. <https://doi.org/10.1126/science.1119092>.
- (9) Parsell, T. H.; Yang, M.-Y.; Borovik, A. S. C–H Bond Cleavage with Reductants: Re-Investigating the Reactivity of Monomeric MnIII/IV–Oxo Complexes and the Role of Oxo Ligand Basicity. *J. Am. Chem. Soc.* **2009**, *131* (8), 2762–2763. <https://doi.org/10.1021/ja8100825>.
- (10) Parsell, T. H.; Behan, R. K.; Green, M. T.; Hendrich, M. P.; Borovik, A. S. Preparation and Properties of a Monomeric MnIV–Oxo Complex. *J. Am. Chem. Soc.* **2006**, *128* (27), 8728–8729. <https://doi.org/10.1021/ja062332v>.
- (11) Fertlinger, C.; Hessenauer-Ilicheva, N.; Franke, A.; van Eldik, R. Direct Comparison of the Reactivity of Model Complexes for Compounds 0, I, and II in Oxygenation, Hydrogen-Abstraction, and Hydride-Transfer Processes. *Chem. Eur. J.* **2009**, *15* (48), 13435–13440. <https://doi.org/10.1002/chem.200901804>.

- (12) Goetz, M. K.; Anderson, J. S. Experimental Evidence for PKa-Driven Asynchronicity in C–H Activation by a Terminal Co(III)–Oxo Complex. *J. Am. Chem. Soc.* **2019**, *141* (9), 4051–4062. <https://doi.org/10.1021/jacs.8b13490>.
- (13) Goetz, M. K.; Hill, E. A.; Filatov, A. S.; Anderson, J. S. Isolation of a Terminal Co(III)-Oxo Complex. *J. Am. Chem. Soc.* **2018**, *140* (41), 13176–13180. <https://doi.org/10.1021/jacs.8b07399>.
- (14) Kojima, T.; Nakayama, K.; Ikemura, K.; Ogura, T.; Fukuzumi, S. Formation of a Ruthenium(IV)-Oxo Complex by Electron-Transfer Oxidation of a Coordinatively Saturated Ruthenium(II) Complex and Detection of Oxygen-Rebound Intermediates in C–H Bond Oxygenation. *J. Am. Chem. Soc.* **2011**, *133* (30), 11692–11700. <https://doi.org/10.1021/ja2037645>.
- (15) Jeong, Y. J.; Kang, Y.; Han, A.-R.; Lee, Y.-M.; Kotani, H.; Fukuzumi, S.; Nam, W. Hydrogen Atom Abstraction and Hydride Transfer Reactions by Iron(IV)–Oxo Porphyrins. *Angew. Chem. Int. Ed.* **2008**, *47* (38), 7321–7324. <https://doi.org/10.1002/anie.200802346>.
- (16) Gardner, K. A.; Kuehnert, L. L.; Mayer, J. M. Hydrogen Atom Abstraction by Permanganate: Oxidations of Arylalkanes in Organic Solvents. *Inorg. Chem.* **1997**, *36* (10), 2069–2078. <https://doi.org/10.1021/ic961297y>.
- (17) Palenik, G. J. Crystal Structure of Potassium Permanganate. *Inorg. Chem.* **1967**, *6* (3), 503–507. <https://doi.org/10.1021/ic50049a015>.
- (18) Arunkumar, C.; Lee, Y.-M.; Lee, J. Y.; Fukuzumi, S.; Nam, W. Hydrogen-Atom Abstraction Reactions by Manganese(V)– and Manganese(IV)–Oxo Porphyrin Complexes in Aqueous Solution. *Chem. Eur. J.* **2009**, *15* (43), 11482–11489. <https://doi.org/10.1002/chem.200901362>.
- (19) Cho, K.-B.; Kang, H.; Woo, J.; Park, Y. J.; Seo, M. S.; Cho, J.; Nam, W. Mechanistic Insights into the C–H Bond Activation of Hydrocarbons by Chromium(IV) Oxo and Chromium(III) Superoxo Complexes. *Inorg. Chem.* **2014**, *53* (1), 645–652. <https://doi.org/10.1021/ic402831f>.
- (20) Cho, J.; Woo, J.; Nam, W. A Chromium(III)–Superoxo Complex in Oxygen Atom Transfer Reactions as a Chemical Model of Cysteine Dioxygenase. *J. Am. Chem. Soc.* **2012**, *134* (27), 11112–11115. <https://doi.org/10.1021/ja304357z>.
- (21) Dhuri, S. N.; Lee, Y.-M.; Seo, M. S.; Cho, J.; Narulkar, D. D.; Fukuzumi, S.; Nam, W. Mechanistic Insights into the Reactions of Hydride Transfer versus Hydrogen Atom Transfer by a Trans-Dioxoruthenium(VI) Complex. *Dalton Trans.* **2015**, *44* (16), 7634–7642. <https://doi.org/10.1039/C5DT00809C>.
- (22) Warren, J. J.; Tronic, T. A.; Mayer, J. M. Thermochemistry of Proton-Coupled Electron Transfer Reagents and Its Implications. *Chem. Rev.* **2010**, *110* (12), 6961–7001. <https://doi.org/10.1021/cr100085k>.
- (23) Wang, D.; Ray, K.; J. Collins, M.; R. Farquhar, E.; R. Frisch, J.; Gómez, L.; A. Jackson, T.; Kerscher, M.; Waleska, A.; Comba, P.; Costas, M.; Que, L. Nonheme Oxoiron(Iv) Complexes of Pentadentate N5 Ligands : Spectroscopy , Electrochemistry, and Oxidative Reactivity. *Chem. Sci.* **2013**, *4* (1), 282–291. <https://doi.org/10.1039/C2SC21318D>.
- (24) Wang, D.; Zhang, M.; Bühlmann, P.; Que, L. Redox Potential and C–H Bond Cleaving Properties of a Nonheme FeIV=O Complex in Aqueous Solution. *J. Am. Chem. Soc.* **2010**, *132* (22), 7638–7644. <https://doi.org/10.1021/ja909923w>.
- (25) Bryant, J. R.; Mayer, J. M. Oxidation of C–H Bonds by [(Bpy)2(Py)RuIVO]2+ Occurs by Hydrogen Atom Abstraction. *J. Am. Chem. Soc.* **2003**, *125* (34), 10351–10361. <https://doi.org/10.1021/ja035276w>.
- (26) Yin, G.; Danby, A. M.; Kitko, D.; Carter, J. D.; Scheper, W. M.; Busch, D. H. Oxidative Reactivity Difference among the Metal Oxo and Metal Hydroxo Moieties: PH Dependent Hydrogen Abstraction by a Manganese(IV) Complex Having Two Hydroxide Ligands. *J. Am. Chem. Soc.* **2008**, *130* (48), 16245–16253. <https://doi.org/10.1021/ja804305x>.
- (27) F. Leto, D.; Ingram, R.; W. Day, V.; A. Jackson, T. Spectroscopic Properties and Reactivity of a Mononuclear Oxomanganese(Iv) Complex. *ChemComm.* **2013**, *49* (47), 5378–5380. <https://doi.org/10.1039/C3CC00244F>.

- (28) Wang, B.; Lee, Y.-M.; Tcho, W.-Y.; Tussupbayev, S.; Kim, S.-T.; Kim, Y.; Seo, M. S.; Cho, K.-B.; Dede, Y.; Keegan, B. C.; Ogura, T.; Kim, S. H.; Ohta, T.; Baik, M.-H.; Ray, K.; Shearer, J.; Nam, W. Synthesis and Reactivity of a Mononuclear Non-Haem Cobalt(IV)-Oxo Complex. *Nat. Commun.* **2017**, *8*, 14839. <https://doi.org/10.1038/ncomms14839>.
- (29) Hong, S.; So, H.; Yoon, H.; Cho, K.-B.; Lee, Y.-M.; Fukuzumi, S.; Nam, W. Reactivity Comparison of High-Valent Iron(Iv)-Oxo Complexes Bearing N -Tetramethylated Cyclam Ligands with Different Ring Size. *Dalton Trans.* **2013**, *42* (22), 7842–7845. <https://doi.org/10.1039/C3DT50750E>.
- (30) Lam, W. W. Y.; Yiu, S.-M.; Yiu, D. T. Y.; Lau, T.-C.; Yip, W.-P.; Che, C.-M. Kinetics and Mechanism of the Oxidation of Alkylaromatic Compounds by a Trans-Dioxoruthenium(VI) Complex. *Inorg. Chem.* **2003**, *42* (24), 8011–8018. <https://doi.org/10.1021/ic034782j>.
- (31) Che, C. M.; Tang, W. T.; Wong, W. T.; Lai, T. F. Novel Ruthenium-Oxo Complexes of Saturated Macrocycles with Nitrogen and Oxygen Donors and x-Ray Crystal Structure of Trans-[Ru(IV)(L)O(H₂O)][ClO₄]₂. *J. Am. Chem. Soc.* **1989**, *111* (25), 9048–9056. <https://doi.org/10.1021/ja00207a010>.
- (32) Che, C.-M.; Zhang, J.-L.; Zhang, R.; Huang, J.-S.; Lai, T.-S.; Tsui, W.-M.; Zhou, X.-G.; Zhou, Z.-Y.; Zhu, N.; Chang, C. K. Hydrocarbon Oxidation by β-Halogenated Dioxoruthenium(VI) Porphyrin Complexes: Effect of Reduction Potential (RuVI/V) and C-H Bond-Dissociation Energy on Rate Constants. *Chemistry – A European Journal* **2005**, *11* (23), 7040–7053. <https://doi.org/10.1002/chem.200500814>.
- (33) Abraham, M. H.; Grellier, P. L.; Prior, D. V.; Duce, P. P.; Morris, J. J.; Taylor, P. J. Hydrogen Bonding. Part 7. A Scale of Solute Hydrogen-Bond Acidity Based on Log K Values for Complexation in Tetrachloromethane. *J. Chem. Soc., Perkin Trans. 2* **1989**, No. 6, 699–711. <https://doi.org/10.1039/P29890000699>.
- (34) Luo, Y.-R. *Handbook of Bond Dissociation Energies in Organic Compounds*; CRC Press: Boca Raton, 2003.
- (35) Bordwell, F. G.; Bares, J. E.; Bartmess, J. E.; McCollum, G. J.; Van der Puy, M.; Vanier, N. R.; Matthews, W. S. Carbon Acids. 12. Acidifying Effects of Phenyl Substituents. *J. Org. Chem.* **1977**, *42* (2), 321–325. <https://doi.org/10.1021/jo00422a032>.
- (36) Bordwell, F. G. Equilibrium Acidities in Dimethyl Sulfoxide Solution. *Acc. Chem. Res.* **1988**, *21* (12), 456–463. <https://doi.org/10.1021/ar00156a004>.
- (37) Bordwell, F. G.; Drucker, G. E.; McCollum, G. J. Stabilization of Carbanions by Polarization of Alkyl Groups on Nonadjacent Atoms. *J. Org. Chem.* **1982**, *47* (13), 2504–2510. <https://doi.org/10.1021/jo00134a002>.
- (38) R. Carter Hill; William E. Griffiths; Guay C. Lim. *Principles of Econometrics*, 4th ed.; Wiley: Hoboken, NJ, 2011.
- (39) Freedman, D. *Statistical models: theory and practice*; Cambridge University Press: Cambridge, 2005.
- (40) Reid, J. P.; Sigman, M. S. Holistic Prediction of Enantioselectivity in Asymmetric Catalysis. *Nature* **2019**, *571* (7765), 343–348. <https://doi.org/10.1038/s41586-019-1384-z>.
- (41) Hill, T. L. *An Introduction to Statistical Thermodynamics*; Dover Publications: Newburyport, 2012.
- (42) Snelgrove, D. W.; Lusztyk, J.; Banks, J. T.; Mulder, P.; Ingold, K. U. Kinetic Solvent Effects on Hydrogen-Atom Abstractions: Reliable, Quantitative Predictions via a Single Empirical Equation. *J. Am. Chem. Soc.* **2001**, *123* (3), 469–477. <https://doi.org/10.1021/ja002301e>.
- (43) Warren, J. J.; Mayer, J. M. Predicting Organic Hydrogen Atom Transfer Rate Constants Using the Marcus Cross Relation. *Proc. Natl. Acad. Sci. U.S.A.* **2010**, *107* (12), 5282–5287. <https://doi.org/10.1073/pnas.0910347107>.
- (44) Cramer, C. J.; Truhlar, D. G. Density Functional Theory for Transition Metals and Transition Metal Chemistry. *Phys. Chem. Chem. Phys.* **2009**, *11* (46), 10757–10816. <https://doi.org/10.1039/B907148B>.

- (45) Harvey, J. N. On the Accuracy of Density Functional Theory in Transition Metal Chemistry. *Annu. Rep. Prog. Chem., Sect. C: Phys. Chem.* **2006**, *102* (0), 203–226. <https://doi.org/10.1039/B419105F>.
- (46) Neese, F. A Critical Evaluation of DFT, Including Time-Dependent DFT, Applied to Bioinorganic Chemistry. *J Biol Inorg Chem* **2006**, *11* (6), 702–711. <https://doi.org/10.1007/s00775-006-0138-1>.
- (47) Abraham, M. H.; Grellier, P. L.; Prior, D. V.; Morris, J. J.; Taylor, P. J. Hydrogen Bonding. Part 10. A Scale of Solute Hydrogen-Bond Basicity Using Log K Values for Complexation in Tetrachloromethane. *Perkin Trans. 2* **1990**, No. 4, 521–529. <https://doi.org/10.1039/P29900000521>.
- (48) Weigend, F.; Ahlrichs, R. Balanced Basis Sets of Split Valence, Triple Zeta Valence and Quadruple Zeta Valence Quality for H to Rn: Design and Assessment of Accuracy. *Phys. Chem. Chem. Phys.* **2005**, *7* (18), 3297–3305. <https://doi.org/10.1039/B508541A>.
- (49) Harper, K. C.; Bess, E. N.; Sigman, M. S. Multidimensional Steric Parameters in the Analysis of Asymmetric Catalytic Reactions. *Nature Chemistry* **2012**, *4* (5), 366–374. <https://doi.org/10.1038/nchem.1297>.
- (50) Bondi, A. Van Der Waals Volumes and Radii. *J. Phys. Chem.* **1964**, *68* (3), 441–451. <https://doi.org/10.1021/j100785a001>.
- (51) Rowland, R. S.; Taylor, R. Intermolecular Nonbonded Contact Distances in Organic Crystal Structures: Comparison with Distances Expected from van Der Waals Radii. *J. Phys. Chem.* **1996**, *100* (18), 7384–7391. <https://doi.org/10.1021/jp953141+>.
- (52) Usharani, D.; Janardanan, D.; Li, C.; Shaik, S. A Theory for Bioinorganic Chemical Reactivity of Oxometal Complexes and Analogous Oxidants: The Exchange and Orbital-Selection Rules. *Acc. Chem. Res.* **2013**, *46* (2), 471–482. <https://doi.org/10.1021/ar300204y>.
- (53) Waidmann, C. R.; Zhou, X.; Tsai, E. A.; Kaminsky, W.; Hrovat, D. A.; Borden, W. T.; Mayer, J. M. Slow Hydrogen Atom Transfer Reactions of Oxo- and Hydroxo-Vanadium Compounds: The Importance of Intrinsic Barriers. *J. Am. Chem. Soc.* **2009**, *131* (13), 4729–4743. <https://doi.org/10.1021/ja808698x>.
- (54) Marcus, R. A. ON THE THEORY OF OXIDATION—REDUCTION REACTIONS INVOLVING ELECTRON TRANSFER. V. COMPARISON AND PROPERTIES OF ELECTROCHEMICAL AND CHEMICAL RATE CONSTANTS. *J. Phys. Chem.* **1963**, *67* (4), 853–857. <https://doi.org/10.1021/j100798a033>.
- (55) Marcus, R. A.; Sutin, N. Electron Transfers in Chemistry and Biology. *Biochim. Biophys. Acta, Rev. Bioenerg.* **1985**, *811* (3), 265–322. [https://doi.org/10.1016/0304-4173\(85\)90014-X](https://doi.org/10.1016/0304-4173(85)90014-X).
- (56) Bím, D.; Maldonado-Domínguez, M.; Rulišek, L.; Srnec, M. Beyond the Classical Thermodynamic Contributions to Hydrogen Atom Abstraction Reactivity. *Proc. Natl. Acad. Sci. U.S.A.* **2018**, *115* (44), E10287–E10294. <https://doi.org/10.1073/pnas.1806399115>.
- (57) Radón, M. Revisiting the Role of Exact Exchange in DFT Spin-State Energetics of Transition Metal Complexes. *Phys. Chem. Chem. Phys.* **2014**, *16* (28), 14479–14488. <https://doi.org/10.1039/C3CP55506B>.
- (58) Neese, F. Software Update: The ORCA Program System, Version 4.0. *Wiley Interdiscip. Rev. Comput. Mol. Sci.* **2018**, *8* (1), e1327. <https://doi.org/10.1002/wcms.1327>.
- (59) Neese, F. The ORCA Program System. *Wiley Interdiscip. Rev. Comput. Mol. Sci.* **2012**, *2* (1), 73–78. <https://doi.org/10.1002/wcms.81>.
- (60) Matsuo, T.; Mayer, J. M. Oxidations of NADH Analogues by Cis-[RuIV(Bpy)₂(Py)(O)]²⁺ Occur by Hydrogen-Atom Transfer Rather than by Hydride Transfer. *Inorg. Chem.* **2005**, *44* (7), 2150–2158. <https://doi.org/10.1021/ic048170q>.